

Near infrared quantitative chemical imaging as an objective, analytical tool for optimization of  
the industrial processing of wheat

by

Mark Daniel Boatwright

B.S., Kansas State University, 2009  
M.S., Kansas State University, 2012

AN ABSTRACT OF A DISSERTATION

submitted in partial fulfillment of the requirements for the degree

DOCTOR OF PHILOSOPHY

Department of Biochemistry & Molecular Biophysics  
College of Arts and Sciences

KANSAS STATE UNIVERSITY  
Manhattan, Kansas

2018

## **Abstract**

The technique of near infrared chemical imaging has been widely used for many industrial applications. It offers selectivity and/or sensitivity for numerous organic functional groups. The advantage of the near infrared spectroscopic region is the linear relationship of absorbance and concentration that enables quantitation. This universally employed technique has been a boon for research studies in the industrial process of wheat milling for the production of flour. The milling process has numerous sequential grinding and sieving steps that enable selective physical segregation of a starch rich endosperm product from wheat. Thousands of spectra of purified endosperm and non-endosperm standards are collected to develop a spectral library. Quantitation of the purity of individual processing streams is accomplished by applying a partial least squares calibration that is based upon the spectral library. The quantitative chemical imaging technique is useful for determination of endosperm purity profiles for mill flour streams. These plots reveal purity changes as less pure streams are added to produce a flour blend. The chemical structural basis furthermore allows comparison of purity even with changes in the wheat blend being milled with representative standardization. Furthermore, whereas a certain section of sieves is responsible, for designating the material defined as flour, application of the spectroscopic method is obvious. Select examples of key processing streams were studied to show the possibility of sieve-by-sieve analysis of the physical separation to provide mill optimization. These novel methods of analysis would not be possible without the sensitive and selective method of quantitative chemical imaging. Application of this technique to a few select unit processes is projected to reasonably affect a 1% increase in the yield of high quality flour. This amounts to a significant financial gain against low profit margins.

Near infrared quantitative chemical imaging as an objective, analytical tool for optimization of  
the industrial processing of wheat

by

Mark Daniel Boatwright

B.S., Kansas State University, 2009  
M.S., Kansas State University, 2012

A DISSERTATION

submitted in partial fulfillment of the requirements for the degree

DOCTOR OF PHILOSOPHY

Department of Biochemistry & Molecular Biophysics  
College of Arts and Sciences

KANSAS STATE UNIVERSITY  
Manhattan, Kansas

2018

Approved by:

Major Professor  
Dr. John Tomich

Approved by:

Major Professor  
Dr. David Wetzel

# **Copyright**

© Mark Boatwright 2018.

## **Abstract**

The technique of near infrared chemical imaging has been widely used for many industrial applications. It offers selectivity and/or sensitivity for numerous organic functional groups. The advantage of the near infrared spectroscopic region is the linear relationship of Absorbance and concentration that enables quantitation. This universally employed technique has been a boon for research studies in the industrial process of wheat milling for the production of flour. The milling process has numerous sequential grinding and sieving steps that enable selective physical segregation of a starch rich endosperm product from wheat. Thousands of spectra of purified endosperm and non-endosperm standards are collected to develop a spectral library. Quantitation of the purity of individual processing streams is accomplished by applying a partial least squares calibration that is based upon the spectral library. The quantitative chemical imaging technique is useful for determination of endosperm purity profiles for mill flour streams. These plots reveal purity changes as less pure streams are added to produce a flour blend. The chemical structural basis furthermore allows comparison of purity even with changes in the wheat blend being milled with representative standardization. Furthermore, whereas a certain section of sieves is responsible, for designating the material defined as flour, application of the spectroscopic method is obvious. Select examples of key processing streams were studied to show the possibility of sieve-by-sieve analysis of the physical separation to provide mill optimization. These novel methods of analysis would not be possible without the sensitive and selective method of quantitative chemical imaging. Application of this technique to a few select unit processes is projected to reasonably affect a 1% increase in the yield of high quality flour. This amounts to a significant financial gain against low profit margins.

# Table of Contents

List of Figures .....	ix
List of Tables .....	xiii
Chapter 1 - Industrial Processing of Wheat.....	1
1.1 Wheat.....	1
1.2 Wheat Milling Background .....	5
1.3 Mill Optimization.....	10
1.4 Spectroscopic Analysis.....	13
1.4.1 Study of Biological Materials.....	13
1.4.2 Spectroscopic Chemical Imaging .....	16
1.4.3 NIR Chemical Imaging Background .....	20
1.4.4 Spectroscopic Bands of Grains.....	21
1.5 NIR Chemical Imaging of Wheat.....	23
1.5.1 Previous Experimentation .....	23
1.5.2 Experimental Optimization .....	25
1.6 Wheat Milling Sample Acquisition.....	28
1.7 Analytical Considerations for Quantitative Chemical Imaging.....	29
1.8 Abbreviations .....	32
1.9 References.....	32
Chapter 2 - Endosperm Purity Profiling: Commercial Mill Streams Preceded by Debranning via Application of Quantitative Chemical Imaging.....	35
2.1 Abstract.....	35
2.2 Introduction.....	36
2.3. Experimental .....	39
2.3.1. Commercial Wheat Mill.....	39
2.3.2. Specimens.....	41
2.3.3. Instrumentation.....	42
2.3.4. Quantitative Near Infrared Imaging Procedure .....	44
2.4 Results and Discussion .....	45
2.5. Summary .....	50

2.6. Abbreviations .....	51
2.7. References.....	51
2.8. Footnotes.....	52
Chapter 3 - Endosperm Purity Profile Comparison of Different Milling Operations.....	53
3.1 Introduction.....	53
3.2 Experimental .....	55
3.2.1 Wheat Milling Operations.....	55
3.2.2 Specimens.....	55
3.2.3 Instrumentation.....	57
3.2.4 Quantitative Near Infrared Imaging Procedure .....	57
3.3 Results and Discussion .....	58
3.3.1 Construction of the Endosperm Millers' Curve.....	58
3.3.2 Preprocessing Comparison: Debranning vs. Tempering.....	61
3.3.3 Comparison of Multiple Milling Operations.....	63
3.4 Conclusion .....	65
3.5 List of Abbreviations.....	66
3.6 References.....	66
Chapter 4 - Novel Optimization of Wheat Milling Sieving Operation and Unit Process Mass	
Balance Utilizing Selective Near Infrared Chemical Imaging .....	68
4.1 Introduction.....	68
4.2 Experimental .....	73
4.2.1 Instrumentation.....	73
4.2.2 Commercial Milling Operation .....	75
4.2.3 Milling Operational Settings .....	82
4.3 Results & Discussion.....	85
4.3.1 Sieving Experiments .....	85
4.3.2 Break System Balance .....	94
4.3.3 Reduction Operation .....	96
4.4 Summary.....	99
4.5 Abbreviations .....	100
4.6 References.....	101

Chapter 5 - Summary and Future Direction .....	102
Appendix A - Copyright Permission for Chapter 2 .....	104
Appendix B - Reasoning for the term matza .....	105

## List of Figures

Figure 1.1 Diagrams of the wheat kernel with labeled botanical parts (left) and cross-section (right) with major regions. [Reprinted from 2] .....	2
Figure 1.2 Typical flow diagram for a milling process indicating grinding, sieving, and purifier operations complete with operational settings and stream destinations. [Reprinted from 7] ..	6
Figure 1.3 Photograph of a typical sifter box (left) and a diagram of a sifter frame (right). [Reprinted from 8] .....	8
Figure 1.4 Price in dollars/cwt of wheat (bottom) and flour (top) from quarterly reports over 2010-2016. Note that the Minneapolis (□, ○) and Kansas City (◇, Δ) markets are displayed for each commodity (9). .....	10
Figure 1.5 Millers' plots of ash (left) and ferulic acid (right) indicating increasing contamination as additional streams are added. Note the ferulic acid plot indicates an earlier purity distinction between two wheat varieties because of the chemical specificity. [Reprinted from 14] .....	12
Figure 1.6 Visual representation of diffuse reflectance pathways through a granular sample. [Reprinted from 7] .....	14
Figure 1.7 Optical diagram of the NIR FPA imaging system. [Reprinted from 23] .....	16
Figure 1.8 Photograph of the Middleton Spectral Vision near infrared imaging spectrometer. ...	18
Figure 1.9 Mean spectra obtained from wheat starch, wheat gluten, and an entire kernel. Note that the distinctive bands for starch and protein are subdued in the intact wheat kernel. ....	22
Figure 1.10 Chemical images displaying endosperm purity in warm false colors arising from specifying near infrared bands selective for endosperm (top right) and non-endosperm (bottom right), respectively. Note the expanded color scale. [Reprinted from 23] .....	23
Figure 1.11 False color images of purifier streams before (left) and after (right) adjustment. Note the calculated % endosperm and mass balance (red). After adjustment, the product yield (FC & SC) increased from 65% to 77% with a corresponding reduction in rework. Note the expanded color scale that indicates endosperm purity with warm false colors. [Reprinted from 23] .....	24

Figure 1.12 (Left) Truncated spectra of endosperm (red) and non-endosperm (blue). (Right) Partial least squares factor loadings 1-4 (red, blue, green, and purple, respectively). Note that factor loading 1 resembles the library standard spectrum of endosperm.....	26
Figure 1.13 Example of spectra in a linear space with varying amounts of two components (left). The spectra plotted against the calculated best fit regression coefficients upon which they are based. [Reprinted from 25].....	27
Figure 1.14 Endosperm quantitative result of same mixture over starting time.....	31
Figure 1.15 Chemical images (left) and photomicrographs (right) showing mixtures of wheat bran flakes and a granular wheat endosperm mixture. . Note the expanded color scale that indicates endosperm purity with warm false colors. Images were taken from well-mixed (top), agitated (middle), and additionally agitated (bottom) mixtures. ....	31
Figure 2.1 Flow sheet of the 204 CWT/24 hour commercial flour mill equipped with abrasive debranning technology.....	39
Figure 2.2 Cumulative percent endosperm calculated from endosperm purity multiplied by flow rate. As each successively inferior stream is added, value for the combination is recalculated. ....	46
Figure 2.3 The cumulative reflectance intensity of visible light showing limited contrast for cumulative percent total product (■). A Konica Minolta reflectance Chroma Meter (CR-410) was used to obtain visible color (L* value) measurements. Shown to scale with endosperm measurement (■).....	47
Figure 2.4 False color images and respective endosperm purity for flour streams collected from DD1 1 (99.4%), DD1#2 1 (94.8%), C1 1 (94.0%), DD2-1 (91.6%), and DD2 2/3 (81.2%). Note the expanded color scale that indicates endosperm purity with warm false colors.. Each is representative of different points across the cumulative endosperm curve. ....	48
<b>Figure 2.5.</b> Ash residue after ignition in a muffle furnace reveals the mineral content that is not related to the organic non-endosperm content of each flour stream. The result of plotting ash vs. endosperm purity produces a shotgun pattern. ....	49
Figure 3.1 Flow diagram for the Hal Ross flour mill.....	56
Figure 3.2 Cumulative endosperm curve for the Jerusalem commercial mill without preprocessing. Note the four slopes changes as inferior product is added to the flour blend. ....	59

Figure 3.3 Cumulative endosperm curve for the Jerusalem commercial mill reduction system. Note the departures in the curve in comparison to the original plot. ....	61
Figure 3.4 Cumulative endosperm curve comparison of a conventional pilot mill and commercial mill equipped with debranning.....	62
Figure 3.5 Milling system comparisons of total flow and endosperm purity for a mill with and without debranning.....	63
Figure 3.6 Cumulative millers' curves for a conventional pilot scale ( $\diamond$ ), commercial scale with debranning ( $\square$ ), and a pretreatment free commercial scale ( $\Delta$ ) milling operation with an expanded scale.....	64
Figure 3.7 Cumulative millers' curves for a conventional pilot scale ( $\diamond$ ), commercial scale with debranning ( $\square$ ), and a pretreatment free commercial scale ( $\Delta$ ) milling operation with a common scale.....	65
Figure 4.1 Typical sifter diagrams indicating sieve by sieve details (left), flow of overs (left center), flow of thrus (right center), and the positioning of exit spouting (right).....	69
Figure 4.2a Flow diagram of the Em Hachita soft wheat commercial mill. ....	77
Figure 4.3. Milling diagrams for the second break (top) and fourth break (bottom) grinding and sieving operations.....	84
Figure 4.4. Diagram of the B3 sieving operation (left) and chemical images for the overs and thrus (right). Note the expanded color scale that indicates endosperm purity with warm false colors. ....	86
Figure 4.5. Sieving diagram for the C1b reduction process.....	87
Figure 4.6. Chemical images of the C1b flour sieve overs and thrus. Note the enriched flour product and similar intensity of F1 and F2 flour images. Note the expanded color scale that indicates endosperm purity with warm false colors. ....	88
Figure 4.7. Flow sheet diagram of the C2 sifting process. Note the fine and coarse flour streams from 8-140 $\mu\text{m}$ sieves and 5-160 $\mu\text{m}$ sieves, respectively.....	89
Figure 4.8. Chemical images resulting from the C2 sieving analysis. Note the expanded color scale that indicates endosperm purity with warm false colors.....	90
Figure 4.9. Flow sheet diagram of the C4 sifting process (left). Note the flour stream from 8-140 $\mu\text{m}$ sieves. Corresponding chemical images of the overs and thrus are also shown (right). Note the expanded color scale that indicates endosperm purity with warm false colors. ....	92

Figure 4.10. Flow sheet diagram of the Div 3 sifting process (left). Note that two flour streams are produced from 6-125  $\mu\text{m}$  (coarse) and 4-112  $\mu\text{m}$  (fine) sieves. Corresponding chemical images of the overs and thrus are also shown (right). Note the expanded color scale that indicates endosperm purity with warm false colors. ....93

Figure 4.11. Purity comparisons of second break operations for a laboratory and commercial scale milling operations. Note that the experimental operation had an optimized first break and second break grinding with tempering of the wheat. The 2016 construction had limits for the incoming stock and grinding because of the lack of pretreatment and contracted engineer settings, respectively. Note the expanded color scale that indicates endosperm purity with warm false colors.....95

Figure 4.12. Chemical images indicating distribution of C2 stock into streams of varying purity. The destination operations included a coarse C4 stock, two C3 streams, a fine flour fraction, and a coarse flour fraction. Note the expanded color scale that indicates endosperm purity with warm false colors.....97

Figure 4.13. Chemical images indicating distribution of C4 stock into streams of varying purity. The destination operations included a coarse B4 stock, a C5 stream, and a single lower quality flour fraction. Note the expanded color scale that indicates endosperm purity with warm false colors.....98

Figure 4.14. Purity comparisons of reduction operations for a laboratory and commercial scale mill flow. Note that the both operations feature relatively pure incoming stock and segregate it between a significant mass of product, the next reduction step, and some further processing step. The optimized experiment understandably had higher purity incoming stock and flour. Note the expanded color scale that indicates endosperm purity with warm false colors. ....99

## List of Tables

Table 2.1 Flour stream rank by endosperm purity.....	45
Table 4.1 B3 Flour Sieve Endosperm Values.....	86
Table 4.2 C1b flour sieve data for overs (+) and thrus (-).....	88
Table 4.3 C2 flour sieve data for overs (+) and thrus (-). ....	90
Table 4.4 Div 3 flour sieve data for overs (+) and thrus (-). ....	93

## Chapter 1 - Industrial Processing of Wheat

### 1.1 Wheat

Wheat has the largest growing distribution of any cultivated cereal (1). It is also the second largest source for worldwide caloric consumption. As such, it is a very important food crop with interest at a global level. The basic chemical components of wheat kernel that provide nutritional value include starch, protein, and cellulosic material. There are also several minor constituents such as lipids, minerals, and vitamins.

The wheat plant is classified as a grass (family Gramineae) under the genus *Triticum* (2). The primary wheat plant that is milled is the species *Triticum aestivum* or common wheat. Common wheat is traditionally divided into multiple subclasses based upon the growth pattern, pigmentation of the outer bran layer, and kernel characteristics (3). The differences between subclasses affect the processing characteristics and end use of the wheat with selective breeding further meeting these needs.

The wheat kernel has an oblong shape that is larger, and rounded at one end. The kernel has two asymmetrical sides. The dorsal side is smooth and rounded and contains a dent where the germ is located. The ventral side is rounded, but contains a horizontal crease along the longest axis. The average kernel varies from 8-10 mm in length (4). The shape and size have greatly defined the development of processing and refinement methods over time.

The individual kernel of wheat is organized into several distinct botanical parts (**Fig. 1.1**). The major botanical parts of the wheat kernel are the bran (the seven outermost protective layers), the endosperm (energy source for the growing seed), and the germ (the embryo). The bran is the outer, protective portion of the wheat kernel and consists of several layers contributing to approximately 8% of the kernel weight. The outermost layers are called the outer

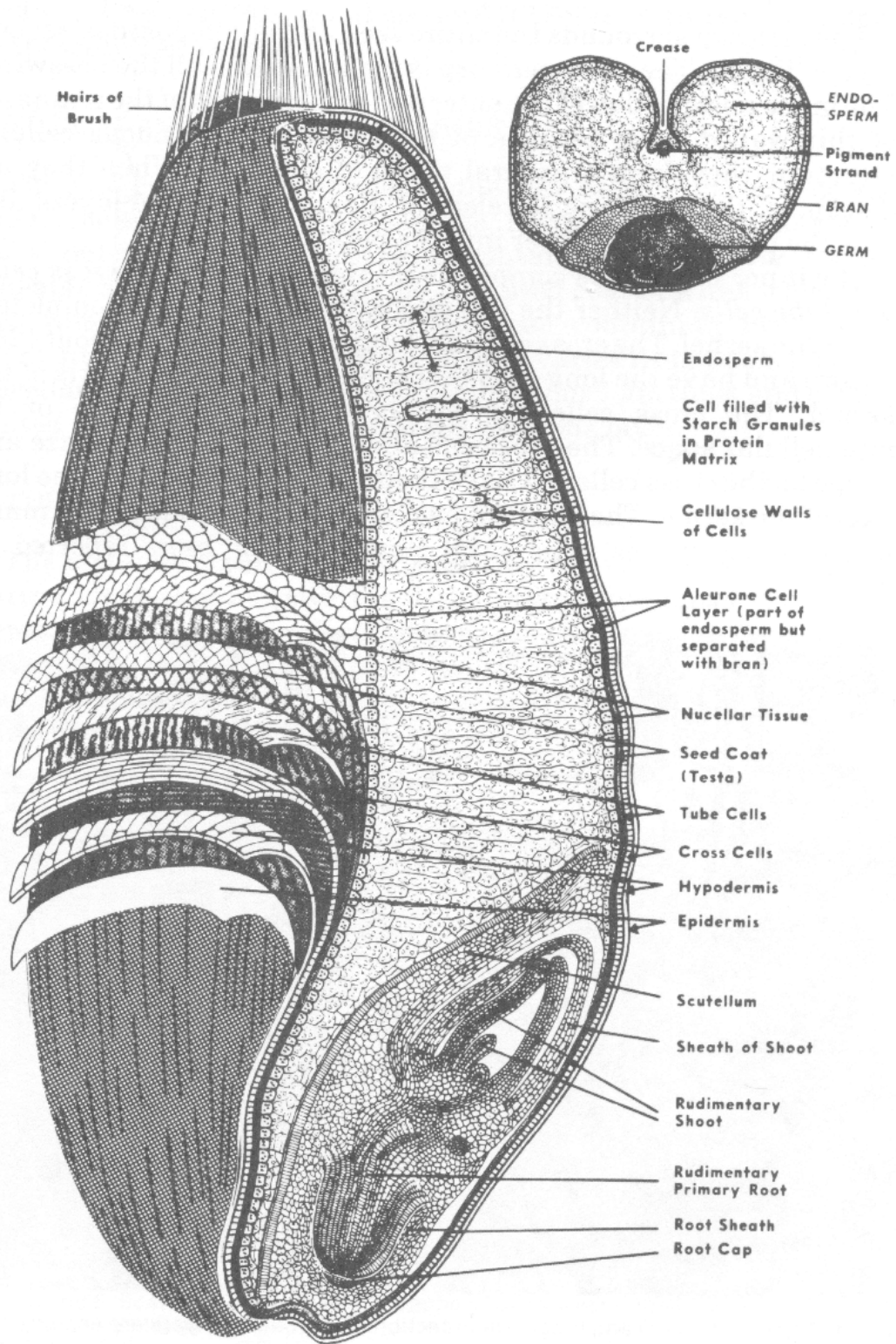


**Figure 1.1** Diagrams of the wheat kernel with labeled botanical parts (left) and cross-section (right) with major regions. [Reprinted from 2]

pericarp and consist of epidermis and the hypodermis. The adjacent inner pericarp has the intermediate cells, cross cells, and tube cells. The innermost layer of the bran is the seed coat, which is composed of the testa, pigment strand, and nucellar layers. These inner layers provide additional structure and the pigment strand gives the wheat kernel its coloration.

The endosperm component has the largest contribution at 83% of the total kernel. The purpose of the endosperm is to provide the food source for the growing embryo. As such, it is a very important source of calories for human consumption. The endosperm is located inwards past the aleurone layer and changes from peripheral, prismatic, to central endosperm; each with a slightly modified chemistry and structure. Endosperm consists of starch granules embedded within a matrix of cellulosic cell walls and protein bodies. Wheat starch is further subdivided between “A” and “B” granules that are approximately 12-30 and 1-10  $\mu\text{m}$ , respectively (5). While the individual starch granules are fairly small, the endosperm cells, composed of cell walls, protein matrix, and starch granules, are a minimum of 60  $\mu\text{m}$  (6). There are approximately 30,000 individual starch endosperm cells within a single wheat kernel.

The smallest region of the major wheat kernel botanical parts is the germ. The germ is surrounded by an epithelial layer and contains the embryonic axis (the growing portion of the germ) and the scutellum that provide nutrients in the form of lipid and protein. There are health benefits from the inclusion of germ in the diet including the desirable lipid composition; however, the chemistry of the germ makes it unreasonable for its inclusion in wheat products due to rancidity upon storage.

Any chemical analysis of wheat must take into account the variation of the chemistry between and within the botanical parts of the kernel. These chemical compounds include starch, protein, water, and lipid in significant amounts (78%, 14%, and 3% by mass, respectively). The

starch composition of wheat is fairly constant. Protein has the largest variation per unit weight of the three major chemical components. This variation can occur even within kernels of the same cultivar (up to 10%). Regarding specific proteins, the amount of gluten between wheat cultivars can differ by a factor of three. This is significant because gluten storage proteins often eclipse 50% of the total protein content of wheat.

The wheat kernel initially begins with a significant mass of water during the growth process. However, when the wheat kernel matures, it begins to dry out to a moisture content of approximately 9-12% and metabolic activity begins to cease. The greatest amount of moisture is present within the endosperm, but highly variable. Lipid has a fairly minor presence in the wheat kernel. It is enriched within the bran and germ, but there is also a small amount buried within the endosperm cells.

Also, there are several minor constituents of the wheat kernel. Wheat has a fair amount dietary fiber primarily in the form of nonstarch polysaccharides. These are divided amongst arabinoxylan and beta-glucan primarily. There is also a relevant fraction of mineral content (ash) that is enriched in the bran and germ. The average concentration of mineral present for the entire wheat kernel is 1.58%.

Given the importance of the endosperm regarding human consumption of wheat, the chemical composition has been widely studied. On average, wheat endosperm contains 80% starch, 10% protein, and 10% of other chemical components (1). The variation of starch composition is highly dependent on variables during the development of individual kernels. Protein composition is interdependent with several external factors including soil, fertilization, etc.

## 1.2 Wheat Milling Background

Separation science has been applied to the refinement of naturally occurring materials to isolate the high value component. For industrial scale refinements, intermediate steps are required to produce a value-added material. Grain refinement (milling) is often necessary to obtain desired texture of end product and increase the shelf life of flour or flour products (3). This causes many vitamins and minerals to be removed, but they are easily with supplemental additives. Thus, the selected endosperm measurement focuses not on just a valuable measurement, but the components which negatively affect the performance of the product or shelf life. Non-endosperm particles are known to adversely affect the taste of mouth feel, including bitterness and dryness. Baking is also affected, because bran and germ soak up additional moisture and add weight to the dough preventing rising. More importantly, bran particles with their irregular shapes can break air bubbles.

The wheat milling process consists of a combination of gradual grinding for particle size reduction and repeated classification by sifting. The overall efficiency of the process is measured by the purity and yield of product in the form of fine particulates of wheat endosperm (flour). Raw wheat is shipped from local elevators and sent immediately to storage bins in the mill. Initial separations steps include a magnet and coarse sieve to remove potential contaminants. Directly before the milling process, more significant cleaning and conditioning occurs. The first premilling cleaning step is aspiration, where airflow picks up the lightweight chaff and dust. A destoner follows to separate similar sized particles like rocks or glass based upon density. The seed separator is used to remove seeds and other material that has a different shape or length than the typical wheat kernel. The traditional milling process uses a period of soaking called



tempering. The theory is that the moisture weakens the interaction between the bran and endosperm while softening bran to prevent its' shattering into small pieces. Alternative preprocessing steps can follow including debranning to remove the outermost layers of bran with abrasive action.

The milling process is routinely described by a flow sheet (**Fig. 1.2**) where successive grinding operations with subsequent sifting stages are shown in detail (7). Sifting is performed with a stack of sieve frames with sieves of different apertures stretched upon them. This process is based on the principle of sorting the incoming stock after each grinding stage to different particle sizes with descending sieve apertures. Groups of sieves in the range between 110–220 microns are generally shown in the flow sheet for the separation of enriched endosperm as flour.

The flow diagram displays each unit process with a summation of incoming material (with shorthand notation of the origin) entering a grinding, sieving, or purifier process. Each unit process is also designated with a short form. The material is shown to enter a pair (or pairs) of grinding rolls that are denoted with the number of roll pairs, energy consumption, the pitch, the differential, the spiral, and the roll surface.

**Fig. 1.3** demonstrates a typical sifting surface (8). Note that a wooden frame is present upon which a sieve cloth is stretched. Material will typically approach the first sieve from the middle. As the sifter box gyrates in a mechanistic fashion, the wheat intermediate stock is also shaken back and forth from one side to another. In this manner, some material goes through this sieve cloth and the rest makes its way towards what is referred to as the tail of the sieve where it passes towards the side nail and down to the next sieve (**Fig 1.3**). The materials hit the next sieve from one side, known as the head of the sieve and the material passes down so forth. The thrus are collected in the pan and guided towards the thrus channel which goes down the side of

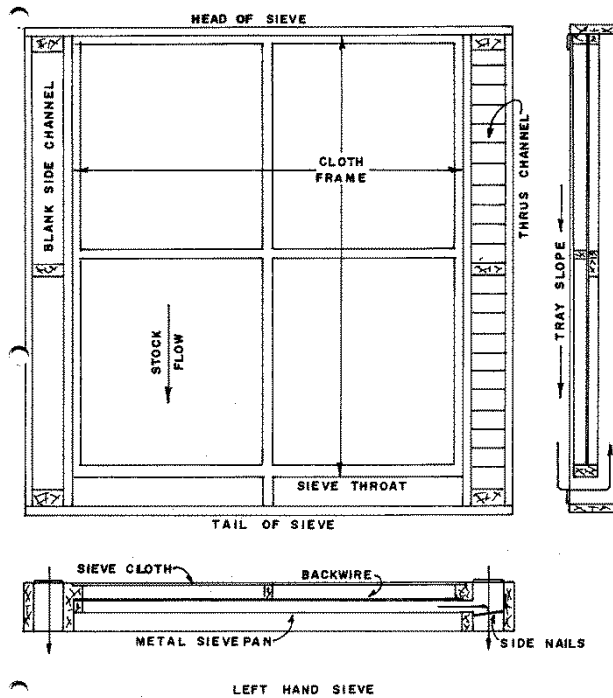


**Figure 1.3** Photograph of a typical sifter box (left) and a diagram of a sifter frame (right). [Reprinted from 8]

the section, reaches the bottom, and exits through a cloth sifter sock.

The milling process is broken down into several stages, each with a particular goal. The first set of operations, referred to as the break system (Bk), consists of grinding action with corrugated rolls with the purpose of tearing the kernel apart to remove endosperm from the bran in large pieces. There are typically 5-6 break operations, beginning with the first milling step in the rupture of the intact wheat kernel. The material over a 1040  $\mu\text{m}$  sieve for each of these processes is sent to the next break operation and the other sieves produce a small amount of flour and selectively redistribute endosperm and non-endosperm to additional processing steps. Often, additional sifting surface is available for these high-volume operations in the form of a Division sifter.

The next milling system for the majority of milling operations is a sizings step. This process is not featured in every mill, but it selectively breaks down endosperm particles and flattens the bran to ease the particle size based separation via sieving. A sizable amount of flour is produced here while providing pure endosperm for later steps and redistributing material to rework step. Alternatively, there is a break redust system to redistribute intermediate stock from the early break systems (typically 1, 2, 3 Bk) to appropriate operations. The purifier operation also performs a similar function. This system uses sieving under the effect of air turbulence to provide stock classification rather than a grinding procedure. Material is selectively graded based upon density and particle size into at least five stocks. These stocks are often purified middlings (coarse particles of purified endosperm) and non-endosperm fractions going back to the break system.

The next stage is the middlings reduction system. This system is provided with clean middlings and uses smooth rolls that reduce the material to a particle size appropriate for flour (< 220  $\mu\text{m}$ ). The general goal is to produce as much flour as possible as quickly as possible. The sifters often redistribute material only to the next reduction operation, however, sometimes stock is sent back to the late break or rework systems.

Many milling systems feature a residue or low-grade system. These processes may include the tail end of the break and/or reduction systems. The purpose of these processes is to produce additional flour if possible and to classify the non-endosperm streams to maximize value. By definition, as a commodity industry, wheat milling operates with high volumes and low margins where every increase in value is beneficial.

### 1.3 Mill Optimization

An optimized milling operation requires consideration of efficiency of several processing factors to maximize profits. The raw wheat (grist) is the largest expenditure for the mill and comprises 80% of the total production costs. In the purchasing of wheat, the mill owner must consider the cost, extraction rate (% flour) potential, and the moisture content. The physical characteristics of wheat that are used to define millability are plumpness, uniformity, soundness, cleanliness, wheat hardness, lack of impurities, and contamination. The price of wheat products and byproducts fluctuates often within a calendar year. Over recent years, the overall price of flour has trended downward (Fig. 1.4). There are discrepancies in prices within the US market, but the overall trends are the same. It can be noted that the prices of both byproducts and products exhibit opposing trends.

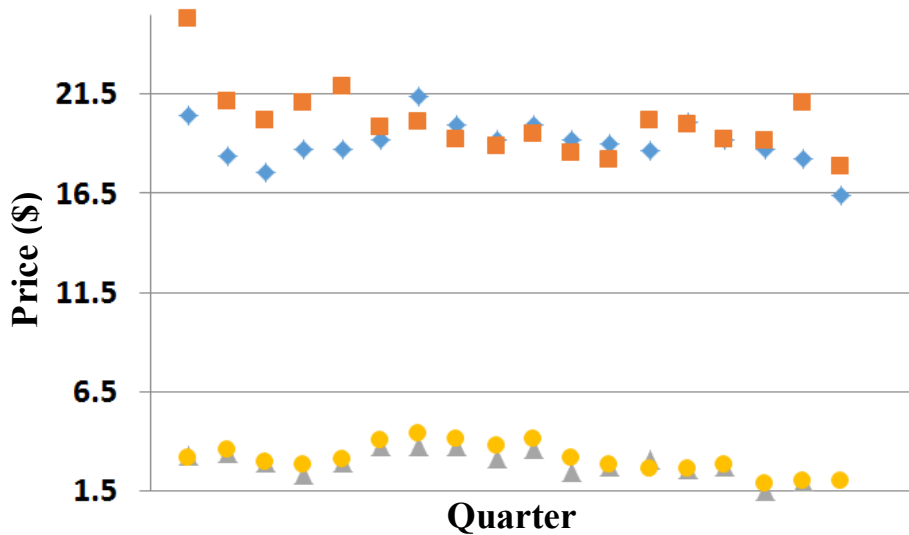


**Figure 1.4** Price in dollars/cwt of wheat (bottom) and flour (top) from quarterly reports over 2010-2016. Note that the Minneapolis (□, ●) and Kansas City (◇, △) markets are displayed for each commodity (9).

Blending with wheat stock that is already in the mill's storage bins is also an option.

Wheat must be purchased at the cheapest available price to produce flour of a specified quality

requested by the buyer/consumer. The relative price of product and byproduct at a particular point in time is also a key consideration. Electricity, capital, and salaries are secondary to the wheat grist. However, these costs can be limited by optimizing the overall process efficiency (10). Optimization of the operational efficiency is quite important. The flour milling industry in the US uses the measurement of the hundredweight (cwt) in pounds to describe the mass. The average U.S. mill approximately handles 10,000 cwt of wheat/24-hour period; however, the trend is towards larger mills greater than 18,000 cwt (11). As such, in the terms of flour mill wheat requirements or flour output, a 1% difference represents hundreds of thousands of dollars over the course of a year. Thus, optimization to improve yield is obvious given the low margins.

After considering potential costs, the miller must meet certain flour quality characteristics, specified by the consumer or buyer. Flour purity is routinely determined by methods such as low mineral ash or a high brightness measurement, indicating the lack of non-endosperm, and the miller must maximize the extraction rate to obtain a reasonable margin. This requires the efficiency of separation to be optimized for every individual unit process (10). With the average capacity of U.S. mills doubling since the 1980s and a subsequent increase in flow rates, this is a significant undertaking in terms of the potential economic benefit.

Good processing efficiency and mill management requires several levels of monitoring. The mill manager is often regularly informed of the mill's capacity, flour output, and extraction by an electronic readout (10). The mill laboratory receives flour samples several times daily and reports measurements for percent moisture, water absorption, protein content, and flour color. Many of these flour measurements are directly indicative of the baking quality of the flour. Traditionally, the mineral ash is also determined for the mill's patent flour stream.

In the absence of a direct molecular organic chemical determination, the weight of the inorganic residue remaining after ignition of the organic material at 550 °C is used. Because the ash content of wheat grown in different soils of different geographical locations influenced the mineral content of the wheat kernel, the validity of flour ash value is diminished. In lieu of a direct measurement of endosperm purity, the latter brightness measurement provides an alternative that approximately reveals the purity of the flour samples (12). In some milling circles, the brightness measurement is touted as a better indicator of flour purity than ash. High performance liquid chromatographic data specific to ferulic acid was also used (13). The ferulic acid content of endosperm is negligible; therefore, a bran selective compound was available for spectroscopic calibration and implementation. The high performance liquid chromatographic ferulic acid based calibration was a technical success, but was not readily adaptable or accepted by the industry based upon unfamiliarity and the entropy of the phytochemical content.

A typical method of visualizing the contribution of each flour stream to the purity is the miller's curve (Fig. 1.5). Each flour stream is ordered by descending purity. The weighted

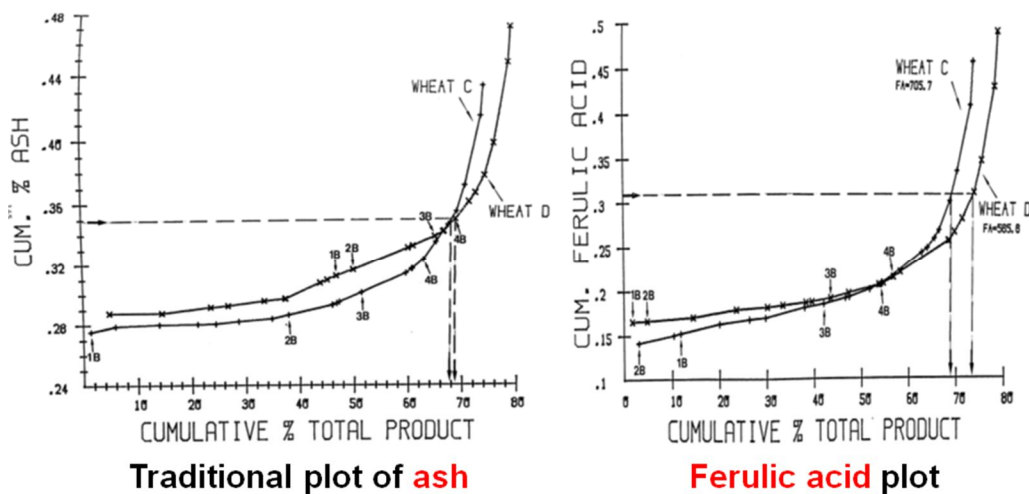


**Figure 1.5** Millers' plots of ash (left) and ferulic acid (right) indicating increasing contamination as additional streams are added. Note the ferulic acid plot indicates an earlier purity distinction between two wheat varieties because of the chemical specificity. [Reprinted from 14]

summation of impurity is then plotted vs. the cumulative amount of product when each additional flour stream is added. This process can be used to evaluate blends, determine when specifications are no longer met, and to enable targeted optimization. However, the current methodology lacks a true, objective measure of the amount of endosperm present in flour streams.

## **1.4 Spectroscopic Analysis**

### **1.4.1 Study of Biological Materials**

The infrared region of the electromagnetic spectrum has been widely used for the analysis of biological materials. Spectral bands are observed as the absorption of light, which is a function of a change in dipole moment for a particular molecule or chemical functional group. Typically, mid-IR spectral bands are caused by stretching or bending vibrations of molecules. The mid-infrared region ( $4000\text{-}400\text{ cm}^{-1}$  or  $2500\text{-}25,000\text{ nm}$ ) provides semi-quantitative information that is typically defined by peak heights, peak areas, and ratios thereof (15). Several key mid-IR bands have been identified in the past that correlate to the chemical structure distinct to the various botanical parts of the wheat kernel (16). This includes the major contributing botanical parts, endosperm and bran. Wheat endosperm has a characteristic, complex carbohydrate peak, a broad O-H stretching band, and muted amide bands. The outer pericarp is enriched in lipid content and features a detailed hemicellulose band and higher intensity protein absorptions.

The adjacent near infrared (NIR) region ( $12,800\text{-}4000\text{ cm}^{-1}$  or  $780\text{-}2500\text{ nm}$ ) consists of the overtone ( $n \times \text{frequency}$ ) and combination ( $\text{frequency X} + \text{frequency Y}$ ) bands of the fundamental mid-IR absorption phenomenon. These NIR peaks are broad and overlapping;

however, this relatively linear region of the electromagnetic spectrum better adheres to Beer's law (17). The Absorbance ( $A$ ) at a particular wavelength is defined by Beer's law as equal to the product of an absorptivity coefficient, the pathlength, and the concentration. Thus, when all other factors are held constant, the near infrared region is beneficial for quantitative determination of analyte concentrations.

Typically, near infrared analysis is performed with diffuse reflectance measurements. Diffuse reflectance is simply defined as the reflection of rays of light as they bounce through or among a particulate or granular sample (**Fig. 1.6**). After several absorption events, the intensity of the ray decreases, and eventually some light is collected by an instrument lens and guided to a detector.

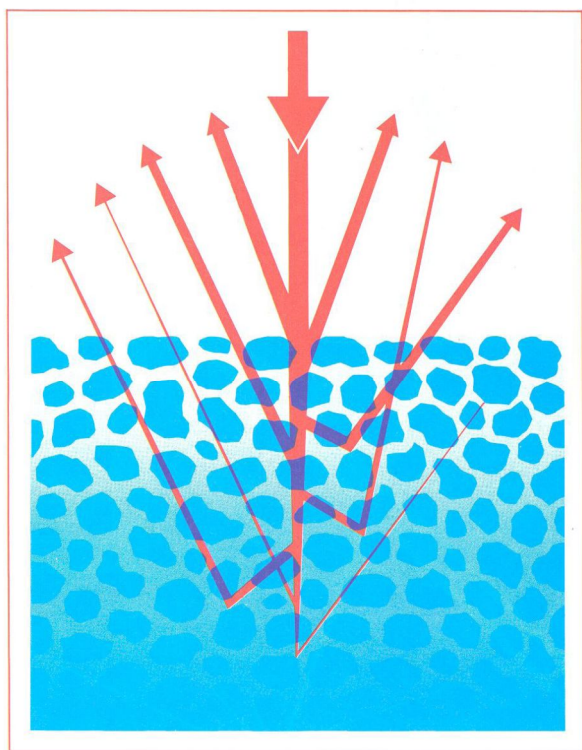


**Figure 1.6** Visual representation of diffuse reflectance pathways through a granular sample. [Reprinted from 7]

Near infrared analysis became routine for the field of agriculture where rapid analyses were needed to measure quality factors such as protein content, moisture, etc. (18). The first major application of near infrared analysis in the study of wheat was performed in 1976 (19). Prof. David Wetzel of Kansas State University used the technique to analyze the protein content of various farmers' wheat samples. The NIR method was calibrated vs. the classical Kjeldahl protein determination. By testing individual farmers' wheat crops before reaching an elevator location, high protein content necessary for bread quality wheat was identified and enabled segregation for different grist (blends). This method determined that wheat characteristics could be analyzed accurately and reliably. The technique was carried on to the breeding program where low-protein cultivars were removed from the gene pool and resulted in a 2.5% absolute increase in protein while maintaining other key desirable breeding characteristics.

Near infrared analysis of individual flour streams was introduced by Wetzel and Posner in 1987 (14). The near infrared online analysis of the milling operation utilized cellulosic content to approximate the impurity present in a particular flour millstream. These calibrations using cellulose wavelengths were calibrated against high performance liquid chromatography (HPLC) methods for ferulic acid. Future experiments used fluorescence imaging to determine the relative concentration of ferulic acid within the sample. The initial calibrations for wheat purity used various samples, such as weighted mixtures of pure and impure material, ferulic acid content, and different granulations. However, there were several instrumental inadequacies and the analytical focus was on determination of the contaminant rather than the actual analyte (purified endosperm).

### 1.4.2 Spectroscopic Chemical Imaging

The combination of spectroscopic techniques and microscopy have been attempted since the 1950's (20). The technique of spectroscopic imaging provides a wealth of data with the benefit of chemical information with the spatial distribution. Commercial distribution of viable microspectroscopic imaging systems with a point by point mapping procedure became available in the 1990's (21). The pioneering work of Neil Lewis and Ira Levin in 1994 (22), led to the development of array detection that allowed for simultaneous acquisition of greater than 80,000 pixels.

The commercial product resulting from that patent was the Spectral Dimensions Sapphire™ (Malvern Instruments, Columbia, MD) chemical imaging system. It was equipped with liquid crystal tunable filter (LCTF) programmable electronic wavelength switching and a thermoelectrically-cooled 320 x 256 Indium Antimonide (InSb) focal plane array (FPA) detector sensitive in the 1100-2400 nm range. The lens used to capture the radiation diffusely reflected off of the specimen on the stage provided a 12.8 x 10.2 mm field of view (FOV), resulting in a 40 μm pixel size (Fig. 1.7).

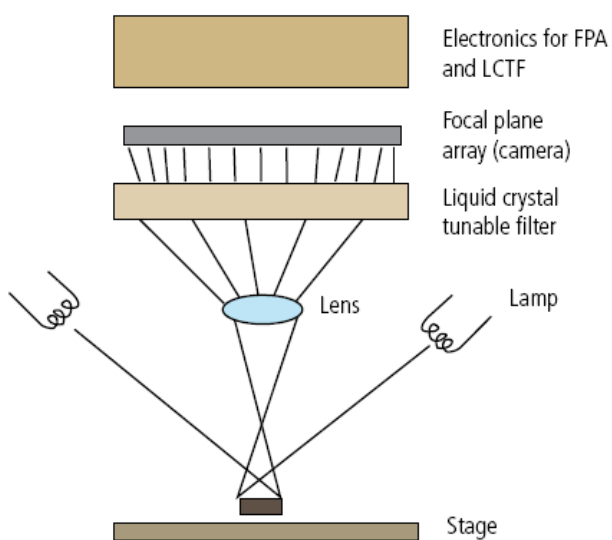


**Figure 1.7** Optical diagram of the NIR FPA imaging system. [Reprinted from 23]

Alternatively, 38.4 mm x 30.7 mm and 3.2 mm x 2.6 mm FOVs with 120  $\mu\text{m}$  and 10  $\mu\text{m}$  pixel sizes, respectively, were available from the manufacturer. A defocused highly polished stainless steel plate or similar material is used to set the dark current. The maximum reflection (or background current) is defined using a ceramic reflectance standard (available from a number of commercial vendors) in focus on the stage. These spectral standards are optimized by monitoring and maximizing the oscilloscope reading for image intensity and uniformity on the diagnostic screen. They are used to standardize the reflectance measurement for the particular instrumental settings. Microprocessor controlled stare time and electronic wavelength switching were used to acquire data.

Alternatively, linear (push broom) array instruments have been developed with a microprocessor controlled stage to enable large scale data acquisition. Commercial instruments are currently available from Middleton Spectral Vision (Middleton, WI) and Specim (Finland). These instruments feature a linear mercury cadmium telluride (MCT) detector array with 256 individual elements (**Fig. 1.8**). Each individual detector pixel for the array had a spatial resolution of 30  $\mu\text{m}$ , for a sum total x-dimension of 1 cm and the scanning for the y-dimension of the stage allows acquisition of a total FOV of approximately 15  $\text{cm}^2$ . The instrument requires a four stage thermoelectric cooling process to minimize thermal noise. The default spectral resolution for the instrument is 5 nm and covers a range of 1100-2500 nm for a total of 256 data points. The linear array instrument requires optimization of the stage scanning and camera settings to avoid distortion of the image.



**Middleton Spectral Vision  
SWIR Camera (MRC-303005-1)**

**Electronics for MCT linear  
array detector**

**Macro lens**

**Two pairs of 4 source lamps**

**Microprocessor controlled stage**

**Figure 1.8** Photograph of the Middleton Spectral Vision near infrared imaging spectrometer.

The spectroscopic data for both instruments are exported in the form of reflectance data. Conversion to Absorbance is necessary to develop linear relationships for concentration. Spectral truncation allows for the removal of non-analyte bands and those that shift, such as the water band at 1940 nm. These and other transformations can be accomplished with spectral imaging software such as ISys (Malvern Instruments, Columbia, MD). A common way to think of spectroscopic data is in an amalgam of chemical information and noise. Ideally the information would overrun the noise; however, sometimes chemometric analysis is needed to get the most out of the data (24). Chemometric techniques allow the user to remove noise, extract the most from the data, and use the information to produce quantitative results. However, one must exhibit caution and be assured that there is information within the data that relates to the sample properties or analyte.

One such chemometric technique is partial least squares (PLS). Developing a spectral library requires absorbance data corresponding to a range of concentration data. The formation of a data set enables calibration. A calibration set should use all mixture components, show mutual independence, span all conditions or chemical contrast, and cover the concentration range. Our simple binary measurements, the entire concentration range is covered, however, the concentrations in between are not. This is remedied by the similarly mixed chemical response for both the endosperm and non-endosperm standards. The major advantage of PLS as an analytical technique is that the concentrations of every chemical species present within the analytical matrix is not necessary for quantitative analysis.

Normalization and other spectral preprocessing techniques are often required to correct for external factors that could adversely affect quantitative analysis such as atmospheric changes and detector drift. Baseline subtraction helps account for atmospheric drift in the spectrum. The normalization procedure used for our method is defined as “mean center and scale to unit variance by spectrum”. For this procedure, the amplitude of each image spectrum is adjusted individually according to the mean spectrum to remove differences due to pathlength while preserving the band shapes to increase the effectiveness of the spectral classification (25). The exact details of this normalization technique are protected by the developer, Spectral Dimensions, Inc. (Olney, MD).

For our NIR quantitative chemical imaging technique, application of a novel PLS algorithm is necessary to distinguish between binary mixtures. The differentiation is derived from the multivariate characterization via spectral libraries of the components present in the solid binary mixture. ISys<sup>TM</sup> dedicated imaging software furnished by the manufacturer (Malvern

Instruments, Columbia, MD) was used to calculate the numerical analytical results. Post-run image contrast was produced with the benefit of histogram truncation of the PLS image.

### **1.4.3 NIR Chemical Imaging Background**

Vibrational spectroscopic chemical imaging enables noncontact quantitative analysis within the FOV in microscopic or macro dimensions. Near infrared chemical imaging has its roots in the pharmaceutical industry (26). For these examples, the sharp spectral bands for chemical substances enables easy distinction and imaging provides useful information on the distribution of active ingredients by highlighting them in false colors. Although identifying and assessing the census and distribution of active ingredients in a matrix of excipient for a pharmaceutical tablet is now commonplace from vibrational hyperspectral chemical imaging, application to solid mixtures in general is relatively uncommon.

The technology has found limited use in the commodity industry and has been used for food adulteration (27), process characterization (28), and for bacterial contamination (29). The first application of near infrared chemical imaging in our laboratory was to determine the ease to germination of wheat kernels (30). This method used a principal components analysis (PCA) to analyze key factors based upon spectroscopic responses that would highlight the regions of the kernel where evidence of active growth of the embryo was presented. Another classification technique was used to determine the class of wheat, waxy vs. non-waxy wheat (31). The waxy wheat was enriched in lipid content and several key wavelengths enabled effortless detection.

In analytical chemistry, physical isolation of the analyte is necessary as a part of its identification and determination; e.g., chromatographic separation precedes measurement by a detector with suitable sensitivity and selectivity. Chemical imaging takes a completely different

approach. In quantitative imaging, the spatially resolved pixels are spectroscopically identified as analyte. Our first application of near infrared quantitative chemical imaging provided a solution to determine the efficiency of mixing for solid commodity mixtures for the animal feed industry (28). Formulated feeds require proper mixing to assure uniformity before further processing such as extrusion cooking; however, in practice, a minimum residence time is preferable to avoid unmixing and additional processing costs. The use of near infrared chemical imaging enabled use of formulation components as a tracer. This was preceded by the use of traditional inorganic tracers that have aberrant mixing characteristics and are inedible. The feed ingredients studied included a high starch base (corn meal) and two high protein supplements (soybean meal and bloodmeal).

The large chemical differences between the starch, lipid, and protein concentration for the filler and protein supplements enable easy spectroscopic discrimination to quantitate the mixture composition. Chemical imaging was used in this application to show single wavelength spectroscopic contrast to distinguish between different formulated feed ingredients within a mixture. Subsequent applications studied binary mixtures to determine the efficiency of mixing as a function of screw conveyor mixing cycles. Mixing efficiency was determined by minimum standard deviation between samples taken from different parts of the mixer. These experiments were the basis for the development of the binary PLS algorithm.

#### **1.4.4 Spectroscopic Bands of Grains**

The fundamental vibrations in the mid-IR region have several distinct bands that have enabled contrast between each botanical part of wheat (16). Some of these differences remain in the near infrared overtones and combination bands (18). **Fig. 1.9** illustrates the large spectral

differences between the two purified major chemical components of wheat, starch and protein (gluten). However, the mean spectrum of wheat features overlap of many of these bands, and the signal for protein and cellulosic material is diminished in the mixture, hence the need for chemometrics. The raw spectra of bran vs. endosperm exhibit smaller spectral differences than the individual components, but these features are sufficient to make the distinction (**Fig. 1.10**).

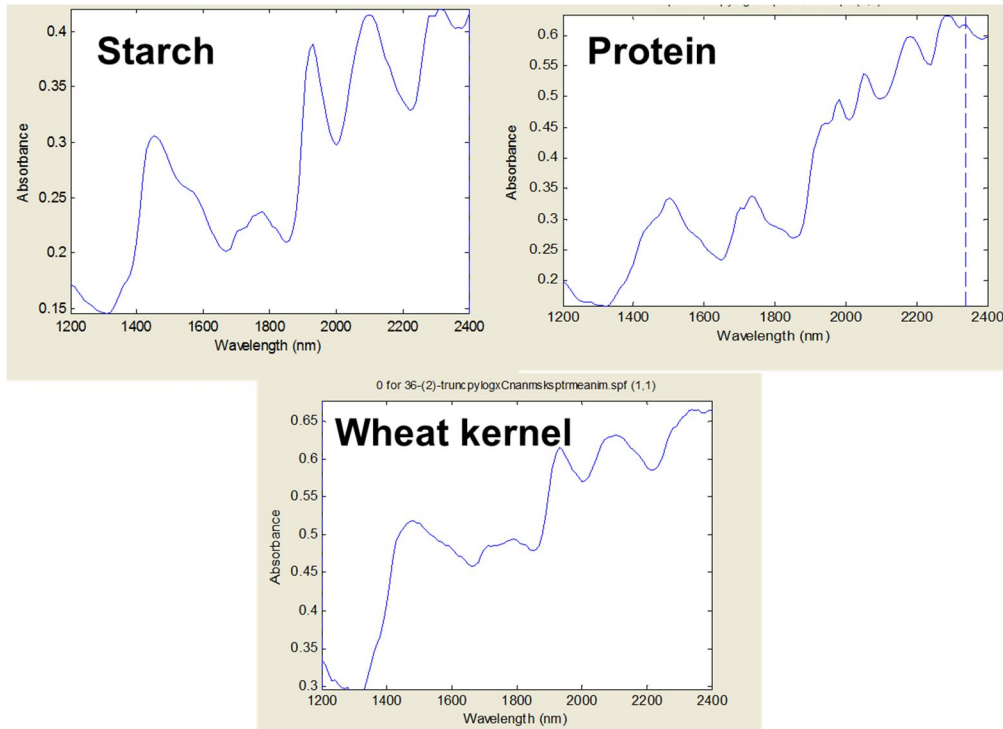


**Figure 1.9** Mean spectra obtained from wheat starch, wheat gluten, and an entire kernel. Note that the distinctive bands for starch and protein are subdued in the intact wheat kernel.

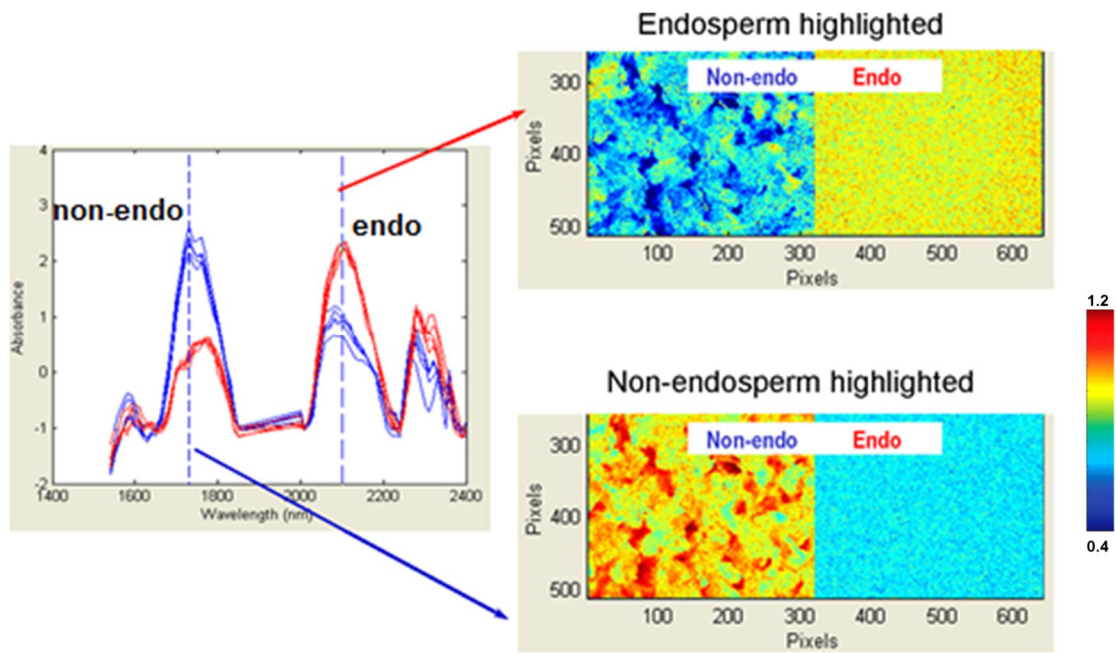


**Figure 1.10** Chemical images displaying endosperm purity in warm false colors arising from specifying near infrared bands selective for endosperm (top right) and non-endosperm (bottom right), respectively. Note the expanded color scale. [Reprinted from 23]

## 1.5 NIR Chemical Imaging of Wheat

### 1.5.1 Previous Experimentation

The complex chemical composition of wheat requires significant statistical calculations of spectral data to obtain reliable quantitation. The experimental averaging of thousands of spectra as spectroscopic standards for endosperm and non-endosperm defines the unique chemical

composition of that portion of the kernel. The variation between the ratio of starch to protein, among other components, fluctuates between different wheat varieties, individual kernels, and even specific regions of the kernel. Thus, the spectral libraries must be comprehensive and unique to the wheat blend (grist) being milled.

The first application of the chemical imaging technique to wheat milling featured samples from a Brazilian commercial mill (23). This experiment involved the optimization of unit process settings for a single purifier operation. The purpose of the purifier operation is to take

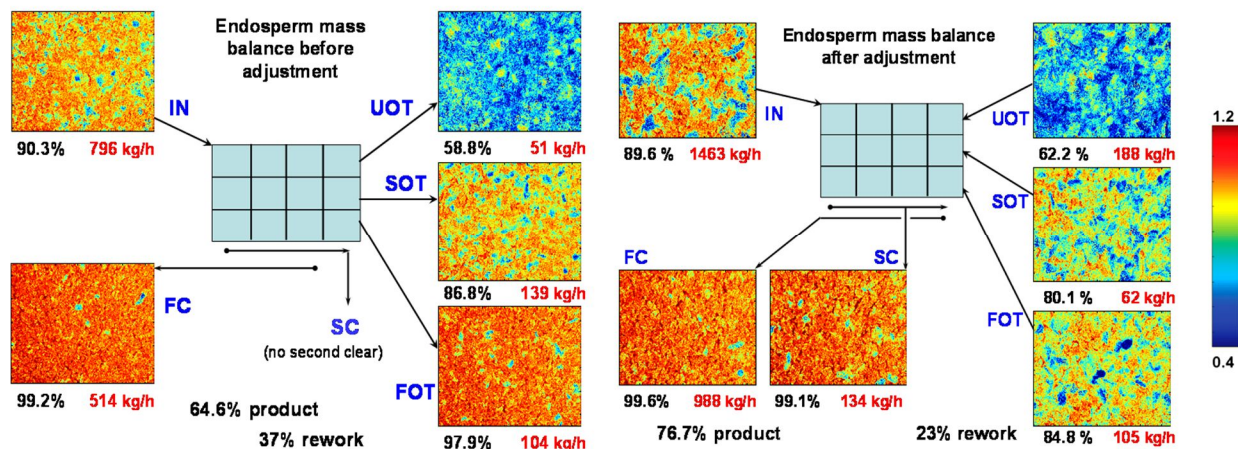


**Figure 1.11** False color images of purifier streams before (left) and after (right) adjustment. Note the calculated % endosperm and mass balance (red). After adjustment, the product yield (FC & SC) increased from 65% to 77% with a corresponding reduction in rework. Note the expanded color scale that indicates endosperm purity with warm false colors. [Reprinted from 23]

processing streams containing both endosperm and non-endosperm from the initial break system and selectively direct them to further processing steps (**Fig. 1.11**). For the initial experimentation, a modified false color scale was used.

A secondary milling experiment was designed to show a typical distribution of endosperm after a grinding and sieving operation for the first break and second break unit processes (23). This experiment took place in the Kansas State University Pilot Mill in Shellenberger Hall. The rudimentary NIR imaging procedure was customized in further experiments, but featured the unique development of an algorithm to average the results of separate PLS determinations for endosperm and non-endosperm. Subsequently, a significant laboratory scale experiment was conducted on laboratory scale mills in the Grain Science Department to study the effect of different combinations of roll gap openings for the first break

and second break grinding rolls in purity terms (32). Efficiency was defined as the fraction of endosperm that was released before the fourth break grinding operation.

The construction of a cumulative endosperm millers' curve was presented by acquiring the combined flour streams from the more recently constructed pilot scale Hal Ross Mill on the Kansas State University campus (33). The general purpose for a millers' curve is to find the combinations of flour streams that can be included in the blend for the production of a pure, high value patent flour from a mill. The review article primarily discussed prior methods for determining the purity (or lack thereof) for individual millstreams.

Chemical imaging has also been used to illustrate that the wheat kernel could be treated in a ternary manner. A quantitative method was developed to show distinction between the endosperm, bran, germ, and aleurone portions of the wheat kernel. These portions were chosen because they are readily separated or dissected in sufficient quantity. The four individual components were isolated and used to develop a spectral library. That enabled subsequent quantitation of each wheat kernel component present within synthetic mixtures produced from the pure substances.

### **1.5.2 Experimental Optimization**

The fundamental vibrational frequencies in the mid infrared are the basis of near infrared combination and overtone bands and the mid infrared spectra of distinct botanical parts of the wheat kernel have been well documented (18). However, the major molecular components also have many similar bands in the mid infrared spectrum. The major distinctions are the shape of O-H stretch vs. N-H stretch, the ratio of the Amide I band to those of other frequencies, and the

shape of the polysaccharide or cellulosic component. Also, quantitation of the mid infrared bands is difficult based upon the adherence to Beer's law.

The near infrared region of the electromagnetic spectrum is quite useful in spite of lower intensities and broad, overlapping bands because linearity is achieved in a useful region. The two major distinctions in the near infrared spectrum for endosperm vs. non-endosperm are revealed as the ratio of a pair bands appearing between 1650 nm and 1850 nm, and the shape of the starch band at 2100 nm is altered by the contribution from the two protein bands at 2060 nm and 2180 nm (Fig. 1.12). Almost every individual agglomerate produced from the milling of wheat

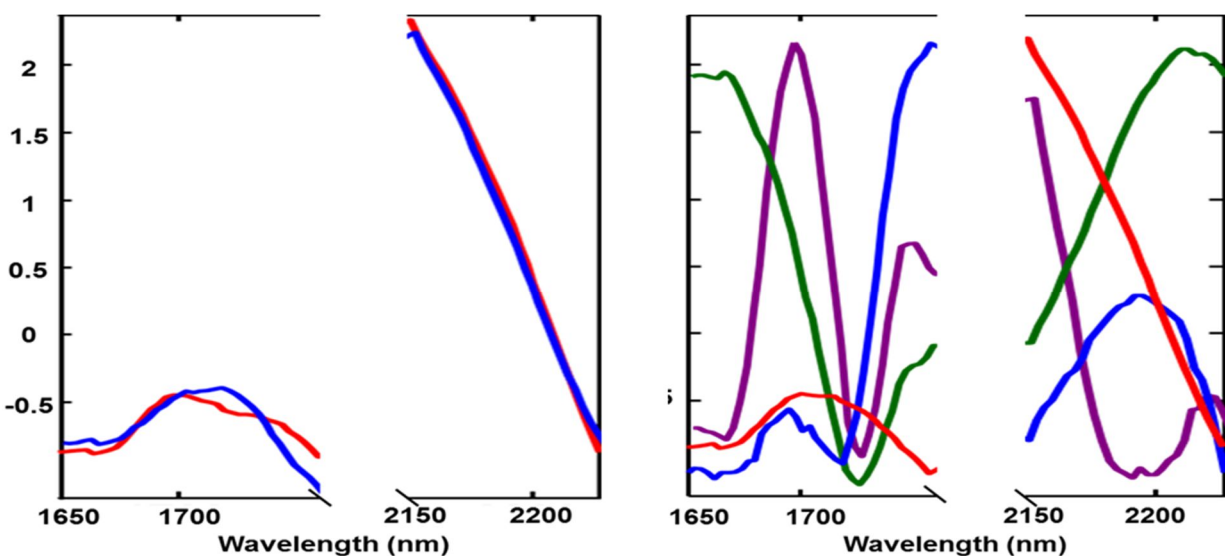


**Figure 1.12** (Left) Truncated spectra of endosperm (red) and non-endosperm (blue). (Right) Partial least squares factor loadings 1-4 (red, blue, green, and purple, respectively). Note that factor loading 1 resembles the library standard spectrum of endosperm.

contains a mixture of several different chemical components. Each class of wheat has a different range of the protein to starch ratio for endosperm and non-endosperm. PLS statistical analysis can produce quantitation of the mixture of chemical components or constituents. The first experiments leading to the quantitation of endosperm (23) utilized the data acquisition software default (1200-2400 nm at 10 nm increments). The water band at 1940 nm (1850-2000 nm) and

adjacent spectral valleys are truncated from the spectrum because the heat from the NIR source causes significant fluctuation as moisture content changes. The region from 1200-1540 nm was also removed because baseline correction of this region was difficult.

The partial least squares data treatment operates by developing factors for the interrelated matrices of concentration data and spectroscopic data in the form of scores and loadings (24). The spectral and concentration data are first expressed as matrices. The data is then projected upon calculated factors as vectors (**Fig.1.13**). The best fit linear vectors are then calculated (Fig. XXX) and models are developed to account for variance that occurs between the concentrations of analytes of interest and the absorbance (or scaled variant thereof). Numerous PLS factors are generated in the process to quantify the variance, however, a minimum number should be included to provide a robust calibration. Often, an extensive number of factors attributed only to noise within the spectrum are present depending on the number of mixture components.

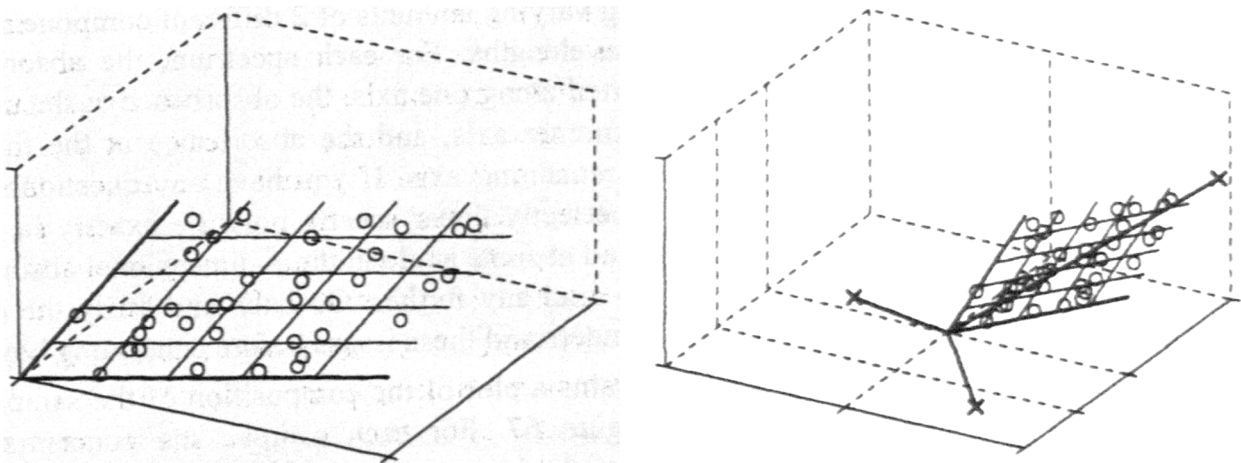


**Figure 1.13** Example of spectra in a linear space with varying amounts of two components (left). The spectra plotted against the calculated best fit regression coefficients upon which they are based. [Reprinted from 25]

A predicted residual sum of errors (PRESS) plot is used to determine when the number of factors has produced a robust calibration (24). For the analysis of a binary mixture, four factors

appears to be an ideal number. The individual factor loadings can be extracted to see if chemical information is still being included in the variance between analytes. Note from **Fig. 1.12**, that factors one through four exhibit significant sharp bands. Factors 1 and 2 bear strong statistical significance and match the spectral features of endosperm. Sharp bands corresponding to protein and starch are still present in Factors 3 and 4. The factor loadings are presented as an intensity index or multiplier at each wavelength of the spectrum. Multiplication of the coefficients to the spectral values provides the quantitative result according to the chosen data class.

The consistent goal since the original proof of principle has been to limit the spectral window. The next experimentation removed the bands of relatively low intensities found at shorter and longer wavelengths (32). These regions also had lower overall contributions in the PLS loadings. Variation in intensities among individual pixels was highest in these regions. The most recent milling experimentation has focused on a shorter wavelength range at 3 nm increments. These feature the carbohydrate band slope (2150-2230 nm) furthest from the water band which overlaps with the protein combination band at 2180 nm. The second spectral region used is from 1650-1788 nm where the changing band ratio occurs. In addition, a baseline point is present at 2230 nm.

## **1.6 Wheat Milling Sample Acquisition**

Specimens are routinely collected for analysis from various milling product or intermediate streams during operation of either commercial, pilot, or laboratory scale mills. For the purpose of the spectroscopic measurement for endosperm content, bran and the very purest endosperm stream isolated during the milling process are obtained for standards for non-endosperm and endosperm, respectively. Samples of processing streams are readily collected

during routine operation of a mill. Flour mills often have custom spouting that allows for direct sample collection. Alternatively, samples can also be grabbed from below the grinding rolls or from below the sifter. Sample collection is usually done concurrently with a stopwatch measurement to approximate the flow rate.

The samples are well mixed before imaging to reduce error. There are numerous options for sample presentation, but the sample must be flattened or compacted to reduce scattering and have a level plane for imaging. Typically, this includes a sample cup and a glass slide for mild compression. Spectra for each image pixel in the field of view are then collected simultaneously to enable quantitative summation.

### **1.7 Analytical Considerations for Quantitative Chemical Imaging**

Focal plane array near infrared imaging reveals the distribution and local relative prominence of a select analyte in a solid matrix (26). Quantitative analysis is achieved by statistical multivariate pattern recognition. Thus, the validity of results from employing quantitative chemical imaging is subject to analytical image precision among replicate fields of view. Pixel size compatibility with particle size is a matter of concern; an adequate FOV that both attains representative sample area, and produces a practical pixel size is preferred. Using fresh replicate FOVs vs. replicate images from the same sample eliminates the variable of change over time. Replicate specimens of the same lot are essential for coarse granular heterogeneous solid mixtures, whereas in contrast, a single finely ground homogeneous endosperm specimen may, in fact, be representative.

For near-infrared quantitative imaging, luck of the draw determines if the FOV subjected to analysis is, in fact, representative of the bulk for heterogeneous mixtures. Averaging fields of

view depends on the nature of the particulate material involved and the heterogeneity of the mixture. The size and shape of the specimen particles also has an influence. Vibrational spectroscopic (chemical) imaging has proven useful and practical, but it is not necessarily part of the classical chemical instrumental analysis toolbox; consequently, questioning its analytical validity is appropriate.

The analytical validity of quantitative analysis of solid binary mixtures is dependent on the photometric precision of a single FOV as well as the precision among multiple FOVs taken from the same solid mixture lot. In either case, producing distinct, reproducible image contrast is an important issue. With the use of a biological sample of an intermediately sized wheat milling processing stream (approximately 750  $\mu\text{m}$ ), the precision among seven replicate FOV's taken after vigorous mixing from the same lot had a respectable relative standard deviation of 1.9%. The coarsest streams ( $> 1000\mu\text{m}$ ) had a relative standard deviation of approximately 3%. The relative standard deviation for fine flour streams were shown to average approximately 0.8%

Afterwards, the effect of replicate sequential spectra for staring over time was observed. These were collected at periods of four minutes with continuous staring at the same FOV for a total of 28 minutes. While spectra were obtained, some heat from the four illuminating lamps was dissipated by a continuously operated fan. For a series of seven successive images from staring at the same FOV, the apparent percentage endosperm decreased from an initial value of 85.4% to a final reading of 80.0%. This resulted in a mean endosperm concentration of 82.3% with a relative standard deviation of 4.0%. **Fig. 1.14** shows the decrease in the percent endosperm over time. This shows that there are definitely some concerns in reusing the same sample of leaving the sample on the stage too long.

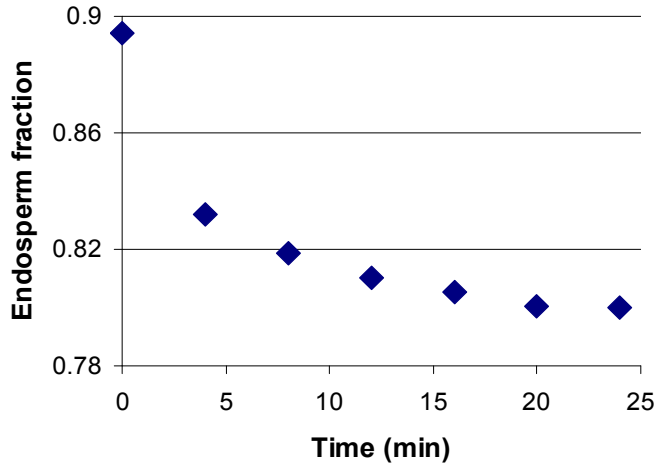


**Figure 1.14** Endosperm quantitative result of same mixture over starting time.

**Fig. 1.15** shows the result of imaging a handmade mixture of small particles of flour and large flakes of bran. Large bran flakes covering the small particles could obscure or completely substitute the chemistry of the smaller particles. Note the emergence of pixels containing

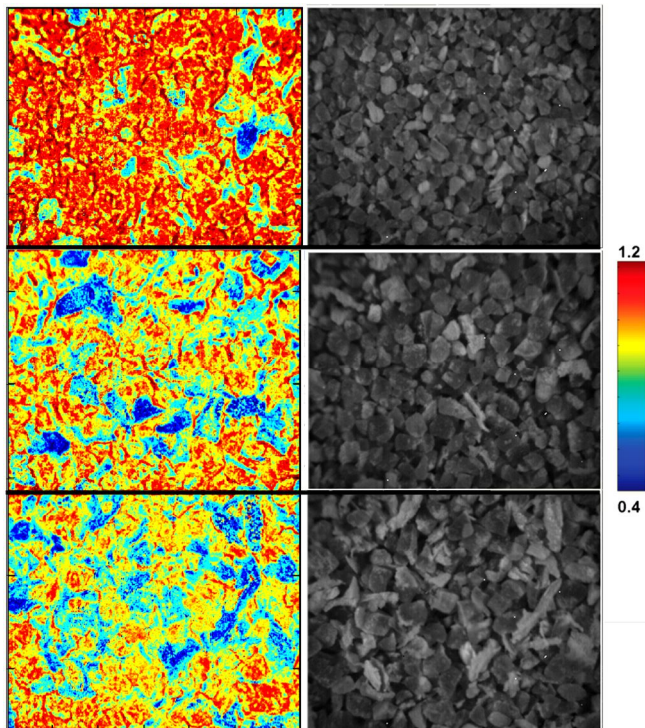


**Figure 1.15** Chemical images (left) and photomicrographs (right) showing mixtures of wheat bran flakes and a granular wheat endosperm mixture. . Note the expanded color scale that indicates endosperm purity with warm false colors. Images were taken from well-mixed (top), agitated (middle), and additionally agitated (bottom) mixtures.

non-endosperm after lightly shaking the sample container between measurements. With near-infrared spectroscopic imaging, the greater depth of penetration of diffuse reflection partially compensated for the surface coverage; however, if the large flakes are completely covered with fine, highly scattering particles, then the chemistry of the small particles will largely substitute for that of the flakes. The only solution to this dilemma is to acquire replicates for each sample and develop a consistent mixing/sampling procedure.

## 1.8 Abbreviations

Bk – Break

CWT – Hundredweight

NIR – Near infrared

HPLC – High performance liquid chromatography

InSb – Indium Antimonide

FPA – Focal plane array

FOV – Field of view

MCT – Mercury-cadmium-telluride

PLS – Partial least squares

PCA – Principle components analysis

PRESS – Predicted residual sum of errors

## 1.9 References

1. Shewry, P.R., Hawkesford, M.J., Piironen, V., Lampi, A.M., Gebruers, K., Boros, D., & Ward, J.L. (2013). Natural variation in grain composition of wheat and related cereals. *Journal of agricultural and food chemistry*, 61(35), 8295-8303.
2. Hosney, R.C. (Ed.). (1998). Structure of cereals. In: *Principles of Cereal Science and Technology*. American Association of Cereal Chemists Inc: Minnesota.

3. Posner, E.S.; Hibbs, A.N. (Eds.). (1997). *Wheat Flour Milling*. American Association of Cereal Chemists Inc: Minnesota.
4. MacMasters M.M.; Hinton, J.J.C.; Bradbury, D. (1971). Microscopic structure and composition of the wheat kernel. In: *Wheat Chemistry and Technology*; Pomeranz, Y. (Ed.). American Association of Cereal Chemists Inc: Minnesota. Vol.7, pp. 511-14.
5. Sandstedt, R.M., Schaumburg, L., and Fleming, J. (1954). The microscopic structure of bread and dough. *Cereal Chem.* 31, 43-49.
6. Bradbury, D., Cull, I. M., & MacMasters, M. M. (1956). Structure of the mature wheat kernel. I. Gross anatomy and relationships of parts. *Cereal chemistry*, 33(6), 329-342.
7. Gwartz, J.A., personal communication, July 2012.
8. Posner, E.S., personal communication, August 2017.
9. Atwell, W. (2016). *Wheat flour*. Elsevier, Amsterdam.
10. Wheat Intake/Mill Performance/Quality Control. Module 11. (1989). In: *Workbook Series; The Incorporated National Association of British and Irish Millers Limited*. London, England.
11. North American Grain & Milling Annual. (2016). Sosland Publishing, Kansas City, MO.
12. Shuey, W. C. (1975). Flour color as a measurement of flour quality. *Bakers digest*. October, 18-26.
13. Pussayanawin, V., Wetzel, D. L., & Fulcher, R. G. (1988). Fluorescence detection and measurement of ferulic acid in wheat milling fractions by microscopy and HPLC. *Journal of Agricultural and Food Chemistry*, 36(3), 515-520.
14. Posner, E. S., & Wetzel, D. L. (1986). Control of flour mills by NIR on-line monitoring. *Association of Operative Millers Bulletin*, 4711-4720.
15. Robinson, J.W; Frame, A.M.S.; Frame II, G.M. (2005). Infrared Spectroscopy. In: *Undergraduate Instrumental Analysis*. Marcel Decker. New York; 213-310.
16. Wetzel, D.L. Microbeam molecular spectroscopy of biological materials. (1995). In: *Food Flavors: Generation, Analysis and Process Influence*; Charalambous, G., (Ed.). Elsevier Press; pp. 2039-2108.
17. Wetzel, D.L. (1983). Near-infrared reflectance analysis: Sleeper among spectroscopic techniques, *Anal. Chem.* 55, 1165A-1176A.
18. Wetzel, D.L. (1998), Analytical Near IR Spectroscopy. In: *Instrumental Methods in food and Beverage Analysis*; Wetzel, D.L.B. and Charalambous, G. (Eds.). Elsevier Science, B.V.
19. Wetzel, D. L. (1976). Kansas wheat harvest on site protein preview. *Report of the Department of Grain Science and Industry, Kansas State University at Manhattan*.
20. Kwiatkowski, J.M. and Reffner, J.A. (1987). FTIR microspectrometry advances. *Nature*. 328(27):837-838.
21. Sting, D. W., Messerschmidt, R. G., & Reffner, J. A. (1991). *U.S. Patent No. 5,019,715*. Washington, DC: U.S. Patent and Trademark Office.
22. Lewis, E.N., Levin, I.W. and Treado, P.J. (1996). *U.S. Patent No. 5, 528, 368*.
23. Wetzel, D. L., Posner, E. S. and Dogan, H. 2010. Indium antimonide (InSb) focal plane array chemical imaging enables assessment of unit process efficiency for milling operation. *Appl. Spectrosc.* 64(12):1320-1324.
24. Kramer, R. (1998). *Chemometric techniques for quantitative analysis*. CRC Press, Boca Raton, FL.
25. ISys™ 4.0 User's Manual. (2005). Malvern Instruments, Olney, MD.
26. Lewis, E.N., Carroll, J.E., and Clark F. (2001). A Near-Infrared View of Pharmaceutical Formulation Analysis, *NIR News*. 12, 16-18.
27. Manley, M. (2014). Near-infrared spectroscopy and hyperspectral imaging: non-destructive analysis of biological materials. *Chemical Society Reviews*, 43(24), 8200-8214.
28. Wetzel, D.L., Brewer, L.R., and Boatwright, M.D. (2010). Granular solid formulation commodity mixture uniformity revealed via InSb focal plane array chemical imaging, *Vib. Spectrosc.* 53(1):83-87.
29. Dubois, J., Lewis, E.N., Fry Jr., F.S., and Calvey, E.M. (2005). Bacterial identification by near infrared chemical imaging of food specific cards. *Food Microbiology*. 22:577-583.

30. Koc, H., Smail, V.W., Wetzel, D.L. (2008) Reliability of InGaAs Focal Plane Array Imaging of Wheat Germination at Early Stages, *J. Cereal Sci.* 48, 394-400.
31. Dogan, H., Smail, V. W., & Wetzel, D. L. (2008). Discrimination of isogenic wheat by InSb focal plane array chemical imaging. *Vibrational Spectroscopy*, 48(2), 189-195.
32. Boatwright, M. D., Gwartz, J. A., Posner, E. S., & Wetzel, D. L. (2013). A quantitative near infrared imaging study of 1, 2, 3 break system endosperm yield from variation of 1BK/2BK roll gap combinations. *Int. Miller.* 3, 35.
33. Wetzel, D. L. (2013). Positive assessment of mill stream endosperm purity using chemical imaging. *Cereal Foods World.* 58(3), 133-137.

## **Chapter 2 - Endosperm Purity Profiling: Commercial Mill Streams Preceded by Debranning via Application of Quantitative Chemical Imaging**

### **2.1 Abstract**

The following chapter was slightly modified from its original publication as: Boatwright, M. D., Posner, E. S., Lopes, R., & Wetzel, D. L. (2015). Profiling endosperm purity of commercial mill streams preceded by debranning using quantitative chemical imaging. *Cereal Foods World*, 60(5), 211-216 (<https://doi.org/10.1094/CFW-60-5-0211>). Vibrational spectroscopic data obtained simultaneously in a rectangular detector array enables analysis of a heterogeneous mixture of solids that constitute wheat flour by the pixel. The analyses of 81,920 near infrared spectra following followed by partial least squares data treatment enables determination of the endosperm purity vs. non-endosperm content for each individual pixel. Heterogeneity is revealed by the resulting image and a mathematical weighted summation provides the composite composition for the field of view. The advantages of the solid state technology employed in this modern method include high sensitivity of individual Indium Antimonide detector elements and programmed electronic wavelength switching of the liquid crystal tunable filter operating with no moving parts. The organic chemical content of endosperm (primarily starch and protein) is compared to non-endosperm (cell walls, aleurone, pericarp, etc.) by the vibrational spectroscopic response of different molecules within the solid mixture. This objective quantitative chemical imaging method is applied to determine the endosperm purity profile for 29 flour streams of a commercial flour mill in which the break system is preceded by a debranning operation. A cumulative flour endosperm purity plot reveals distinct changes in purity as successively less pure streams are incorporated to increase the yield. The sensitivity and

chemical structural basis of the endosperm purity method described should be useful to assess the effect on the efficiency of new equipment installation or significant changes of operational settings on a commercial milling process.

## **2.2 Introduction**

Abrasive debranning has been the norm for covered grains resulting in traditional “polished” white rice (1). At present, in common wheat milling, preceding the break system with debranning equipment is definitely not yet commonplace. The increased energy cost and the capital cost of the hardware are issues that require economic justification based on the overall mill efficiency and product purity considerations. However, a significant capacity increase for existing mill equipment, with appropriate changes in the flow sheet, results in a reduction in energy cost (kWh/ton of wheat) for pre-debranning usage. Hard wheat milling is one area where adaptation of the debranning prior to milling has become an option that reportedly results in a practical pay back (2). The ideal debranning operation in hard wheat milling would evenly remove the outer layers of the pericarp without losing any endosperm or breaking kernels. Potential benefits include the removal of harmful elements from the kernel surface, flour streams with higher “brightness”, and increased flour extraction and mill capacity (3). Debranning operations also allow optimization to provide a high quantity of aleurone product. Removal of these outer layers can also help reduce the alpha-amylase activity, particularly for wheat that has been subject to sprout damage.

Direct endosperm purity assessment of individual mill streams by the chemical imaging technique was previously introduced (4-6). Those studies were restricted to individual unit processes such as an individual purifier, laboratory table top milling study of the break system,

or ranking flour stream purity of an experimental pilot mill. Laboratory sieving of post-break fractions were also reported (7). In this paper, we report the endosperm purity profile of 29 streams of a commercial flour mill running at a capacity of 204 hundredweight (CWT) per 24 hours in which the break system is preceded by abrasive debranners (3). Our investigation team includes the head operative miller on site. He shouldered the responsibility for each operational parameter setting and supervised the stopwatch timed collection for each of the product streams for weighing and various quality analyses. The specimens produced on site in Brazil during a routine commercial production process were sent by air courier to the Kansas State University Microbeam Molecular Spectroscopy laboratory where the endosperm purity was determined via quantitative chemical imaging with a research model imaging spectrometer (8).

We believe that this is the first reported wheat flour endosperm purity profile of a common wheat commercial milling operation where a debranning process precedes the break system. The objective is to use the best possible chemical definition of wheat endosperm purity to produce this profile. Traditionally, the miller is concerned with the “brightness” of the flour (9, 10) or a low ash value as being a good attribute. However, the “brightness” involves only the part of the electromagnetic spectrum that the human eye can see, whereas the chemical endosperm purity profiling is selective for the endosperm in the presence of non-endosperm, and thus a binary chemical mixture is assessed for purity with respect to endosperm vs. non-endosperm.

In the case reported here, the endosperm purity is directly assessed for 29 individual product mill streams of a commercial wheat mill in which an abrasive debranning operation is a pretreatment. Our purpose is to objectively measure, calculate, and present the numerical endosperm purity multiplied by the yield of the purest stream first and subsequently add the

cumulative contribution of each subsequent, slightly less pure mill stream. As each successive stream is added, the overall yield increases, and a slight degradation in the composite endosperm purity occurs. The resulting endosperm profile enables the operative miller to determine the point at which a cutoff is required to maintain the purity specifications required by the flour customer (10). The chemical composition of the endosperm and non-endosperm is determined from quantitative chemical imaging by the individual pixel. Each image pixel results from an individual near infrared spectrum representing the chemical composition of that pixel (8, 11).

This method represents a totally objective measurement where 81,920 spectra from the field of view produce chemically defined individual analyses. These analyses are tabulated to produce the objective flour stream endosperm purity on a chemical structural basis. The subjective visual appearance of “brightness” of the flour from any given stream or mixture operates from a bulk reflection response rather than from that of individual pixels. Our purpose in this study has been to apply the objective chemically defined pixel counting method of assessing endosperm purity and expecting the “brightness” from bulk color measurement to represent an essentially parallel assessment of purity. The endosperm chemically defined purity is primarily composed of starch and protein (12). The presence of non-endosperm in a field of view is indicative of the incomplete separation of the wheat kernel endosperm from the bran. Ash determination (13), however, merely measures the inorganic (mineral) residue remaining after ignition. Application of the more precise partial least squares (PLS) data treatment to chemically defined endosperm purity is addressed in the imaging subheading under Experimental. The intent is to maximize the yield of flour that meets purity specifications.

## 2.3. Experimental

### 2.3.1. Commercial Wheat Mill

A commercial mill operated in Brazil having a capacity of 204 CWT/24 hours and operating on three shifts (**Fig. 2.1**) was the source of all flour streams used in this experiment.

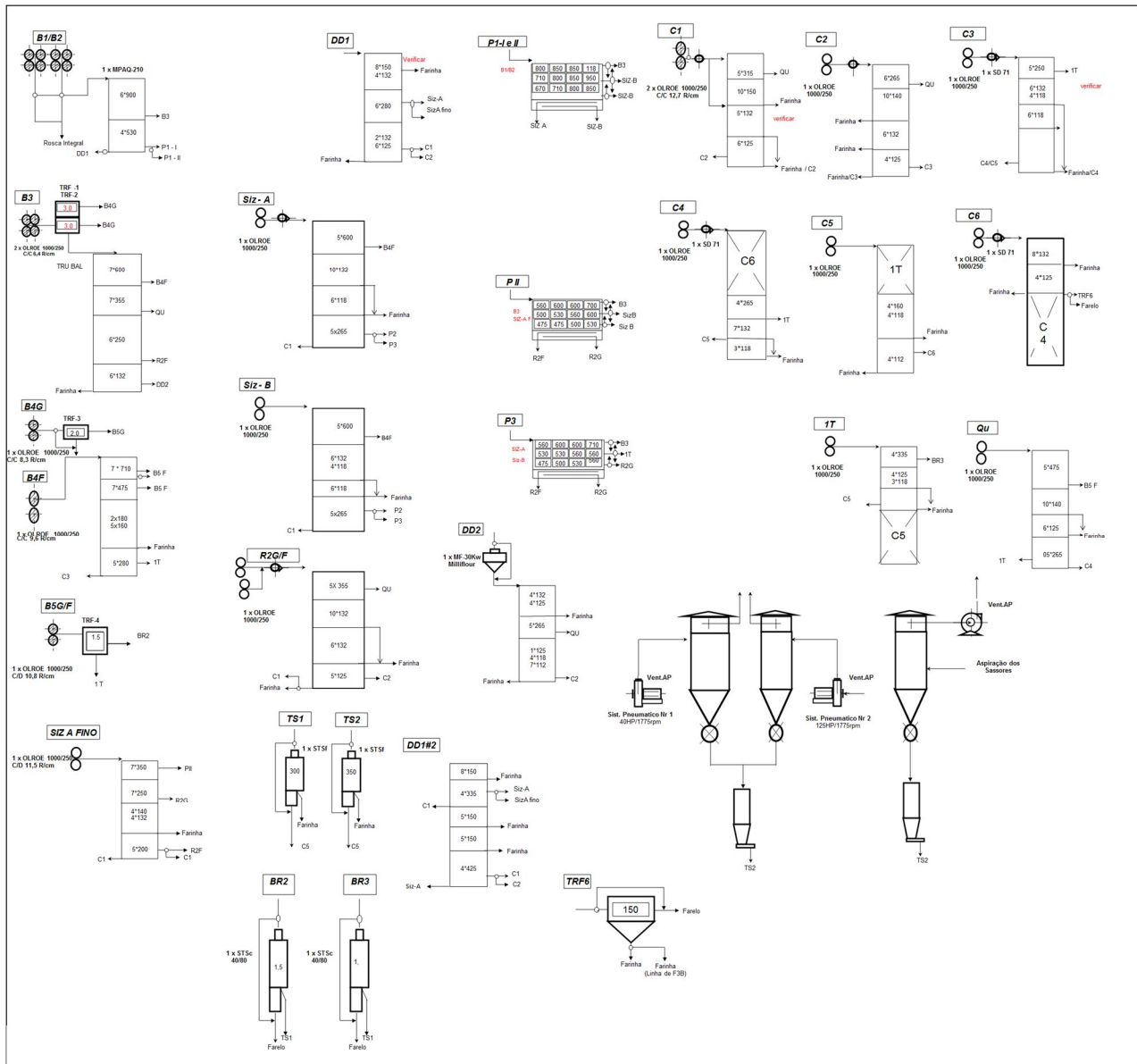


**Figure 2.1** Flow sheet of the 204 CWT/24 hour commercial flour mill equipped with abrasive debranning technology.

The grist for this experiment was from two Brazilian wheat varieties described as Quartzo (70%) and Supera (30%). Both varieties are grown in Brazil on a regular basis and therefore the raw

material used is typical for the flour produced for relatively local consumption. The abrasive debranning equipment was a Satake VTA Abrasion Debranner, model 10AB-L (Hiroshima, Japan). The two units that were installed prior to the double high first/second break rolls have been in operation for approximately 18 months and adjusted to maximize efficiency since that time. A vertically mounted set of stones produces the abrasive action required to remove the bran. A business consideration was responsible for introduction of this step prior to the break system with the object of producing a brighter product at an improved extraction rate. The “brightness” of the final flour is appealing to the customer and obviously constitutes high purity with respect to the bran. Under typical operating conditions, 4%-6% of the total kernel weight is removed from the incoming wheat. The abrasion is applied directly to the cheeks of each wheat kernel that represents approximately 80 percent of the total bran content of the individual kernel. Essentially, abrasive debranning results in removal of all the outer pericarp, the inner pericarp, and to a reasonable extent most of the testa of the exposed portion of the wheat kernel (14).

After the debranning operation, the mill featured only four break (B) operations. This was because less scraping action was required due to most of the bran being removed by the debranning operation. Three divisor (DD) sifters were included to handle the large amount of break stock fines and distribute them to flour, sizings (Siz), and the reduction process (C). The break system also sent a lot of material to the first purifier (P) for sorting by density. The first sifter was responsible for organizing material for the sizings operation. The remainder of the purifiers were responsible for sending material to B3 and R2G/F (break redust), relaying material to and from sizings, and tailings (1T).

The two sizings operations were responsible for preferentially reducing endosperm and flattening any contaminated particles (2). The goal was to produce some additional flour, and

redistribute material to the secondary break system, purifiers, and reduction system. The Mills reduction system consisted of six operations. Each of these processes produces a fair quantity of flour, sends coarse material to the 1T and quality (Qu) reclamation steps, and distributes the intermediate material to the next reduction step. The mill also included two TS (vibrosifters) operations that produced flour and C5 stock. There were also three bran dusters (BR) that produced bran and flour streams. Similar to other milling operations, a high volume of clean stock was also ground into flour by the reduction system.

### **2.3.2. Specimens**

Specimens were collected from each product stream during operation of the mill on a regular production shift. The break release was set to 40% on first break and 70% on second break for the double high break roll. The time of collection was monitored with a stopwatch so that the contents of each sample container would represent the quantity for a specific time interval and could be weighed to reflect the flow rate at that particular position; in parallel with the corresponding purity determination. Twenty-nine streams were sampled this way to produce specimens for subsequent endosperm purity assessment in the analytical research lab at Kansas State University. In addition to collection of flour from each individual product stream and replicates retained for local measurement of color and ash, spectroscopic standards were obtained. Bran specimens obtained from the debranning process and the very purest endosperm from the 1st middlings reduction operation were used as standards to enable calibrating the quantitative imaging method with respect to the raw material, and contrasted to the waste material removed by the debranner and the purest endosperm product from this new mill operation. Addition of the debranning capability has increased production of the mill by 13%.

This analytical experiment represents the first opportunity to use objective chemically defined endosperm purity assessment applied to common wheat milling with a debranner.

### **2.3.3. Instrumentation**

A Sapphire model near infrared imaging system (Malvern Instruments Ltd., Westborough, MA) that provides 81,920 near infrared spectra per field of view was used to acquire spectral data cubes for each flour sample. Data for each sample was collected in triplicate. The operation of this instrument with respect to individual intermediate and flour streams of wheat milling has been described previously (4, 5). The near infrared imaging spectrometer equipped with four quartz tungsten halogen source lamps employs a rectangular thermoelectrically cooled array of Indium Antimonide detector elements (8). A liquid crystal tunable filter provides electronic wavelength switching that enables simultaneous spectral acquisition at each x, y location in the detector array with no moving parts. The associated software controls the optical data acquisition after establishing the maximum reflectance when focusing on the surface of a ceramic standard and obtaining the dark current value with no object at the focal point of the quartz objective. Before spectral acquisition, the granular sample material is placed in a metal planchette and covered with a 1-in. × 1.5-in. glass microscope slide. Within the 1200-2400 nm available wavelength range, select segments were scanned. A scanning step size of 3 nm was used to limit acquisition stare time while providing adequate spectral resolution to discriminate pure endosperm from non-endosperm.

For “brightness” measurements, a Konica Minolta (Ramsay, NJ) reflectance Chroma Meter (CR-410) equipped with a pulsed xenon flash lamp, optical fiber conductor, and diffusing elements illuminates the circular target (50 mm) area. Reflected radiation 90 degrees from the

specimen surface is transmitted to six silicon photodiode detectors. The repeatability standard deviation specification was 0.07 absorbance units. The 1931 CIE defined color space (15) response of three wavelength spectral features for colorimetry were closely matched. Whereas all flour streams have a similar “brightness”, because in the highly white specimens where the optical response slope is small, discrimination between similar flour streams is a photometric challenge. Visible color ( $L^*$  value) was measured on site with the Chroma Meter to obtain a numerical index of “brightness” that the consumer expects. A more sophisticated reflection spectrometer potentially applied to color measurement that is marketed by the same manufacturer and other vendors provides a 10 nm bandpass with a xenon flash lamp source, a fixed spectrograph, and a 60 element silicon photodiode array. Nevertheless, the visible absorption bands of the wheat bran are broad in nature.

Broad band electronic spectra phenomena and vibrational spectra are contrasted in the following consideration. The fundamental distinction is that broad band color results from excitation of electrons. In contrast, the vibrational motion of chemically bonded atoms reveals molecular structural features (16). From first principles, the vibrational features provide chemical discrimination. It is fortuitous that the rate of change in the  $\log(1/\text{Reflectance})$  that accompanies the change in chemical composition is readily measured by the pixel. Chemical heterogeneity is revealed from the image and allows mathematical summation of values within the field of view. The slope of the cumulative endosperm purity curve and the endosperm contribution of each flour stream allows computation of the net purity achieved by selective exclusion of one or more inferior flour streams.

#### **2.3.4. Quantitative Near Infrared Imaging Procedure**

The chemical structural difference between endosperm and non-endosperm was used to sort and identify the pixels of each image spectroscopically. For each pixel, a near infrared spectrum was produced in 3 nm steps from 1650-1788 and 2150-2228 nm. If a simple binary designation of 1 for endosperm and 0 for less than 0.5 endosperm were designated, the arithmetic would amount to simply counting the pixels of endosperm and dividing by the total number of pixels. The area targeted for analysis was 12.81 mm x 10.24 mm and results in a pixel size of 40  $\mu\text{m}$ . The raw image intensity of each image pixel is first converted to Absorbance, which describes optical density. The spectra are then baseline corrected and normalized.

We routinely use a partial least squares data treatment (17) so that the binary designation is replaced by giving an intermediate value to each of the 81,920 pixels in the field of view interrogated. In our previous experimentation, careful establishment of the purity (endosperm) standard was selectively acquired for that purpose, and the impurity (non-endosperm) was spectroscopically defined by clean bran. PLS classification according to spectral libraries (more than 240,000 spectra for each component) defining endosperm and non-endosperm is then applied to determine a pure endosperm multivariate identity reflected in the z-axis value for each pixel. The intensity limits from 1 to 0 for endosperm and non-endosperm correspond to warm and cool colors assigned, respectively to the maximum and minimum of the scale. Skill and experience is required to critically subjectively examine the data and select the appropriate threshold value below which data are excluded. Whereas care is taken in establishing the maximum purity standard and in contrast the impurity of the bran, standardized data handling makes the subsequent routine calculations objective. It is possible with PLS data treatment to

assign a specific endosperm percentage to each pixel and obtain the resulting summation. The relative standard deviation for fine flour streams were shown to average approximately 0.8%

## 2.4 Results and Discussion

**Table 1** ranks the individual flour streams in descending order of endosperm purity with their respective flow and extraction rates listed. Multiplication of a particular endosperm purity

**Table 2.1 Flour stream rank by endosperm purity**

Stream	Rank	% Endo	(kg/h)	Ext'n
DD1 1	1	99.4	309.0	3.9
DD1#2 2/3	2	96.3	261.0	3.3
DD1 2	3	95.8	82.5	1.0
SIZA 1	4	95.3	452.4	5.7
SIZB 1	5	94.9	150.0	1.9
DD1#2 1	6	94.8	232.0	2.9
B3	7	94.4	315.0	4.0
R21	8	94.4	351.0	4.4
SIZA 2	9	94.1	2.4	0.0
C1 1	10	94.0	1112.4	14.0
C2 2/3	11	93.8	21.0	0.3
SIZAF 1	12	93.2	366.0	4.6
C1 2	13	93.1	17.6	0.2
TS2	14	92.6	54.0	0.7
SIZB 2	15	92.4	41.0	0.5
C1 3	16	92.3	8.1	0.1
B4	17	91.8	416.4	5.2
C2 1	18	91.8	370.2	4.6
DD2-1	19	91.6	337.5	4.2
C3 1	20	91.0	249.0	3.1
TRF06	21	91.0	27.0	0.3
TS1	22	90.5	117.0	1.5
C5	23	89.5	135.0	1.7
C4	24	89.2	81.0	1.0

1T	25	88.7	132.0	1.7
QU	26	87.7	113.0	1.4
C3 2/3	27	85.9	160.5	2.0
C6	28	81.9	82.5	1.0
DD2 2/3	29	81.2	16.1	0.2

by the corresponding flow rate produces the individual flour stream contribution of pure endosperm. The weighted combination of successive streams produces an endosperm purity profile in terms of descending purity and increasing yield. The cumulative endosperm purity is shown in **Fig. 2.2**, based upon selective near infrared wavelength absorption data dependent on the chemical structural differences between the endosperm (analyte) and the non-endosperm present in the flour matrix. The rate of change in the optical response is a function of the

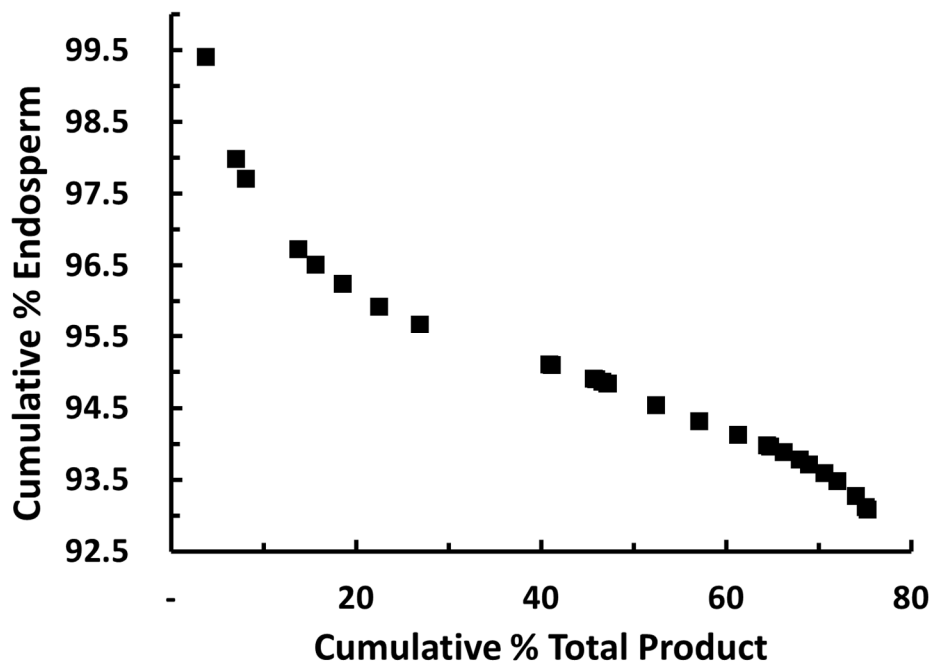


**Figure 2.2** Cumulative percent endosperm calculated from endosperm purity multiplied by flow rate. As each successively inferior stream is added, value for the combination is recalculated.

increased cumulative flour yield as inferior flour streams are added to the product composition.

In contrast, the range of the broad band color measurement is severely limited (**Fig. 2.3**); however, in general, the response is parallel to the negative slope of the objective chemical values shown in **Fig. 2.2**. The permutation of the broad band numerical value differs somewhat from the purity rank that is objective and based on chemical structural contrast. This apparent aberration was anticipated because of the broad band width of 50 nm at the half height of the absorption band produced by the visible color filter with an appropriate wavelength maximum.

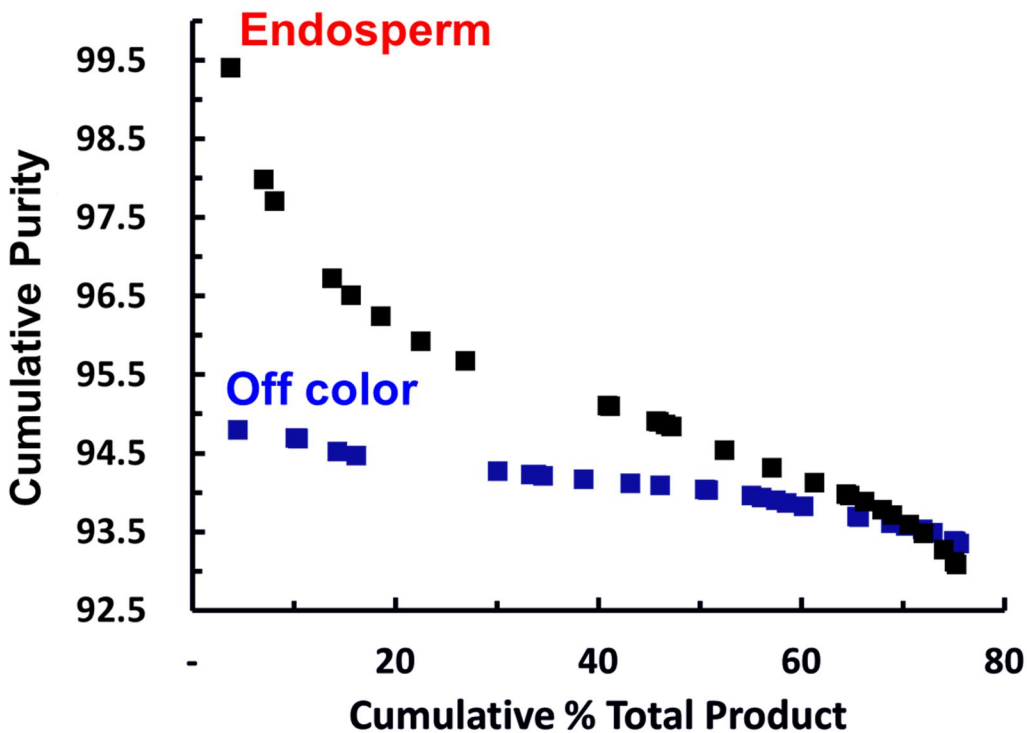


**Figure 2.3** The cumulative reflectance intensity of visible light showing limited contrast for cumulative percent total product (■). A Konica Minolta reflectance Chroma Meter (CR-410) was used to obtain visible color ( $L^*$  value) measurements. Shown to scale with endosperm measurement (■).

Near infrared interference filter instruments typically have a 10 nm band width at half height for each filter. For the liquid crystal tunable filter imaging spectrometer used to produce the direct

endosperm purity profile, three nanometer wavelength increments are reported throughout the selected range.

Based on the premise that the chemical structural basis for endosperm purity is both objective and has a practical range, we have elected to designate the quantitative near infrared image based data as the model. Select near infrared chemical images which highlight endosperm purity in warm (red) colors for individual flour streams appear in **Fig. 2.4**. These images extend over both the endosperm purity range (99.4-81.2%) and the cumulative % total product range for **Fig. 2.2**. In contrast, the broad band color results that are narrowly ranged with sometimes

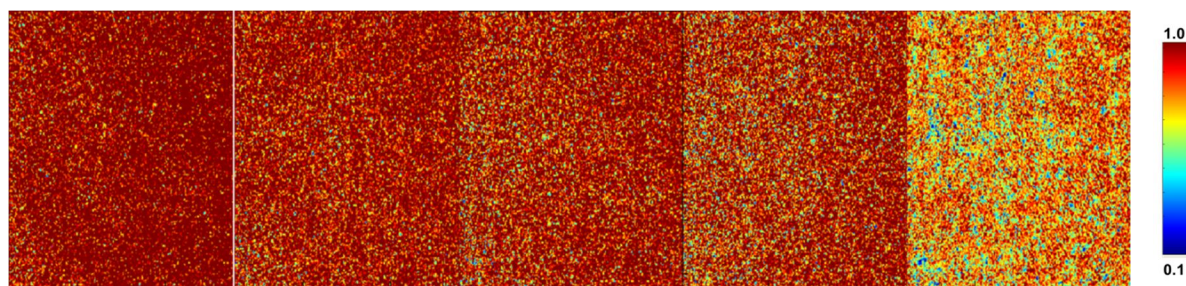


**Figure 2.4** False color images and respective endosperm purity for flour streams collected from DD1 1 (99.4%), DD1#2 1 (94.8%), C1 1 (94.0%), DD2-1 (91.6%), and DD2 2/3 (81.2%). Note the expanded color scale that indicates endosperm purity with warm false colors.. Each is representative of different points across the cumulative endosperm curve.

overlapping values produce a permutation inconsistent with the results from quantitative imaging. Note the sequential list in descending order of endosperm purity of individual color readings and rank (**see footnote 1**). Note also, in the same sequence, the listed ash values and rank (**see footnote 2**). Whereas the ash (mineral residue after ignition) does not reflect the organic species present in the non-endosperm, aleurone, pericarp, germ, etc., the result of plotting ash vs. endosperm purity produces a shotgun pattern with, as anticipated, a somewhat negative slope (**Fig. 2.5**). At a primitive time and place where wheat was locally grown, locally milled,

locally sold, and locally consumed, low ash was a measure of the miller’s resources and skill. A large variation of the mineral content of the soil in which the wheat is grown compromises ash as a meaningful indicator of flour impurity. At long last in the 21st century, a quantitative imaging chemical structural measurement of endosperm purity is defined. This new analytical capability is practical to more accurately assess the result of a change in milling equipment or operating parameters. On a daily basis, however, the broad band color or “brightness” incrementally decreases in concert with chemically defined endosperm purity. Thus, endosperm purity serves as a more objective baseline.

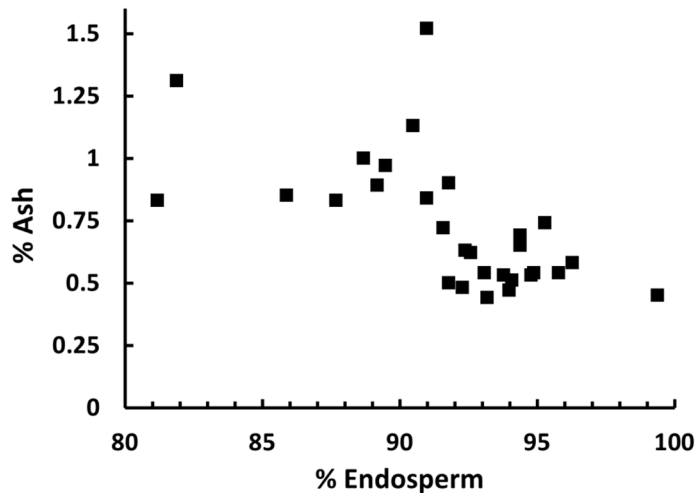


**Figure 2.5.** Ash residue after ignition in a muffle furnace reveals the mineral content that is not related to the organic non-endosperm content of each flour stream. The result of plotting ash vs. endosperm purity produces a shotgun pattern.

From these data, an operative miller can make appropriate decisions to fill orders and meet the specification. This also allows the miller to determine the penalty of adding additional streams in terms of decreasing the endosperm purity. The cutoff point for streams with less endosperm reduces the overall yield but the endosperm purity index for traditional operation allows future calculations for blending where the purity number is retained, but the flow rate is

updated for a different run. A similarity exists between the cumulative endosperm purity obtained for the milling system with debranning and a traditional milling process (6).

In the market that exists for the products of this mill, endosperm purity results in a 10-15% premium for material of certain purity. Just as unconventional, North American hard wheat milling has a ratio of patent to clear flour for a different economic output (2). In this case, the ability to designate and maintain high value flour production sold at a premium price affects the economic benefits derived by careful operation of the mill to get the best possible separation of endosperm from non-endosperm.

## **2.5. Summary**

It can be very informative for the miller to be aware of mill performance in objective terms based on endosperm purity directly determined from detailed quantitative chemical imaging. Unlike flour color, it is not dependent upon the bran color. Also, visual mill inspection is very subjective and the interpretation of results can vary from miller to miller. Methods of flour color determination are often affected by flour particle size. Smaller particles increase the reflectance and may enhance the perceived whiteness of the flour (9).

Unlike ash, the inorganic component of the outer layer of the kernel, the chemical imaging approach does not depend on the soil from which the wheat was grown. While ash fits into Baker specifications and can be useful for adjustment of Mills, ash itself does not affect flour properties. As such, ash may not be the best measurement for flour quality. The near infrared chemical imaging technique with a selective determination of endosperm purity provides a beneficial alternative for optimizing mill flour blends.

## 2.6. Abbreviations

CWT – Hundredweight

PLS – Partial least squares

B – Break

DD – Divisor

Siz – Sizings

C – Reduction

P – Purifier

R2G/F – Redust

T – Tailings

Qu – Quality

TS – Vibrosifter

Br – Bran duster

CIE – Commission Internationael de l’Eclairage

## 2.7. References

1. Dexter, J.E., & Wood, P.J. (1996). Recent applications of debranning of wheat before milling. *Trends in Food Science & Technology*. 7(2), 35-41.
2. Posner, E.S.; Hibbs, A.N. (Eds.). (1997). *Wheat Flour Milling*. American Association of Cereal Chemists Inc: Minnesota.
3. Gregory, D. (2010). Debranning: A miller’s perspective. *International Miller*, Quart. 1, 37.
4. Wetzel, D.L., Posner, E.S., & Dogan, H. (2010). InSb focal plane array chemical imaging enables assessment of unit process efficiency for milling operation. *Applied Spectroscopy*. 64(12), 1320-1324.
5. Boatwright, M.D., Gwartz, J.A., Posner, E.S, and Wetzel, D.L. (2013). A quantitative near infrared imaging study of 1, 2, 3 break system endosperm yield from variation of 1BK/2BK roll gap combinations. *International Miller*. 3, 35.
6. Wetzel, D.L. (2013). Positive assessment of mill stream endosperm purity using chemical imaging. *Cereal Foods World*, 58(3), 133-137.
7. Gwartz, J.A. (2012) New imaging method in milling. *Milling Journal*, 19(4), 56.
8. Lewis, E.N., Levin, I.W. and Treado, P.J. (1996). *U.S. Patent No. 5, 528, 368*.
9. Shuey, W. C. (1975). Flour color as a measurement of flour quality. *Bakers digest*. October, 18-26.

10. Wheat Intake/Mill Performance/Quality Control. Module 11. (1989). In: *Workbook Series; The Incorporated National Association of British and Irish Millers Limited*. London, England.
11. Lewis, E. N., Schoppelrei, J., & Lee, E. (2004). Near-infrared chemical imaging and the PAT initiative. *Spectroscopy*. 19(4), 26-36.
12. Hosenev, R.C. (Ed.). (1998). Structure of cereals. In: *Principles of Cereal Science and Technology*. American Association of Cereal Chemists Inc: Minnesota.
13. Bradbury, D., Cull, I. M., & MacMasters, M. M. (1956). Structure of the mature wheat kernel. I. Gross anatomy and relationships of parts. *Cereal chemistry*. 33(6), 329-342.
14. Gys, W., Gebruers, K., Sørensen, J. F., Courtin, C. M., & Delcour, J. A. (2004). Debranching of wheat prior to milling reduces xylanase but not xylanase inhibitor activities in wholemeal and flour. *Journal of Cereal Science*. 39(3), 363-369.
15. Smith, T., & Guild, J. (1931). The CIE colorimetric standards and their use. *Transactions of the Optical Society*. 33(3), 73.
16. Robinson, J.W; Frame, A.M.S.; Frame II, G.M. (2005). Infrared Spectroscopy. In: *Undergraduate Instrumental Analysis*. Marcel Decker. New York; 213-310.
17. Kramer, R. (1998). *Chemometric techniques for quantitative analysis*. CRC Press, Boca Raton, FL.

## 2.8. Footnotes

- 1) Permutation of color values (with their respective purity ranking) in order were 94.8 (12), 94.6 (1), 94.5 (10), 94.2 (16), 94.1 (18), 94.0 (18), 94.0 (9), 94.0 (6), 93.9 (13), 93.8 (3), 93.7 (5), 93.7 (2), 93.5 (14), 93.3 (15), 93.2 (11), 93.0 (7), 92.8 (8), 92.3 (19), 92.2 (4), 92.2 (26), 92.2 (29), 92.2 (20), 92.1 (27), 92.0 (24), 91.9 (17) 91.5 (23), 90.8 (25), 89.7 (22), 88.4 (28), and 88.0 (21).
- 2) Permutation of ash values (with their respective purity ranking) in order were 0.44 (12), 0.45 (1), 0.47 (10), 0.48 (16), 0.50 (9), 0.53 (6), 0.54 (5), 0.54 (13), 0.54 (3), 0.58 (2), 0.62 (14), 0.63 (15), 0.63 (11), 0.65 (7), 0.69 (8), 0.72 (19), 0.74 (4), 0.83 (26), 0.84 (20), 0.85 (27), 0.89 (24), 0.90 (17), 0.97 (23), 1.00 (25), 1.12 (22), 1.30 (28), and 1.51 (21).

## **Chapter 3 - Endosperm Purity Profile Comparison of Different Milling Operations**

### **3.1 Introduction**

The primary goal for the wheat milling industry is to produce a high volume of flour at sufficient purity (1). These values are often contracted with the purchaser; such as a bakery. The construction of a cumulative millers' curve allows the miller to view the effect of individual flour streams being added to the blend for commercial wheat milling operation while maximizing the patent flour yield at the purity specification expected by the buyer (2). All flour streams are ordered from highest to lowest purity and the weighted combination of the purity measurement is plotted vs. the yield for that blend.

Heretofore, the traditional millers' curve has presented the amount of impurity present in the flour. These methods are dependent upon the type of wheat being milled. As such, a direct comparison is not meaningful unless the wheat being milled is the same grist (blend). For our purposes, determination of the endosperm contents combined with the flour stream flow rates would be favorable to show the purity changes after the weighted addition of streams. The chemical structural basis of an endosperm measurement is only limited by the amount of endosperm present in the wheat. The amount of endosperm in the wheat kernel is highly conserved between wheat blends used in the wheat milling industry (3). Wheat selection by the miller and the operation of the cleaning house typically bypasses the inclusion of small kernels that have slightly higher non-endosperm content ratio and thereby decrease the major variable in the analysis.

The standardization to endosperm concentration allows for efficiency comparisons between different wheat blends and milling operations. This includes the ability to express the

difference between different milling operations in meaningful terms. Three milling operations with very different preprocessing steps were selected for the purpose of this comparison (tempering, debranning, and wheat cleaning only).

The preprocessing procedures for wheat milling have remained fairly unchanged in the past few decades or more (1). Rigorous cleaning steps have always been required to provide grist free of impurities that reduce the yield potential, potentially damage equipment, or adulterate the product. Traditionally, tempering of the wheat with fixed, prolonged exposure to moisture with mixing mellows the bran texture and enables effective separation of endosperm from non-endosperm. However, debranning technology before grinding offers several benefits that have shown an ability to outweigh the extra costs in capital equipment and electricity (4, 5). Likewise, the commissioning process for a developing mill with religious stipulations for the production of matza presented a challenge for milling success with the restriction of limited preprocessing. A comparison of the cumulative millers' curves for these three operations details their purity trends, and the benefits and limitations of preprocessing.

The technique of infrared spectroscopic imaging enables the revelation of the chemical environment for microscopic fields of view (6, 7). Infrared imaging studies of wheat have enabled discrimination of the individual botanical parts of plant material including wheat (8-10). However, the near infrared region is better for quantitative studies in comparison to the mid-IR region (11). Near infrared chemical imaging for the selective determination of the organic endosperm content within wheat milling streams has been demonstrated by past experimentation at Kansas State University (5, 12, 13).

## **3.2 Experimental**

### **3.2.1 Wheat Milling Operations**

Three different flour milling operations were studied. This included a previous study (5) at the Hal Ross demonstration mill at Kansas State University with a capacity of 24 metric tons per 24 hours and 15 flour streams (**Fig. 3.1**). This mill had a minimized processing scheme with several combined flour streams, a double high first and second break roll, and limited operational flexibility. The wheat grist during the experimental study was Kansas hard white winter wheat.

The first of the two commercial mills was a Brazilian mill with a capacity of 204 metric tons per 24 hours with 31 flour streams. The mill had recently modified the flow to accommodate a debranning preprocessing operation. The mill details are featured in **Chapter 2** (13). The grist was a unique blend of semi-soft Brazilian wheat.

The second commercial mill was an Israeli mill with no preprocessing that operated at 187 metric tons per 24 hours. The mill was using a grist of Romanian soft wheat at the time of experimentation. The mill had several unit processes divided into fine and coarse flour streams for 44 total product streams. The mill featured flour streams from five breaks (B), three divisor sifters (Div), 12 reduction operations (C), and a vibrosifter (Vibro). For a traditional milling process, flour production is typically weighted toward the first few (primary) reduction operations. The break and divisor sifters primarily handle material of mixed purity and the vibrosifter sieves material from the air handling system.

### **3.2.2 Specimens**

Grab samples of flour streams were collected during standard operation of each mill. This occurred either below the sifter or at a sampling spout. Flow rates are calculated by taking a

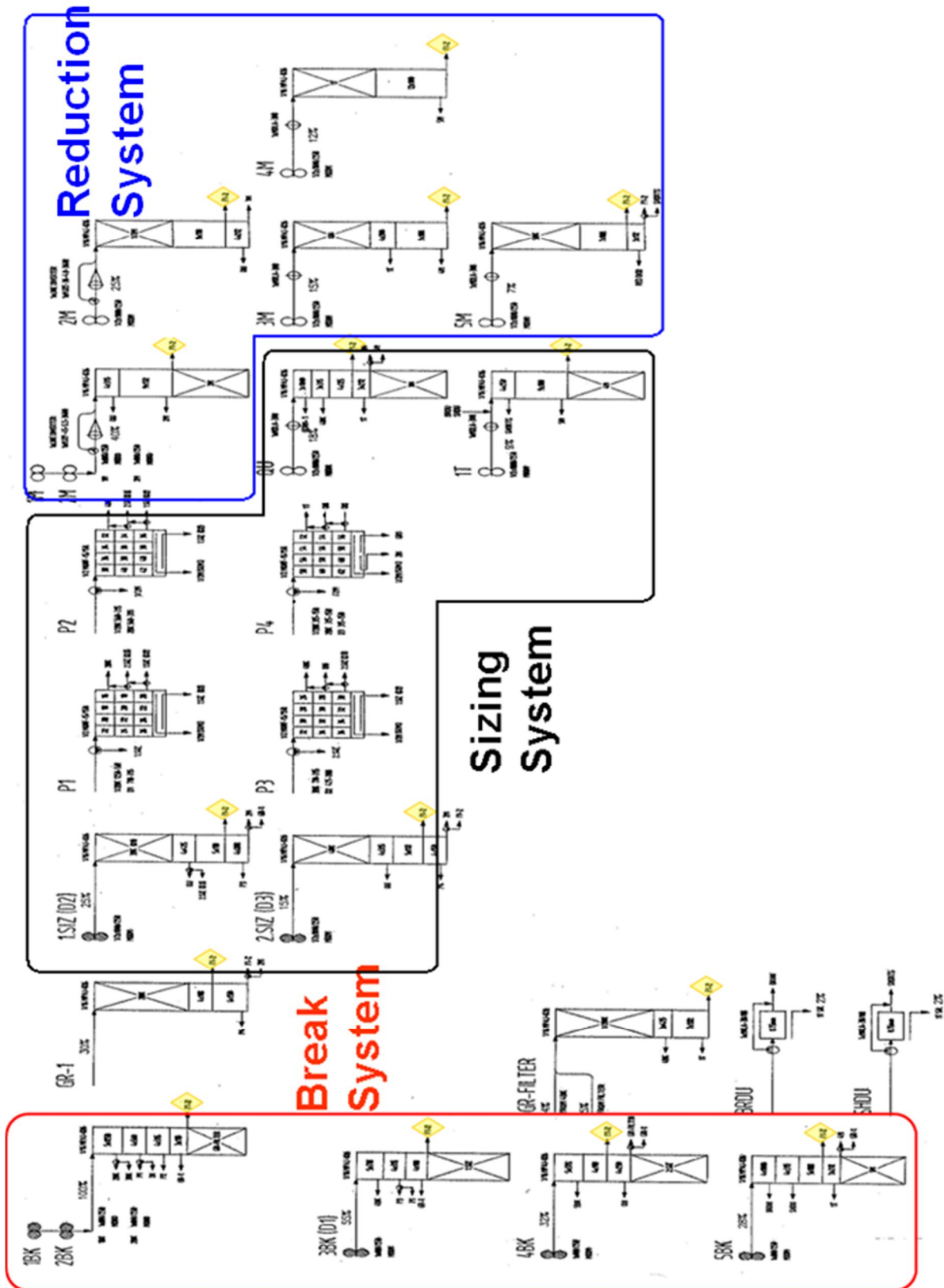


Figure 3.1 Flow diagram for the Hal Ross flour mill.

stopwatch measurement as samples were collected (< 1 minute). The mass of the material was then multiplied out to a 24 hour period.

### **3.2.3 Instrumentation**

The Kansas State and Brazilian milling data was acquired with a Malvern Sapphire® near infrared quantitative imager (Malvern Instruments Ltd., Westborough, MA). A solid state liquid crystal tunable filter (LCTF) enabled scanning the NIR spectrum from a broadband quartz tungsten halogen source (14). A thermoelectrically cooled Indium Antimonide (InSb) focal plane rectangular detector array captured the spectrum for 81,920 individual pixels. The nominal pixel size was 40  $\mu\text{m}$ . Each flour stream was imaged in triplicate. The preliminary experiments at Kansas State University used a spectral windows of 1540-1850 nm and 2000-2400 nm with 10 nm steps. For the Brazilian milling experiment, the spectral region was refined to 1650-1788 and 2150-2228 nm (3 nm steps).

The Israel milling data was acquired later with a Middleton Spectral Vision (Middleton, WI) linear array near infrared imaging spectrometer. The wavelengths were all scanned simultaneously. The spectral window was slightly modified for the new instrument to 1650-1790 nm and 2100-2230 nm. This instrument had a pixel size of approximately 30  $\mu\text{m}$  and the scanning was set for a 256 x 393 pixel data cube.

### **3.2.4 Quantitative Near Infrared Imaging Procedure**

The raw individual pixel intensities for all samples were converted to Absorbance; baseline corrected and normalized before partial least squares (PLS) classification according to

spectral libraries (more than 240,000 spectra for each standard). The individual experiments each required development of independent libraries that represented the wheat grists' specific endosperm and non-endosperm standards. After application of the PLS characterization and algorithm, each pixel was assigned a score from 1 (pure endosperm) to 0 (non-endosperm) and the summation yields the quantitative % endosperm result as in past experiments (5). Details of the spectroscopic measurement and analysis procedure are detailed in **Chapter 1**. Previous studies had determined the relative standard deviation for fine flour streams were to average approximately 0.8%

### **3.3 Results and Discussion**

#### **3.3.1 Construction of the Endosperm Millers' Curve**

The flow rates for flour streams indicated that 50% of the flour was produced from the first six reduction operations. The entire reduction operation was responsible for 72% of the total flour production. The average load for each step of the milling operation was 3.5%. Eight of the 23 milling operations had a value greater than the mean; indicating that the milling yield was distinctly weighted towards a few processes.

The flour production for the Jerusalem mill was essentially divided into 4 categories of flour purity (**Fig. 3.2**).

1. The highest purity material ran from a range of 91.2 to 88.1% endosperm for a 38% contribution to the total flour mass.
2. The second slope region featured material from 87.1 to 78.7% endosperm and contained 40% of the total flour output.

3. The first major drop off for cumulative flour purity consisted of material from a small purity range of 74.7 to 71% with 21.1% of the total flour. This large decrease in cumulative purity was a significant decline in comparison to the previous slope.
4. The last 2.5% of the flour content was added to the byproduct streams for the milling process because it had an endosperm purity of only 66.4 to 50.0%.

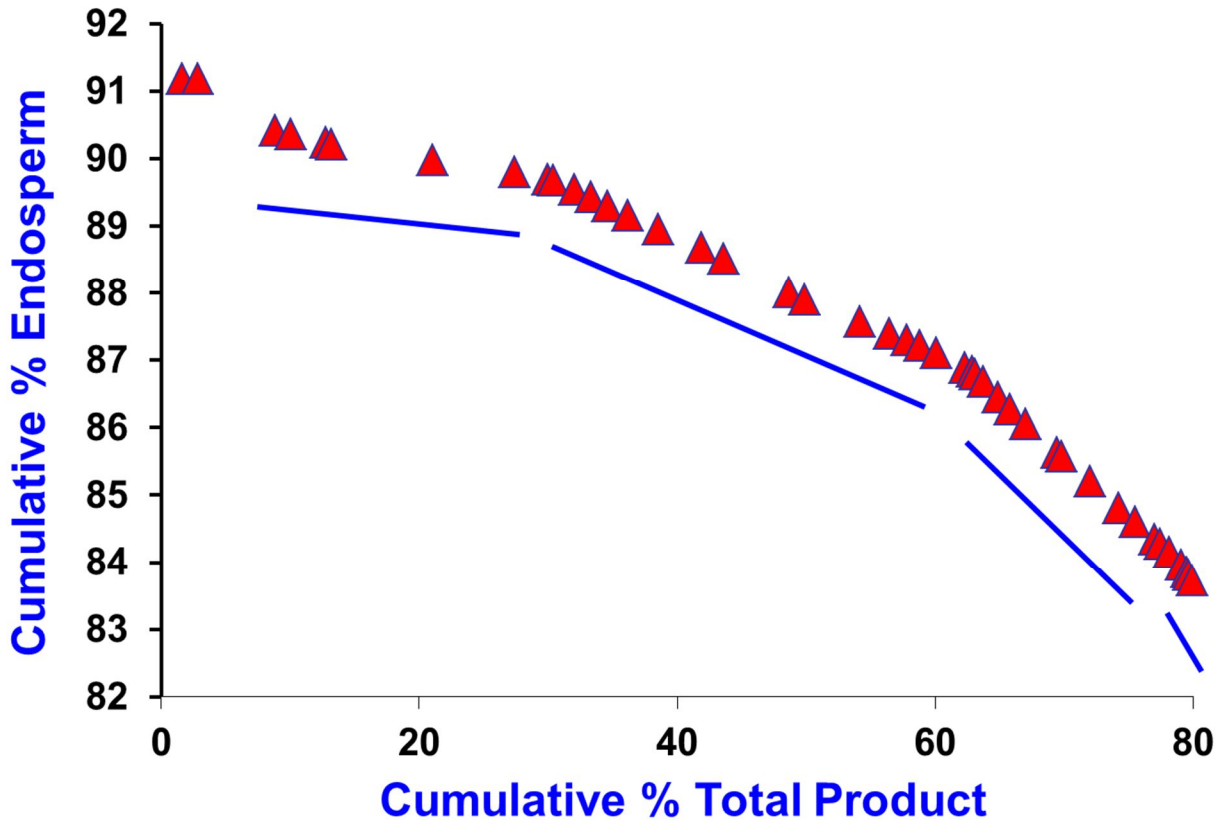


**Figure 3.2** Cumulative endosperm curve for the Jerusalem commercial mill without preprocessing. Note the four slopes changes as inferior product is added to the flour blend.

There were several unexpected trends and inconsistencies in the millers' curve for the mill under contracted commissioning. Several flour streams appeared to be out of order for the current operation of that mill. Many early reduction flours had low purity values, including the fine flours for C3, C4, and C7 at curve positions #21, #22, and #35 respectively. The Vibro flour also had a lower than anticipated flow rate for a soft wheat mill that included a significant

amount of fines. An additional Vibro sifter was added at a later date as a result to handle the more difficult to sift filter flour. All of the C5 and C6 flour streams had endosperm purity values that were relatively high in comparison to the preceding reduction operations.

In theory, for an ideal milling operation, the flour for the fine set of flour sieves would have a higher purity and extraction than the coarse fraction. However, in this case, four milling processes produced a coarse flour at a higher extraction level. The B5 and C5 milling operations in particular had double and triple the amount of coarse flour, respectively. This was anticipated for the B5 operation that handles coarse material with a lot of non-endosperm contamination. However, the C5 milling operation should contain a fairly large amount of purified endosperm to easily produce a significant quantity of fine flour.

Given the importance of the reduction system, a separate curve was subsequently produced to describe this process (**Fig 3.3**). The initial drop off in flour purity for the complete millers curve (**Fig. 3.2**) is shown to have been derived from the reduction process. After the initial drop, the curve levels off for a brief period. However, the middle of the reduction process features a steep decline in flour purity. This would be expected as acceptable for part of the secondary reduction system, but this region of the current working operation included approximately only 15% of the total mill flow for a 3% drop in cumulative endosperm purity.

In contrast, the brightness millers' curve for the Jerusalem mill had a significantly smaller range and instantaneous slopes than the other two curves. However, for this milling operation, the brightness curve serves some use because there are several large observable differences between the streams of high purity. This provides evidence of some usefulness for colorimetry as a quality analysis technique in the milling industry.

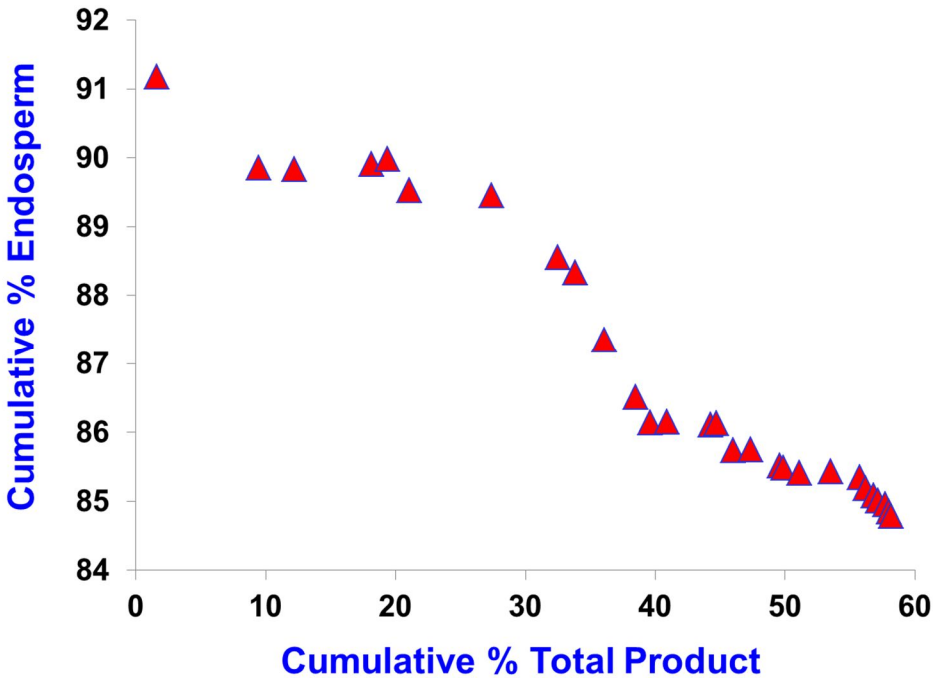


**Figure 3.3** Cumulative endosperm curve for the Jerusalem commercial mill reduction system. Note the departures in the curve in comparison to the original plot.

### 3.3.2 Preprocessing Comparison: Debranning vs. Tempering

The purity profile comparison of flour production provides an enlightening exercise. Near infrared analysis provided an objective terminology that allowed comparison of flour purity from soft and hard wheats (**Fig. 3.4**). We clearly note several benefits for the debranning operation, including the production of high value flour streams, increased overall yield at a fixed purity, and higher value of flour from end of mill processing steps. However, for flours of an average purity value, there was little benefit between the two milling processes. Given our past experiments, a reasonable cutoff for endosperm purity appeared to be 93%. Thus, the debranning operation increased the yield of high-value flour.

From this endosperm purity profile comparison, we note several benefits of the debranning operation: 1) higher purity of “straight grade” flour, 2) increased “straight grade” flour yield, and 3) the production of high purity flour streams. Straight grade flour is generally

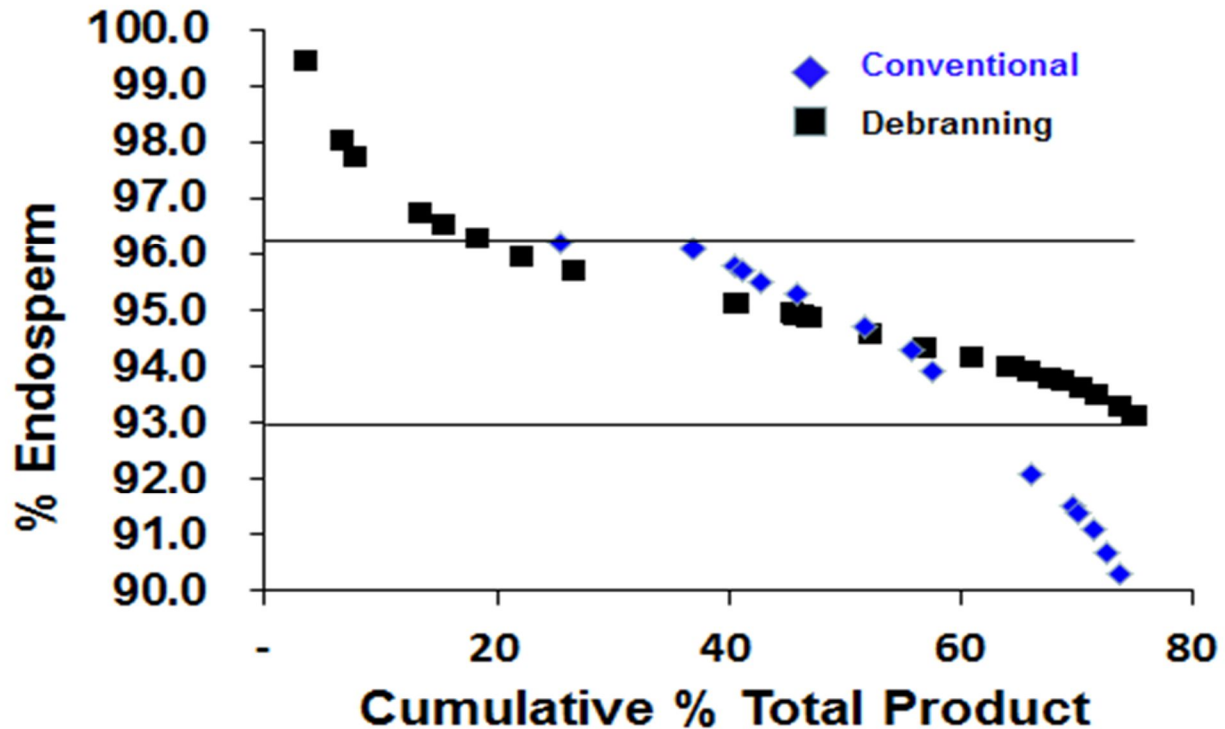


**Figure 3.4** Cumulative endosperm curve comparison of a conventional pilot mill and commercial mill equipped with debranning.

defined as the mixture of all potential flour streams in the mill. Higher purity flour typically ranging from a 50-60% yield is often referred to as "patent" flour. When compared to traditional cutoffs based on color or ash, a reasonable endosperm purity cutoff for patent flour appears to be 93%. Following this reasoning, the debranning operation increases the patent flour yield significantly.

Several differences were seen in the distribution and purity of flour for the different milling systems (**Fig. 3.5**). A significant shift was observed towards earlier flour production in the overall flow for the debranning operation, including a reduced priority of the reduction system. The debranning operation also had a large contribution of redust flour that also precedes the sizings, reduction, or recovery system. The conventional process, in contrast, required significant production from the recovery system.

<b>% total flow</b>	<b>Milling system</b>	<b>Debranning</b>	<b>Conventional</b>
	Breaks	9.2%	9.8%
	Redust	15.5%	-
	Sizings	12.7%	3.6%
	Middlings	28.1%	40.9%
	Recovery	5.6%	15.6%

<b>Milling system</b>	<b>Debranning</b>	<b>Conventional</b>	<b>% endosperm</b>
Breaks	92.9%	82.3%	
Redust	95.3%	-	
Sizings	94.4%	89.4%	
Middlings	91.8%	95.3%	
Recovery	89.5%	84.0%	

**Figure 3.5** Milling system comparisons of total flow and endosperm purity for a mill with and without debranning.

Increased purity was observed for all flour streams produced after the debranning operation with the exception of the reduction system. This differing set of milling priorities presents the opportunity for a shorter milling flow with the help of the debranning operation. As such, the company could either produce a larger amount of patent flour yield or balance the cost of the debranning equipment with less capital cost of equipment and a smaller mill footprint.

### 3.3.3 Comparison of Multiple Milling Operations

Here the three endosperm purity profiles are presented in two ways, an expanded scale and a common scaling. First off is the expanded scale (**Fig. 3.6**) that highlights the trends as a function of the purity range for that particular curve. By using this method, we see that the pilot scale mill maintains a certain level of desired purity for a higher yield, however, the purity falls off the most at the end of the milling process. The conventional pilot mill also featured a limited flour

yield. The Israeli mill had a steady decline in purity but it also rapidly decreased for the last

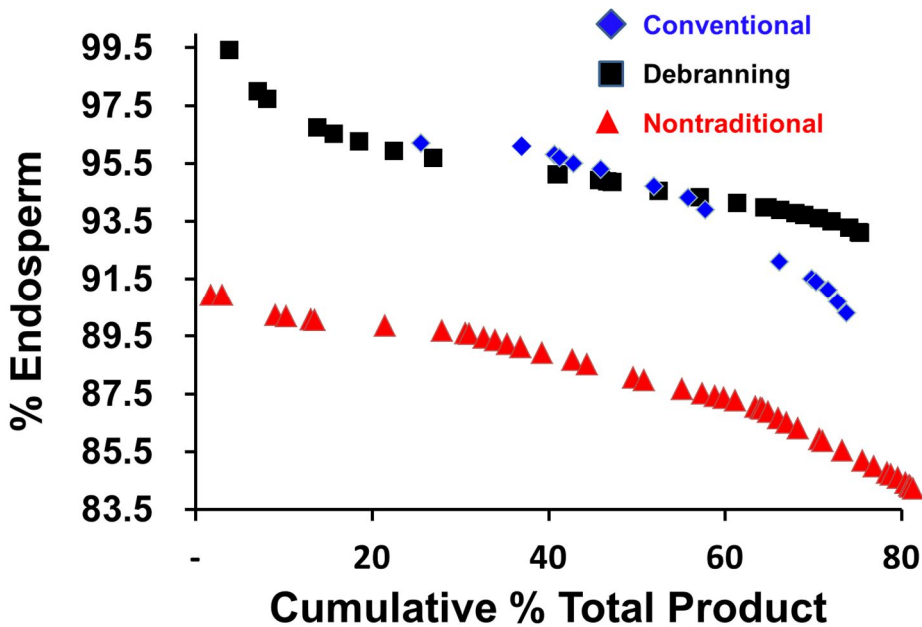


**Figure 3.6** Cumulative millers' curves for a conventional pilot scale ( $\diamond$ ), commercial scale with debranning ( $\square$ ), and a pretreatment free commercial scale ( $\Delta$ ) milling operation with an expanded scale.

few flour streams, but this mill had extraction levels much higher than the milling industry norm.

This mechanism shows that the established mill with debranning had a high initial change in purity, but there was extreme value in maintaining purity over time, with no strong deviation after the first 20% of high value flour.

**Fig. 3.7**, shows the three mills on a common scale. This served well to highlight the differences between a milling operation with and without the preprocessing or pretreatment of wheat. Debranning and tempering of the wheat greatly improved the initial purity of the flour and overall value of the straight grade flour. A steep initial decline in impurity was noted for the start of the debranning operation and the end of the conventional pilot milling process, however, the Israeli millers' curve remains steadier. The other item of note is that the final purity of the

straight grade flour for the other two operations was higher than the initial purity of the Israeli mill by approximately 6%.

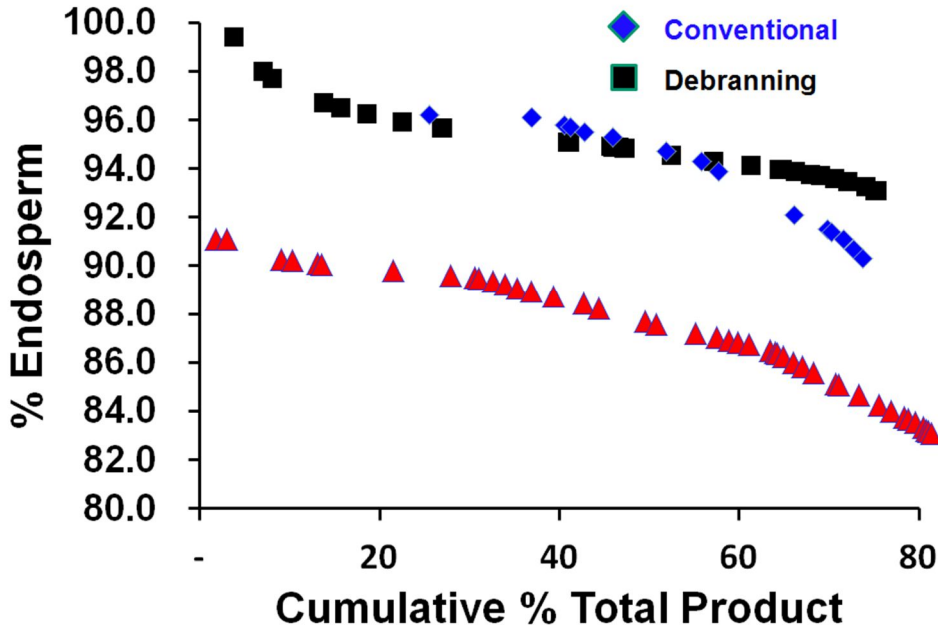


**Figure 3.7** Cumulative millers' curves for a conventional pilot scale (◇), commercial scale with debranning (□), and a pretreatment free commercial scale (△) milling operation with a common scale.

### 3.4 Conclusion

Near infrared chemical imaging enabled direct comparison of different flour mills on the basis of endosperm purity. Each preprocessing step caused redistribution of the high value material, and the lack thereof resulted in lower quality material. The key difference in curve shape is produced by the debranning operation. High value streams are produced and even the lower value streams result in significant value. With the near infrared purity profile, a miller can observe trends over time and reevaluate the performance with wheat changes. The miller can also compare the results to the desired order of production efficiency and make the corrective changes. This method also allows a company to observe the effect of significant processing or

equipment changes and custom tailor or implement them in its other mills. The quantitative chemical imaging technique allows selectivity and sensitivity that is not offered by traditional methods.

### 3.5 List of Abbreviations

CWT – Hundredweight

B – Break

Div – Divisor

C – Reduction

LCTF – Liquid crystal tunable filter

InSb – Indium Antimonide

PLS – Partial least squares

### 3.6 References

1. Posner, E.S.; Hibbs, A.N. (Eds.). (1997). *Wheat Flour Milling*. American Association of Cereal Chemists Inc: Minnesota.
2. Wheat Intake/Mill Performance/Quality Control. Module 11. (1989). In: *Workbook Series; The Incorporated National Association of British and Irish Millers Limited*. London, England.
3. Shewry, P.R., Hawkesford, M.J., Piironen, V., Lampi, A.M., Gebruers, K., Boros, D., & Ward, J.L. (2013). Natural variation in grain composition of wheat and related cereals. *Journal of Agricultural and Food Chemistry*. 61(35), 8295-8303
4. Gregory, D. (2010). Debranning: A miller's perspective. *International Miller*. Quart. 1:37.
5. Wetzel, D. L. (2013). Positive assessment of mill stream endosperm purity using chemical imaging. *Cereal Foods World*. 58(3), 133-137.
6. Robinson, J.W; Frame, A.M.S.; Frame II, G.M. (2005). Infrared Spectroscopy. In: *Undergraduate Instrumental Analysis*. Marcel Decker. New York; 213-310.
7. Budevaska, B.O. (2002). Vibrational spectroscopy imaging of agricultural products. *Handbook of Vibrational Spectroscopy*. Wiley: Hoboken, New Jersey.
8. Budevaska, B.O., Sum, S.T., & Jones, T.J. (2003). Application of multivariate curve resolution for analysis of FT-IR microspectroscopic images of in situ plant tissue. *Applied Spectroscopy*. 57(2), 124-131.
9. Barron, C., Parker, M. L., Mills, E. N. C., Rouau, X., & Wilson, R.H. (2005). FTIR imaging of wheat endosperm cell walls in situ reveals compositional and architectural heterogeneity related to grain hardness. *Planta*. 220(5), 667-677.

10. Philippe, S., Robert, P., Barron, C., Saulnier, L., & Guillon, F. (2006). Deposition of cell wall polysaccharides in wheat endosperm during grain development: Fourier transform-infrared microspectroscopy study. *Journal of Agricultural and Food Chemistry*. 54(6), 2303-2308.
11. Wetzel, D.L. (1983). Near-infrared reflectance analysis: Sleeper among spectroscopic techniques, *Anal. Chem.* 55, 1165A-1176A.
12. Wetzel, D. L., Posner, E. S. & Dogan, H. 2010. Indium antimonide (InSb) focal plane array chemical imaging enables assessment of unit process efficiency for milling operation. *Appl. Spectrosc.* 64(12):1320-1324.
13. Boatwright, M.D., Posner, E.S., Lopes, R., & Wetzel, D.L. (2015). Profiling endosperm purity of commercial mill streams preceded by debranning using quantitative chemical imaging. *Cereal Foods World*. 60(5), 211-216.
14. Lewis, E.N., Levin, I.W. & Treado, P.J. (1996). *U.S. Patent No. 5, 528, 368*.

## Chapter 4 - Novel Optimization of Wheat Milling Sieving Operation and Unit Process Mass Balance Utilizing Selective Near Infrared Chemical Imaging

### 4.1 Introduction

The wheat milling process is gradual, beginning with an intact kernel, requiring selective grinding and reduction of particle size; a technique that has been modified and optimized over the years (1). During the repeated grinding and sieving of the milling process the objective is to reduce the starchy endosperm product from the center of the kernel into particles below a certain size (212  $\mu\text{m}$ ). However, while the grinding operation is responsible for producing material of finer particle size and selectively flattening or reducing particles, the sifting process is responsible for defining the end product of flour milling. Separation by sieving is governed by a several key principles. These include the acceleration of the screen in space (gyration), speed of the material over the sieve surface, the amount of sieve surface (or also the number of sieves), the amount of material reaching each sieve surface, the granulation and shape of material on the sieve surface, and the actual aperture size. However, the single most important determinant of the particle size separation is the sieve aperture (2). Despite the dependence on outside factors to control granulation, the aperture size for sieves often follows a strict pattern and innovation in their organization has been stagnant.

Typically, sifting in flour milling takes place within sections of a sifter box. Each sifter box has spouting overhead that directs material into approximately 6-12 sifter sections. Cloth socks are required to connect the spouting to the sifter because they allow movement with the sifter gyration. **Fig. 4.1** is a typical description and diagram of a single sifter section and its

operation. Material is observed to enter the sifter from the first break rolls. Upon entering the sifter, the material hits a divider and is split into two sets of four sieves. The arrows and labels

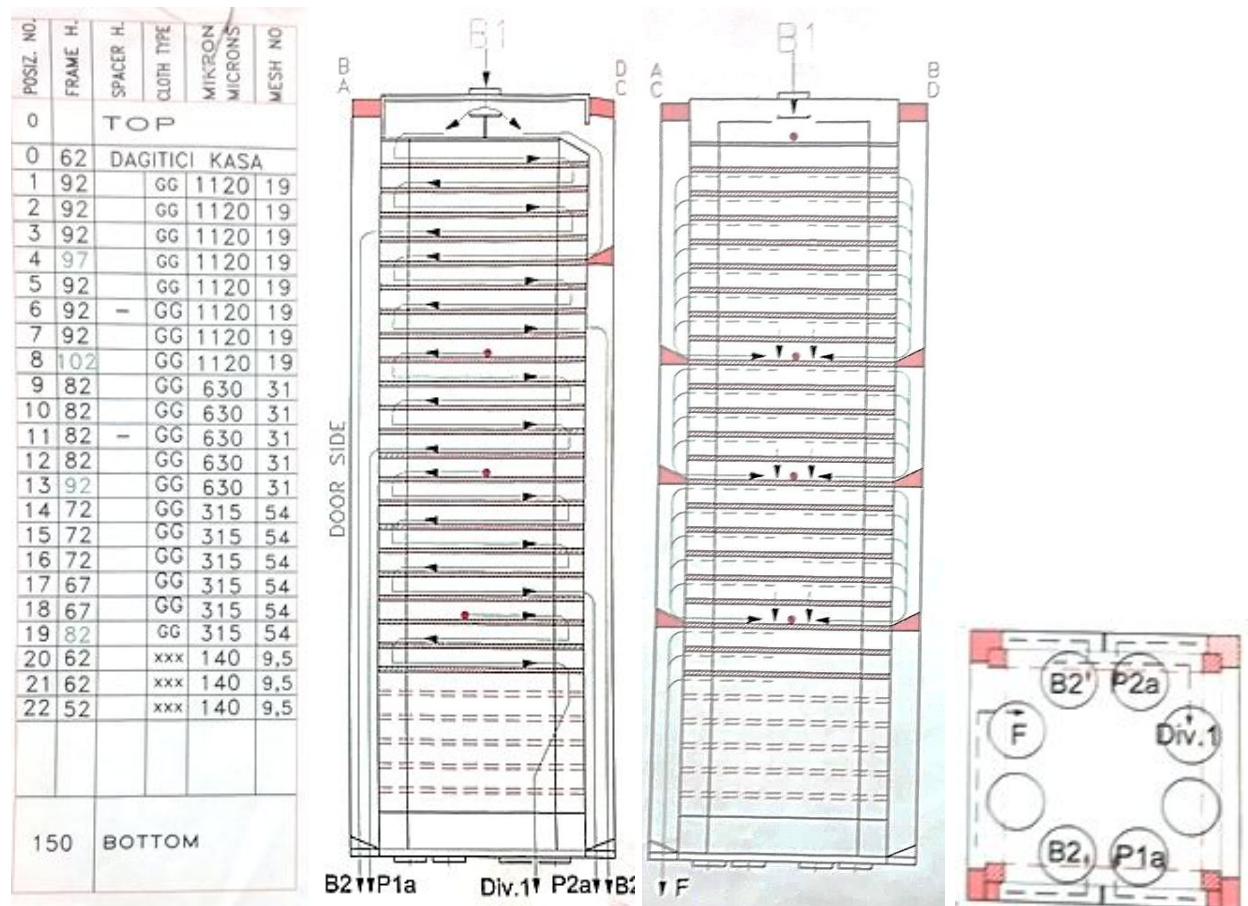


**Figure 4.1** Typical sifter diagrams indicating sieve by sieve details (left), flow of overs (left center), flow of thrus (right center), and the positioning of exit spouting (right).

indicate where the material is transported. The first eight sieves have duplicate sieve apertures. The material that passes over these eight sieves pass on to the second break operation in two separate streams and the thrus pass to the ninth sieve.

On the ninth sieve of the section, there is a dot which indicates that material from above has entered the sieve. The material then progresses through five sieves; the overs of which go to P1a and the thrus continue to the next sieve and so forth. **Fig. 4.1** indicates combination of thrus

and collection in a pan, except for sieves 20-22 that are sent to the flour stream. The fourth diagram indicates the destination of each stream exiting the sifter and where it can be collected.

A common goal for the sifting operation of all mills is to have significant regulation regarding the removal of fines (3). Optimization of the amount of overs and thrus can help prevent “bare” sieving, particularly for flour sieves. Bare sieving is the terminology used to describe an underutilized sifting surface where abrasion and subsequent non-endosperm contamination can occur. One option to prevent bare sieving is to decrease the sieve aperture size to prevent too much material from passing through the sieve. Moderation of this change is important because the smaller sieves opening tend to clog, thereby increasing the time of sifting. For any change of sieve size, the aperture modification does not limit material based on the exact dimension. Sieve openings are square and material approaching 142% of the x, y dimension can still pass through on the diagonal.

Also, the miller must consider that there is no correlation between particle size and endosperm. The sieves after each grinding stage are arranged so a set amount of flour is removed and intermediate streams containing non-endosperm and some endosperm are sent to additional processing stages. Because some of the non-endosperm and endosperm particles are in a mixture of material below 212 microns, sieves with the appropriate micron size are chosen to separate as much pure endosperm (flour) from the mixture.

The action on each sieve frame is inherently dissimilar. However, the traditional method of analysis is to view only the resultant action of multiple sieves. As such, the miller does not have the opportunity to examine the effect of each successive frame. By analysis of the material passing over and through individual sieves, the miller can directly control or monitor the flour being produced. However, traditional methods of analysis have made this heretofore difficult or

impossible (4). The brightness measurements have insufficient contrast between samples and the measurement of mineral ash is ineffective due to high variance and lack of selectivity. In contrast, near infrared chemical imaging provides a sensitive quantitative measurement with a chemical structural basis of endosperm.

Sampling of individual sieves is impossible during regular operation of a flour mill. Each individual sieve frame is contained within the sifter box and direct sampling would require access within the moving sifter. The only way the sieves can be sampled is when the mill is shut down. Given the low margins for the milling process and time required for data acquisition, the only time sieve sampling is feasible would be scheduled shut down for maintenance. In every commercial mill, sifter sections are regularly open and inspected for their condition and maintenance (weekly) according to a set sequence. Thus, the first application of this novel analytical procedure was first proposed during the contracted optimization of a commercial mill.

An Israeli soft wheat milling operation was the location for these unique milling experiments. Full access to sifter sections during the middle of routine operation was provided intermittently, unlike most commercial operations where profits would be affected. For this company, the major consumer of the flour product was the company itself; providing for financial flexibility. The study of soft wheat milling highlights the utilization of the near infrared chemical imaging technique for different milling operations. The unique chemistry of soft wheat varieties (5) also accounted for some differences in processing.

The endosperm of soft wheats is amorphous and friable because the endosperm wedge proteins between the starch granules bond weakly (6). The specific origin of wheat softness has not been verified, but it is often linked to the compound puroindoline that interacts with the protein matrix through unknown mechanisms (7). Another factor is the positive correlation between the

amount of cell walls (8). The kernel is often thicker than hard wheats and more dense. Soft wheats have lower protein (7.0-10.5%) and are used where the final product does not require structural development of dough/batter, such as cookies and cake.

The goal of later processing steps in the milling flow is to maximize the byproduct value and to produce extra flour of additional value with diminishing returns. However, each processing step sends material to several subsequent processing steps. The high volume, low margin nature of the flour milling industry makes it essential to optimize each individual operation and process setting. If a unit process is out of sync, it is important for the miller to quickly identify and solve the problem. Study of a flour mill during the commissioning or contract phase provides a unique opportunity for studying these errors. Several chemical imaging experiments were performed to quantify potential dysfunctional operation of key unit processes for the mill. Each milling process has several outgoing streams and several processing parameters that control the outputs. However, the miller is limited in the monitoring or action of mill processes and must use trial and error (9).

The near infrared chemical imaging technique with chemical and particle size data, results in more informed selection on the granulation and concentration of endosperm analyte for flour milling streams. Chemical images and quantitative endosperm results are shown for the flour sieves of several key sifter sections. Testing in various milling systems of flour extracted from individual sieves show that it is possible to determine the size and presence of any non-endosperm particles among the product streams. Sieve changes can then be proposed to optimize the separation.

## 4.2 Experimental

### 4.2.1 Instrumentation

Two commercial near infrared imaging instruments were used in this study. The Malvern Sapphire<sup>®</sup> near infrared quantitative imager (Malvern Instruments Ltd., Westborough, MA) used for the complementary studies was the basis of the development of the spectroscopic imaging technique for wheat milling streams (10). A solid state liquid crystal tunable filter (LCTF) enabled scanning the NIR spectrum from a broadband source (11). An Indium Antimonide (InSb) focal plane detector rectangular array captured the spectrum for 81,920 individual pixels. The spectral region used was 1650-1788 and 2150-2228 nm (3 nm steps) with a pixel size of 40  $\mu\text{m}$ .

The second instrument was a Middleton Spectral Vision ViaSpec DAQ SWIR model no. MRC-303005-1 push broom array imaging spectrometer (Middleton, WI). The ViaSpec has a linear mercury-cadmium-telluride (MCT) detector with 320 elements at a spatial resolution of approximately 30  $\mu\text{m}$  that requires a four stage thermoelectric cooling process. The microprocessor controlled stage allows for scanning a y-dimension up to 6 inches. For our purposes, a 393 pixel y-dimension was scanned. The default spectral resolution was 5 nm and covered a range of 1000-2500 nm for a total of 256 spectral channels, however, only a portion of this spectral region was necessary for our studies. The acquisition time for one scan was approximately 5 seconds.

Several instrumental parameters were optimized before routine data acquisition could proceed with the Middleton Spectral Vision instrument. The stage scanning settings included speed of acceleration and deceleration that would provide adequate sampling for each pixel. The camera settings included frame rate and exposure time. The stage and camera settings had to be

adjusted simultaneously to avoid distorting the image. The optimized settings for the camera were 286 frames per second and an exposure time of 1600  $\mu$ s.

The ViaSpec spectral data cubes are acquired in the ENVI data format as an .hdr and .raw file. The .hdr file contains the coordinates for the x, y-dimension and the spectral wavelengths scanned. The .raw file contains the spectral data in the form of reflectance counts. Given a slight error for the stage scanning, the y-dimension for each image was either 393 or 394 frames. The spectral data cubes were approximately 125,000 pixels. Each sample measurement must be calibrated to a dark and reference current. These are acquired with a closed shutter and white ceramic standard, respectively. They are retaken every hour to account for atmospheric or detector changes. Spectral data from the ViaSpec are then imported into the Malvern ISys software for data processing. Some adjustments to the ISys analytical procedure were necessary upon transition to another spectroscopic imaging instrument.

The first step for analysis of spectral data cubes is to convert the data into Absorbance. This is accomplished for both instruments (after data conversion for the ViaSpec) by performing spectral math with the sample (S), dark (D), and reference (R) data files. The formula is  $Abs = \log 1/ [(S-D)/(R-D)]$ . The subsequent preprocessing steps are as follows:

1. A baseline subtraction algorithm with a quadratic polynomial function and a baseline range of 0. The points for the baseline are 1650, 1688, 1750, and 2230.
2. For the Middleton Spectral Vision instrument data only, spectral truncation of the excess spectral data from 1000-1650, 1790-2100, and 2230-2500 nm.
3. A normalization (mean center and scale to unit variance by spectrum) procedure is used to reduce the variance between data points that are out of focus.

After preprocessing, spectra from select regions of replicate images of endosperm and non-endosperm sample data are used to develop PLS libraries in excess of 400,000 pixels. Two component classes are created; A, starchy endosperm based upon highly purified streams from the purifier operation; and B, clean bran. The normalized data files are then subjected to 2 separate PLS1 characterization operations for each class (endosperm and non-endosperm). The classification gives each pixel in the image a score from 0 to 1, where 1 is an exact match to spectra for that library class. The two classification images are then entered into an algorithm ( $A/A+B$ ). The mean value for all of the pixels yields the quantitative result. For wheat milling processing streams of an average size (approximately 750  $\mu\text{m}$ ), the relative standard deviation was determined to be 1.9%. The relative standard deviation for the coarsest streams of the milling process ( $> 1000\mu\text{m}$ ) were approximately 3% and 0.8% for fine flour streams

#### **4.2.2 Commercial Milling Operation**

The commercial mill featured in this chapter of the thesis presented a unique opportunity for experimentation. The scheduled and random stop/start operation of the mill, based on constant adjustment by the mill engineer, allowed for regular sampling within the sifter boxes. The soft wheat mill responsible for providing 65% of the Passover matza within Israel and the additional 50% of the total product was exported. The mill only requires operation five days per week to meet the minimum weekly flour needs of the bakery. The bakery produces cookies and various pastries, however, the major product is matza.

The production of matza flour requires several considerations and adjustment throughout the milling process. This level of control exceeds that of the standard soft wheat mill. The traditional milling operation features a conditioning step with water called tempering (1). This

strengthens the bran and weakens the interaction between the non-endosperm and endosperm portions of the kernel. However, Jewish law dictates that nothing must be added to the wheat before it is milled. To limit the negative effect of no tempering, the mill has 4 dedicated air washing units that are responsible for cleaning the air and running humidity control at 65% relative humidity; putting the mill under a pressurized system.

The equipment and flow were designed for the processing of soft wheats. Thus, the sieve configuration, apertures and air flow are often adjusted accordingly. A typical soft wheat milling operation has a smaller flow diagram than hard wheat mills with fewer purification steps; however, the sifting space (area) is larger because the material often sticks together or to the sieve surface (1). Soft wheat mills often have additional bran dusters or air classifiers to aid in the separation of flour, particularly for the break system (12). The Israeli mill has some modifications from the traditional soft wheat mill given the absence of tempering. The milling flow diagram is featured in **Fig. 4.2**. This milling process featured five breaks (B), two purifiers (P), four bran dusters (Br), three divisor sifters (Div), 12 reduction operations (C), and a vibrosifter.

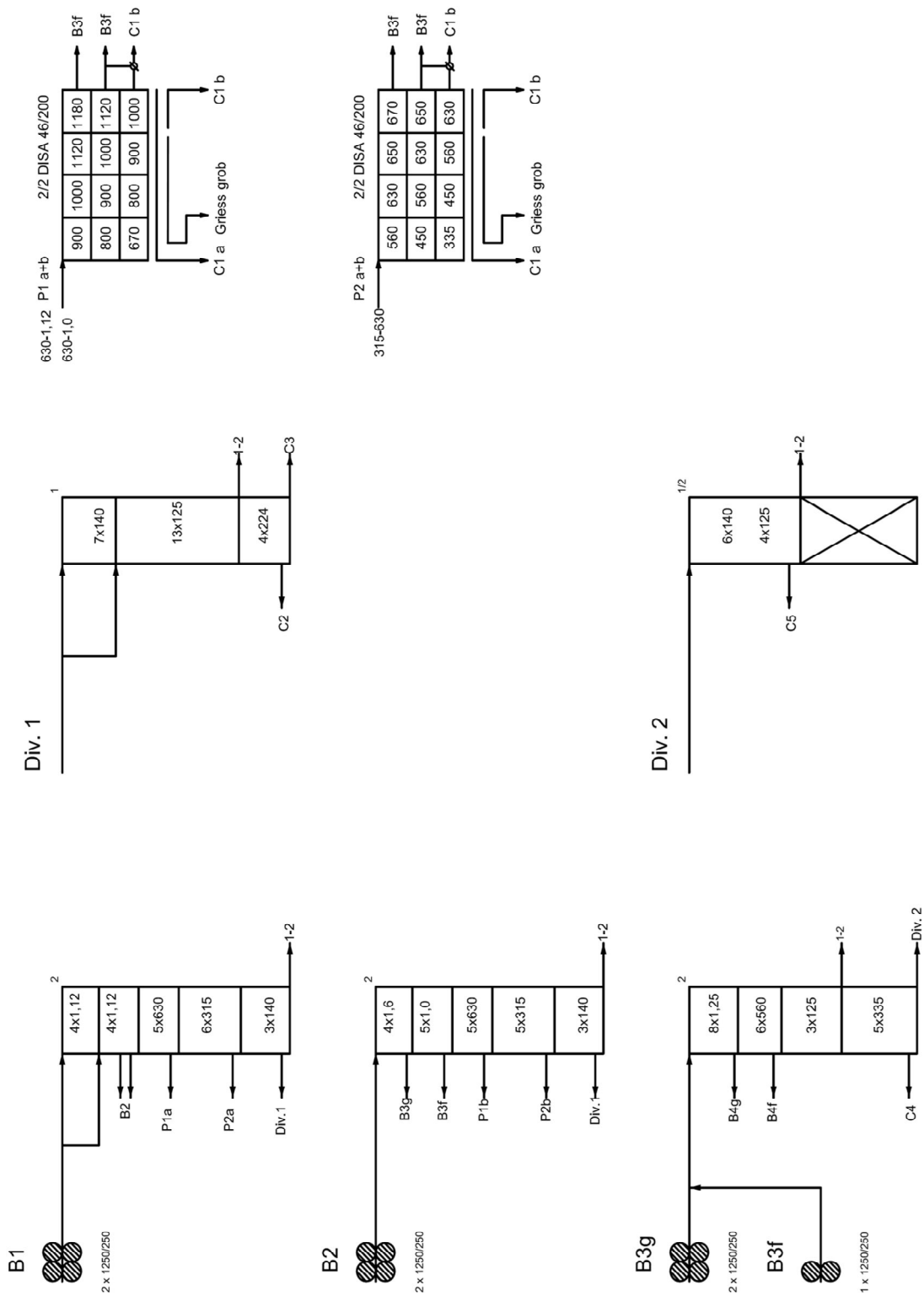
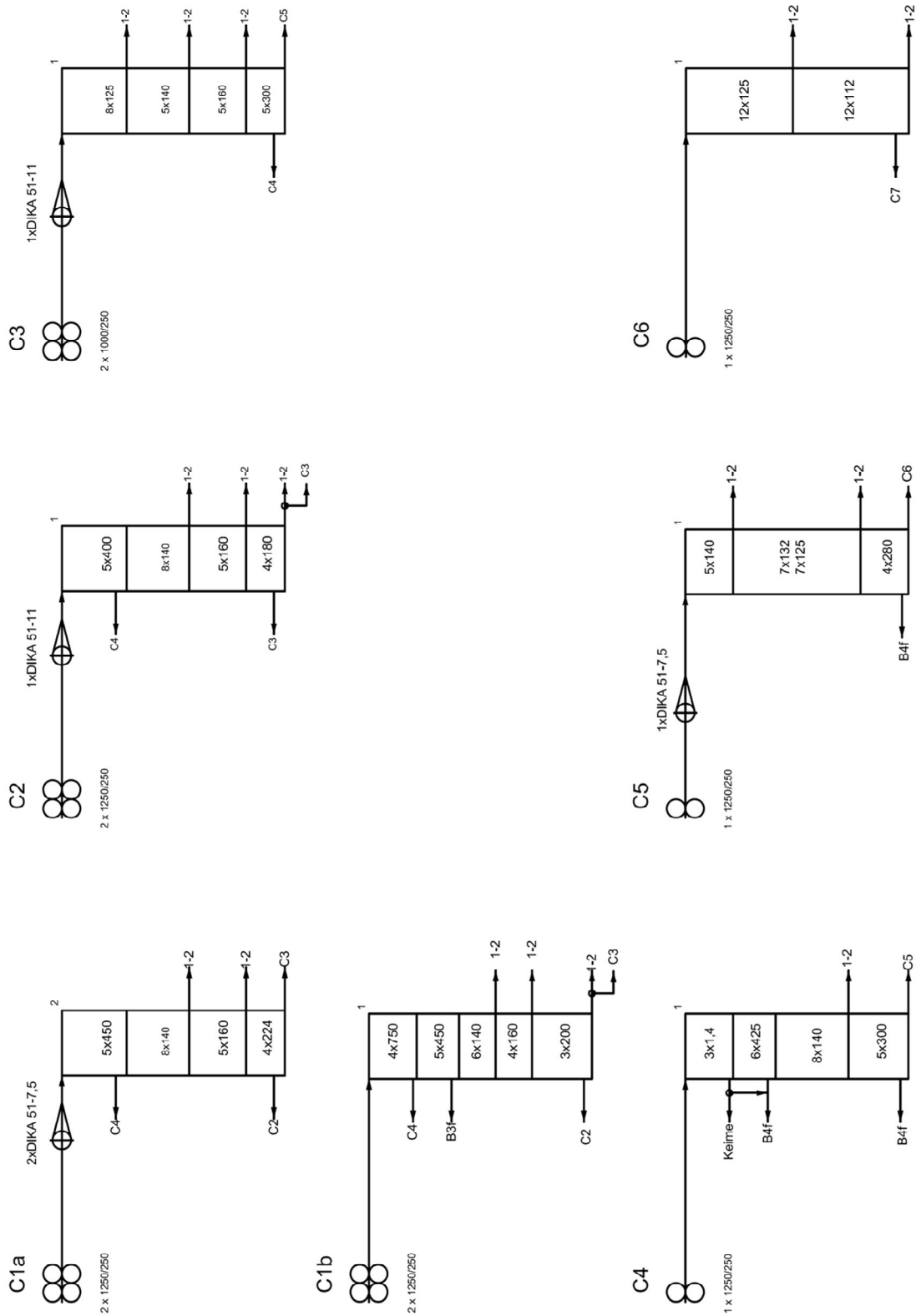
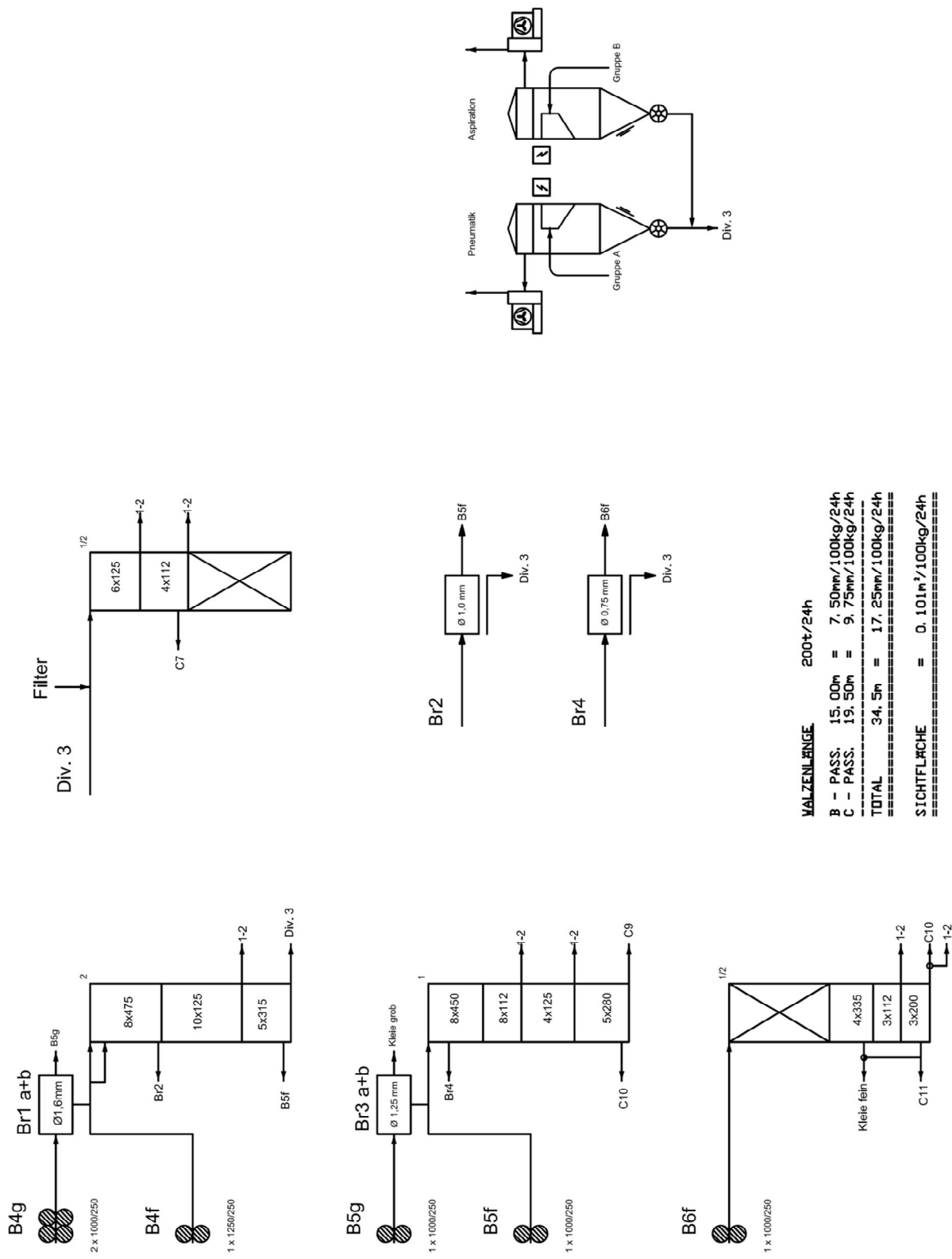


Figure 4.2a Flow diagram of the Em Hachita soft wheat commercial mill.



**Figure 4.2b** Flow diagram of the Em Hachita soft wheat commercial mill.



**WALZENLÄNGE 200t/24h**

B - PASS, 15. 00h	=	7. 50mm/100kg/24h
C - PASS, 15. 50h	=	9. 75mm/100kg/24h
<b>TOTAL 34. 5h</b>	<b>=</b>	<b>17. 25mm/100kg/24h</b>

=====  
**STICHTFLÄCHE = 0. 101m<sup>2</sup>/100kg/24h**  
 =====

Figure 4.2c Flow diagram of the Em Hachita soft wheat commercial mill.

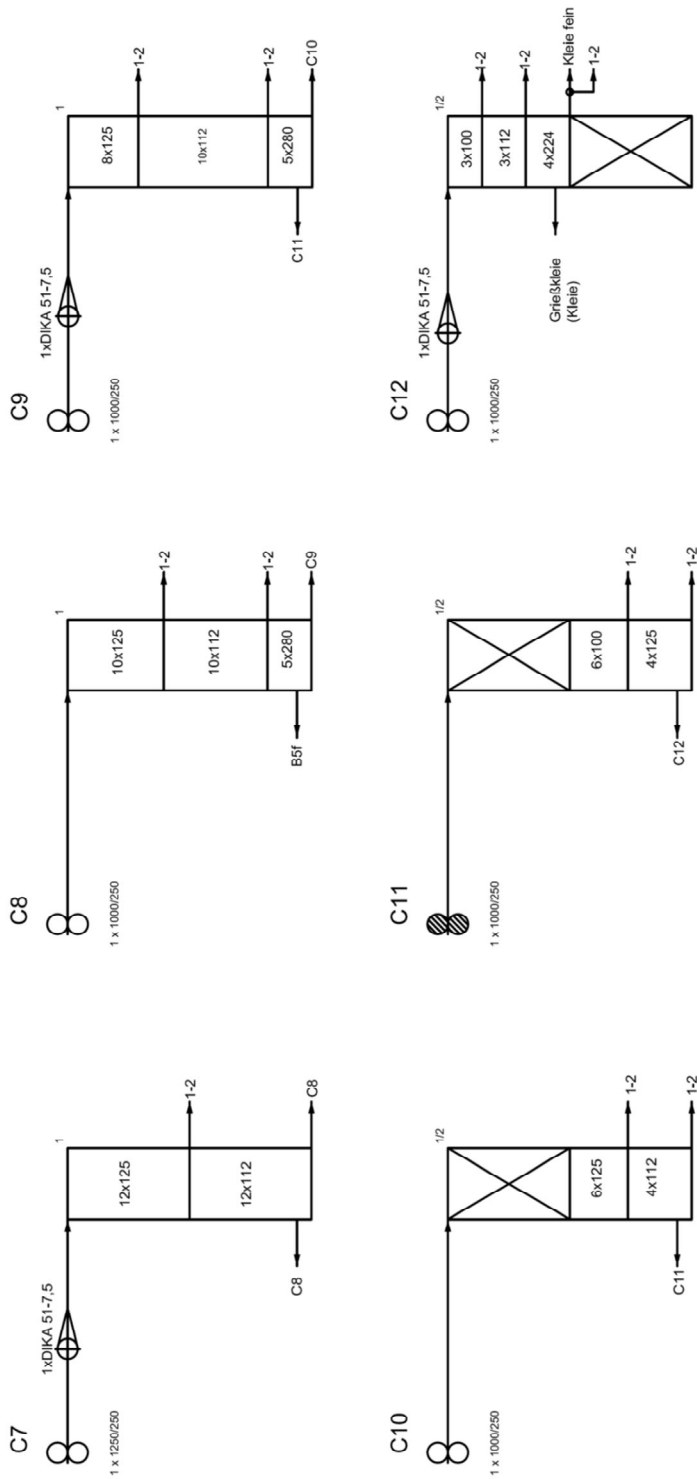


**Figure 4.2d** Flow diagram of the Em Hachita soft wheat commercial mill.

Given the constraints of the unique milling process, the break system has to be gradual and the subsequent milling operations must pick up the slack to extract endosperm without non-endosperm contamination. The primary breaks (B1 and B2) send a lot of material to the purifier where material is selectively sorted for additional processing or grinding for flour production in the reduction system. One key feature present within this mill is the Divisor sifters. These three sifters are an extension of the first four break operations. They handle the excess fine material that could not be separated within the initial sifting section. This process separates a coarse break flour fraction and the overs are sent to the reduction process (C2, C3, C5, or C7).

The secondary break system attempts to maximize the value of byproducts such as clean bran etc., and to extract material of additional value for the secondary reduction system. Bran dusters (BR) that handle break stage material are indicated before the fourth and fifth break sifting, in addition to two standalone operations. Two aspirators are also shown on the diagram. Their purpose is to collect potential product material and send it to the Div 3 sifter. The Israeli mill had primary and secondary reduction systems of seven and six operations, respectively. The goal of the primary reduction system was to grind the purified endosperm into fine flour. The secondary reduction system is handles secondary break stock and attempts to produce additional flour of value.

For the Em Hachita flow sheet, each sifter in the milling operation is denoted with the number of sections and sieves are described by number of sieves  $\times$  sieve aperture size (microns). The diagram (**Fig. 4.2**) either notes that there is one or two (left and right) sifter sections or uses a small notation in the upper right corner. Each box within the sifter section indicates sieves with a common purpose/sieve aperture, where the final overs and or thrus go to a certain destination (i.e. C1 etc.). All product (flour) streams are indicated on the flow sheet with the designation 1-2.

The terms like kleie grobe, kleie fine, griess grob, and greibkleie, indicate the secondary products coarse bran, fine bran, germ, and shorts, respectively (13). The bran is the outer covering of the wheat kernel and the germ is another part of the wheat kernel that contains the developing wheat embryo (14). Shorts are defined as an inseparable mixture of the bran, endosperm, and germ, with lesser value than the individual components.

The spectroscopic standards for the Israeli mill were fairly difficult to define and acquire. For previous experiments (4, 10, 15), samples from the 1<sup>st</sup> middlings reduction top operation (or alternatively a combination of pure flour or purifier streams) and clean bran were acquired for endosperm and non-endosperm, respectively. At the time of the first spectroscopic sampling, none of the streams heading to the C1 reduction operations had been fully optimized to the desired purity. Thus, material for the endosperm standard had to be collected directly from a single isolated fraction of high purity, perhaps feeding into the early reduction operations. After visual observation of the quality of various intermediate streams feeding into or departing low ash or high brightness operations, several purifier fractions of varying particle sizes were combined to produce the endosperm standard. Furthermore, several pieces of non-endosperm contaminant were removed from the sample. The non-endosperm standard was obtained from one of the byproduct streams from the B6f sifter, fine bran, that had the least amount of endosperm adhered to the bran.

#### **4.2.3 Milling Operational Settings**

The Israeli mill used a Romanian soft red winter wheat during the first set of experimental runs. The mill was not fully optimized even though it had been commissioned for regular milling. This was because the buyer and miller were owned by the same company, Em

Hachita Ltd., and any temporary inconsistency was authorized. The mill construction specified for wheat of 12-14% moisture. However, this requirement was secondary to the other specifications (purity etc.) required by the rabbis. The Romanian wheat eventually purchased had a moisture level of approximately 9.75%. This made the wheat milling process without tempering a difficult task.

Several equipment choices hampered the production of a sufficient quantity of pure flour. Each sifter frame contains sieve cleaners that perturb the sieve surface; however, they were not fully functional for many of the flour sieves and had to be replaced. This had caused the sifting space to be inefficient in the separation of fine endosperm. Also, the sieve stockings that connect the sifter to the spouting were not optimized and caused blockages in the sifters from the bottom up and complete mill shutdown. The material being sent to the purifiers was not optimized for the current break release settings; the amount of material released from the break system to other stages of the mill. Likewise, the sieve configuration on the purifier was not allowing proper segregation of products to the reduction operations.

The initial goal for the milling operation was an ash value of 0.65 for patent flour at an extraction level of 80% with a capacity of 8.1 metric tons of wheat/hr. As of the initial experimentation, the milling operation was meeting the brightness specification of 89, but any improvements to color would be of value. The extraction level was only 77%, between the desired extraction level and that of a typical milling operation. This was at a reduced capacity of 7.8 metric tons/hr. with an ash value of 0.68. Another goal was maximization for the value of byproducts. Improvement was a clear option because a limited amount of coarse bran was being produced (5%). Typical milling operations produce up to 8-10% bran (1). Subsequent milling alterations were necessary.

A few key errors in the milling process were chosen for analysis for endosperm mass balance. The first dysfunction studied was the effect of unbalanced grinding operation between duplicate unit processes used to handle the large flow rate. In these cases, either the distribution of material to the two grinding rolls differed or the operational settings for the grind did not match. The second and fourth break (B) operations were studied after observation of discrepancies between mill flow rates during a standard sample collection (**Fig. 4.3**).

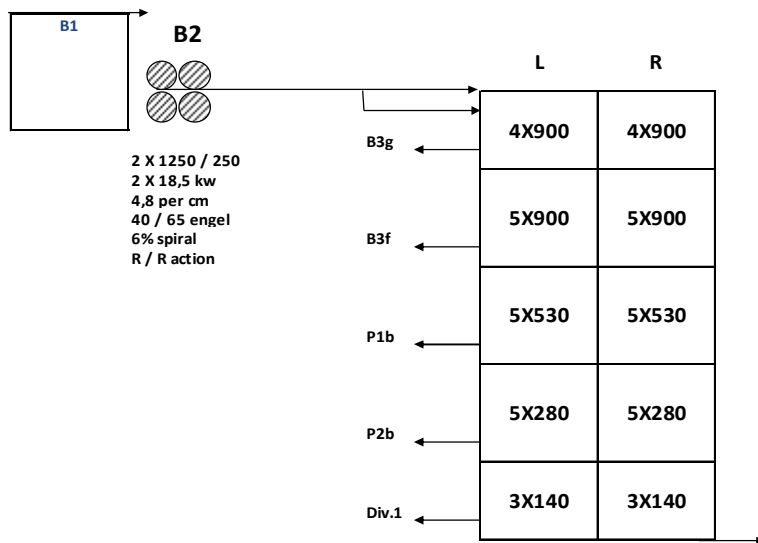


**Figure 4.3.** Milling diagrams for the second break (top) and fourth break (bottom) grinding and sieving operations.

Another experiment sought to highlight the current operation of the primary reduction operations (C2-C5) in the production of flour and distribution of byproducts. When developing the millers' curve for the mill it was noted that flour production had mixed purity and yield for these important steps. This was uncharacteristic as there should be a large flow of pure stock into these unit processes for the production of a high volume of flour. Collection of these samples was primarily below the respective sifter sections of at special sampling spouts. When possible, flow rates were determined to acquire mass balance data. The comparison laboratory milling experiments were collected after grinding and sieving on table top equipment.

## 4.3 Results & Discussion

### 4.3.1 Sieving Experiments

The novel portion of our experimentation is the heretofore unrealized optimization of the individual repeating sieves within a sifter section. The primary goal is to maximize endosperm purity and yield for the material passing through each individual flour sieve and optimizing within the 110-220  $\mu\text{m}$  apertures typically used for flour sieves in the Israeli mill. The sampling procedure for individual streams required the milling operation to be stopped. The sifter boxes were opened for regular maintenance such as checking for sieve blockages and holes. Then, samples could be collected from the material on top of and below each sieve. This allows the miller to see the effective separation for each sieve and compare the effect of subsequent sieves.

The sieving operations studied included B3, C1b, C2, C4, C5, C10, C12, and Div 3. The B3 sifter stack was studied as a matter of convenience, given that there were problems with several sieves in the stack. The B3 sifter required several sieve cleaners to be replaced because material was sticking below the sieve surface. The B3 operation (**Fig 4.4**) begins a transition in the break system where the material has a significantly lower amount of endosperm remaining and comes from the two coarsest fractions resulting from the B2 process ( $> 1000 \mu\text{m}$ ). This sifter section only had three sieves devoted to the production of flour that pass through a 125  $\mu\text{m}$  sieve. The overs were redirected to 355  $\mu\text{m}$  sieves to either C4 (overs) or Div 2 (thrus). The B3 sifting operation had an approximately 34% enrichment for the flour streams, however, the flour was of negligible quality (approximately 75% endosperm).

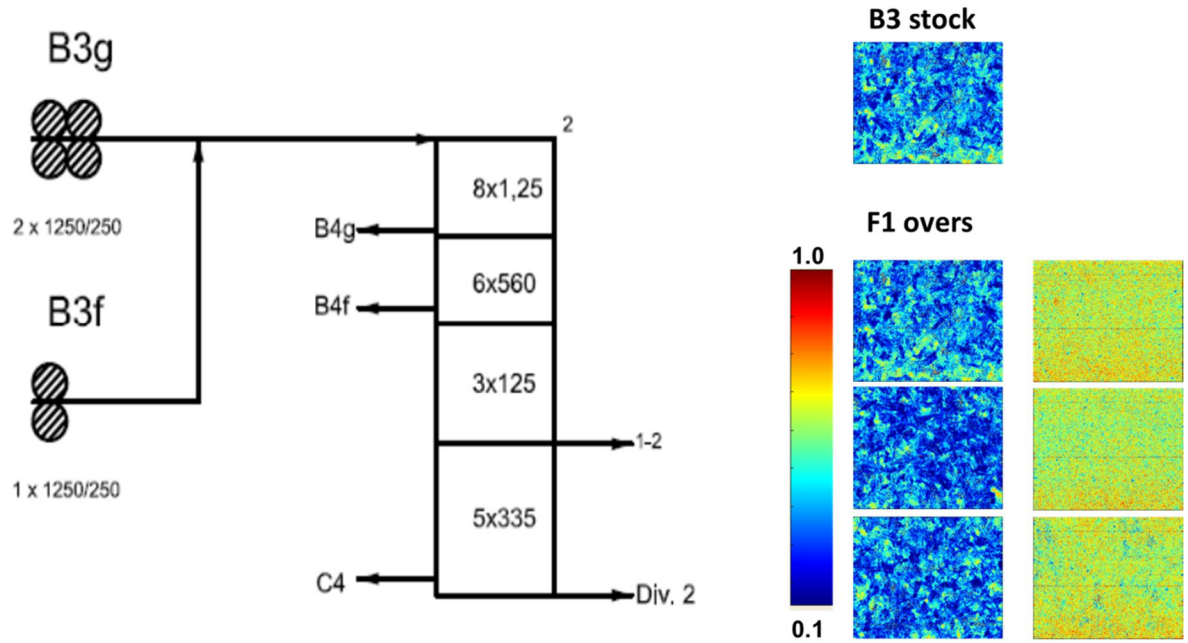


**Figure 4.4.** Diagram of the B3 sieving operation (left) and chemical images for the overs and thrus (right). Note the expanded color scale that indicates endosperm purity with warm false colors.

**Table 4.1** B3 Flour Sieve Endosperm Values

B3 flour sieves				
% Endo		Sieve size (microns)	Sieve #	Sample #
47.07%	+	140	1	D1
76.47%	-		1	D2
41.23%	+		2	D3
75.43%	-		2	D4
39.84%	+		3	D5
77.58%	-		3	D6

The initial stock to the B3 flour sieves was approximately 47% endosperm (**Table 4.1**). The lower purity stock of the overs (39.8%) would either be sent to C4 or Div 2. However, given the purity of this fraction, it is highly likely that this material should head to a reclamation step instead. Otherwise, significant optimization of the first three break operations is necessary to reorganize the granulation. The B3 sieving operation was later adjusted and grab sampling of the

flour indicated a significant increase in purity to approximately 83% endosperm for a moderate yield of flour.

The C1b sifter stack is described in **Fig. 4.5**. The origin of C1b stock is the coarser, dense fines from both the P1 and P2 operation. The C1b operation sends coarse material to C4 and B3. More importantly, there are 6 sieves that produce a fine flour (140  $\mu\text{m}$ ) and 4 sieves below for a coarse flour (160  $\mu\text{m}$ ). The overs of the 160  $\mu\text{m}$  flour sieves are sent to a set of 200  $\mu\text{m}$  sieves and either C2 (overs) or C3 (thrus). The C1b operation had the second smallest flour output of the primary break system at approximately 2% of the total flour.

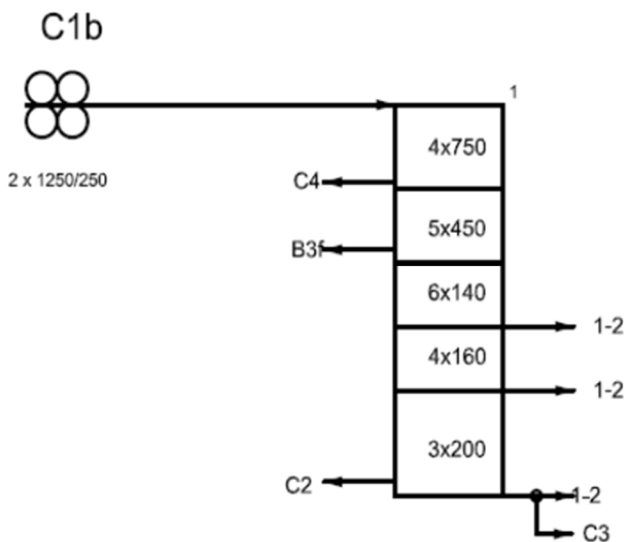


**Figure 4.5.** Sieving diagram for the C1b reduction process.

Each C1b overs stock has similar endosperm values; however, we might see some additional fines in the F1 overs. The C1b sifting experiment exhibited lower ash values for the coarse flour, but a slightly lower endosperm purity value. From **Fig. 4.6**, a large amount of bran contamination was observed in the fourth sieve flour of F1 where the overs had a higher purity than the thrus. Also, for the F2 sieves, the product clearly drops off for the last two sieves.

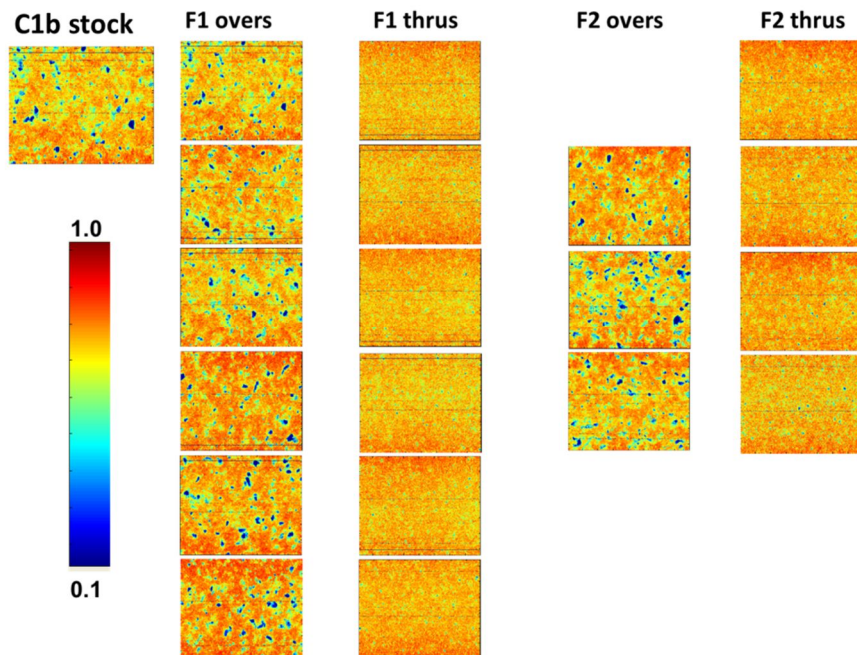


**Figure 4.6.** Chemical images of the C1b flour sieve overs and thrus. Note the enriched flour product and similar intensity of F1 and F2 flour images. Note the expanded color scale that indicates endosperm purity with warm false colors.

**Table 4.2** C1b flour sieve data for overs (+) and thrus (-).

C1b flour sieves					
% Ash	% Endo		Sieve size (microns)	Sieve #	Sample #
0.905%	85.22%	+	140	10	A1
0.669%	88.47%	-		10	A2
0.960%	85.57%	+		11	A3
0.629%	88.82%	-		11	A4
0.928%	85.93%	+		12	A5
0.630%	88.84%	-		12	A6
0.945%	88.49%	+		13	A7
<b>0.642%</b>	87.75%	-		13	A8
0.927%	86.28%	+		14	A9
0.643%	89.45%	-		14	A10
0.966%	87.56%	+		15	A11
0.642%	88.86%	-		15	A12
0.934%	-	+	160	16	A13
0.593%	90.20%	-		16	A14
0.950%	86.97%	+		17	A15
0.599%	90.70%	-		17	A16
1.120%	83.37%	+		18	A17
0.593%	86.02%	-		18	A18
0.993%	82.45%	+		19	A19
0.582%	87.33%	-		19	A20

The ash and endosperm values were contradictory for the sifting experiment indicating that additional aleurone or outer endosperm is present in the flour for this operation (**Table 4.2**). This material would have functional ability for baking etc., but would not meet ash standards. Optimization of the stock sent to the C1b process is the ideal method to increase the purity of the flour. This includes break system and purifier changes. Also, the spectral images and quantitative results indicate that decreasing the sieve aperture should remove some additional non-endosperm particles from the flour.

The C2 sifter stack is described in **Fig. 4.7**. The origin of the incoming stock was the coarse fraction of Div. 1 (224-315  $\mu\text{m}$ ), C1a (160-224  $\mu\text{m}$ ), and C1b (160-200  $\mu\text{m}$ ). There were two flour streams produced on thirteen 140  $\mu\text{m}$  and five 160  $\mu\text{m}$  sieves, respectively. The overs of the C2 160  $\mu\text{m}$  flour sieve are sent to two different classes of C3 material that pass over and through a 180  $\mu\text{m}$  sieve. The C2 enrichment for flour purity was approximately 35%.

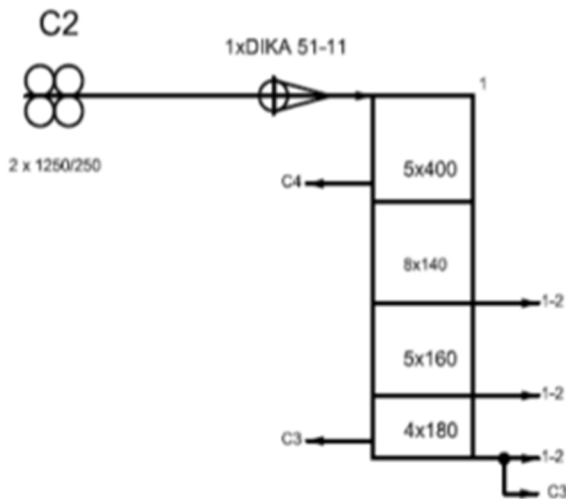


**Figure 4.7.** Flow sheet diagram of the C2 sifting process. Note the fine and coarse flour streams from 8-140  $\mu\text{m}$  sieves and 5-160  $\mu\text{m}$  sieves, respectively.

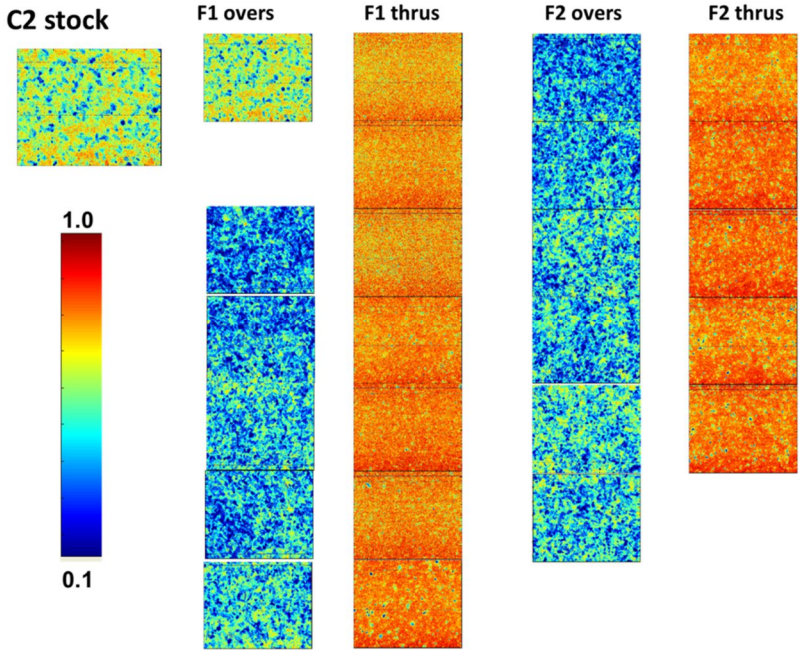


**Figure 4.8.** Chemical images resulting from the C2 sieving analysis. Note the expanded color scale that indicates endosperm purity with warm false colors.

**Table 4.3** C2 flour sieve data for overs (+) and thrus (-).

C2 flour sieves					
% Ash	% Endo		Sieve size (microns)	Sieve #	Sample #
1.797%	71.47%	+	140	6	B1
0.627%	83.92%	-		6	B2
N/A	N/A	+		7	B3
0.571%	85.65%	-		7	B4
3.483%	41.48%	+		8	B5
0.654%	84.98%	-		8	B6
3.790%	44.97%	+		9	B7
0.616%	86.97%	-		9	B8
3.268%	52.50%	+		10	B9
0.561%	88.64%	-		10	B10
3.019%	47.77%	+		11	B11
0.603%	-	-		11	B12
2.850%	55.86%	+		12	B13
0.587%	86.95%	-		12	B14
2.790%	46.02%	+		13	B15
0.719%	87.07%	-		13	B16
2.905%	48.84%	+	160	14	B17
0.653%	86.88%	-		14	B18
3.034%	55.56%	+		15	B19
0.636%	88.39%	-		15	B20
2.571%	51.58%	+		16	B21
0.647%	88.06%	-		16	B22
2.775%	56.16%	+		17	B23
1.508%	86.32%	-		17	B24
2.624%	52.43%	+		18	B25
0.658%	87.78%	-		18	B26

From the initial C2 stock it was noted that there was still a fair amount of product available (**Fig. 4.8**). Likewise, the first initial sieving process removes a lot of product. The purity values for the C2 sieve increase going farther down the stack of 140  $\mu\text{m}$  sieves, indicating that there may be a lot of initial bran contamination in the stream (**Table 4.3**). However, the purity increases for later streams and the coarse flour fraction contains a lot of endosperm in comparison to the fine flour (87.5% vs. 86.3%).

Visual analysis of the sieve fractions shows that sieve #7 contains a lot of extra non-endosperm material in the flour stream. Visual inspection of the second group of flour sieves shows slightly smaller particles of non-endosperm being introduced. Sieve #4 shows the most amount of bran contamination which matches **Fig. 4.8**. In comparison to the C1b stock, we note that the C2 operation produces a similar quality flour with an initial stock that has 14% less endosperm content. Adjustment of the milling procedures provided a similar amount of flour yield as before (the second largest of milling operations), but resulted in flour purity increases to 89.6% and 89.8% endosperm, respectively.

The C4 sifter experiment had 8 sieves (140  $\mu\text{m}$ ) that produced only one flour (**Fig. 4.9**). The C4 operation was hard to control because several moderately coarse streams are combined from C1a, C1b, C2, C3, and B3. However, the C4 operation had the smallest flour yield of all of the primary breaks. Rather, the C4 operation used several coarse sieves to produce germ and B4f stock with apertures of 1400  $\mu\text{m}$  and 425  $\mu\text{m}$ , respectively. The fines were further segregated into B4f (over 300  $\mu\text{m}$ ) and C5 (thrus) stock. The C4 sieving experiment showed an average 31% enrichment of endosperm purity from the raw material to flour.

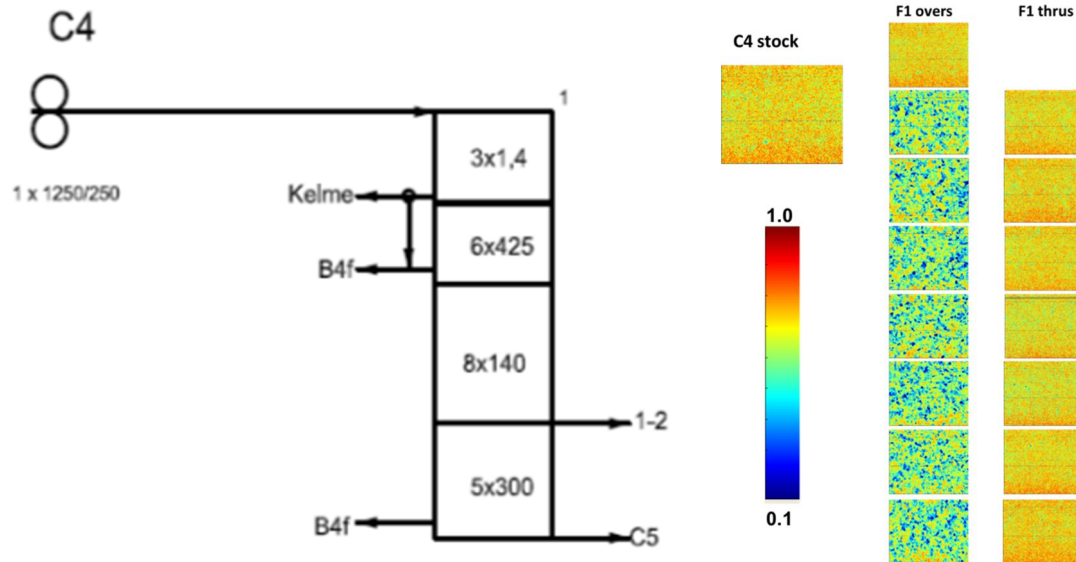


**Figure 4.9.** Flow sheet diagram of the C4 sifting process (left). Note the flour stream from 8-140  $\mu\text{m}$  sieves. Corresponding chemical images of the overs and thrus are also shown (right). Note the expanded color scale that indicates endosperm purity with warm false colors.

The Div 3 sifter stack had 10 sieves (6-125  $\mu\text{m}$  and 4-112  $\mu\text{m}$ ) devoted to the production of two flour streams (**Fig. 4.10**). The remaining material was sent to C7, the beginning of the secondary reduction system. The Div 3 operation handled additional B4 fines and filter flour acquired from the air handling system.

One sample was excluded from the Div 3 analysis, because there was a hole in the second sieve. The incoming material for the process had an endosperm content of approximately 57.5% (**Table 4.4**). Endosperm was readily removed down the sifter for an average enrichment of 12%; however, the flour had minimal value at approximately 69% endosperm throughout the sifter. Approximately 4% of the mill flour was attributed to Div 3, but much of this material is best suited for the secondary reduction system. Minor adjustments alone resulted in an increase in the purity of Div 3 flour to approximately 73.5%. However, the image analysis indicated there is

some need for some purification or a bran duster operation to filter out lightweight

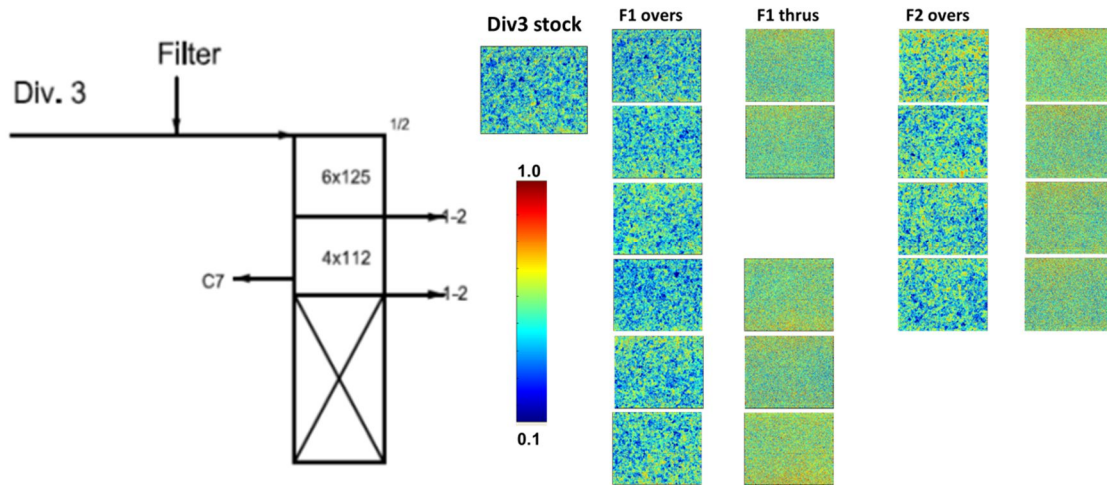


**Figure 4.10.** Flow sheet diagram of the Div 3 sifting process (left). Note that two flour streams are produced from 6-125  $\mu\text{m}$  (coarse) and 4-112  $\mu\text{m}$  (fine) sieves. Corresponding chemical images of the overs and thrus are also shown (right). Note the expanded color scale that indicates endosperm purity with warm false colors.

**Table 4.4** Div 3 flour sieve data for overs (+) and thrus (-).

Div 3 flour sieves				
% Endo		Sieve size (microns)	Sieve #	Sample #
57.52%	+	125	1	C1
68.25%	-		1	C2
58.22%	+		2	C3
-	-		2	C4
59.01%	+		3	C5
68.57%	-		3	C6
54.52%	+		4	C7
70.94%	-		4	C8
58.54%	+		5	C9
69.00%	-		5	C10
60.24%	+		6	C11
73.22%	-		6	C12
58.31%	+	112	7	C13
72.10%	-		7	C14
59.02%	+		8	C15
70.05%	-		8	C16
60.17%	+		9	C17
70.42%	-		9	C18
57.82%	+		10	C19
68.91%	-		10	C20

non-endosperm particles. The cost effective alternative would be to increase the sifter apertures for the flour sieves.

#### **4.3.2 Break System Balance**

The initial problems with imbalance for the break operations were revealed by manually checking the flow rates for each flour stream in the mill. The second and fourth break operations each have two grinding rolls and sifters devoted to their process. Collection of the flour streams provided for a millers' curve showed significant discrepancy between these duplicate processes.

The second break operation features duplicate grinding and sieving operations to handle the material over an 1120 um sieve from the first break operation (**Fig. 4.3**). The second break sieving operations divide the material between third break coarse, third break fine, purifier 1, purifier 2, and a secondary sifter (Div 3) for the classification of fines and flour. The operation of the entire break system is highly regulated because it sets the tone for the entire milling operation. Purifier streams are the largest source of purified endosperm to the reduction system for the production of clean flour.

Spectroscopic detection of endosperm content (**Fig 4.11**) revealed that the incoming material to second break contained 78.2% endosperm when these samples were acquired. Given

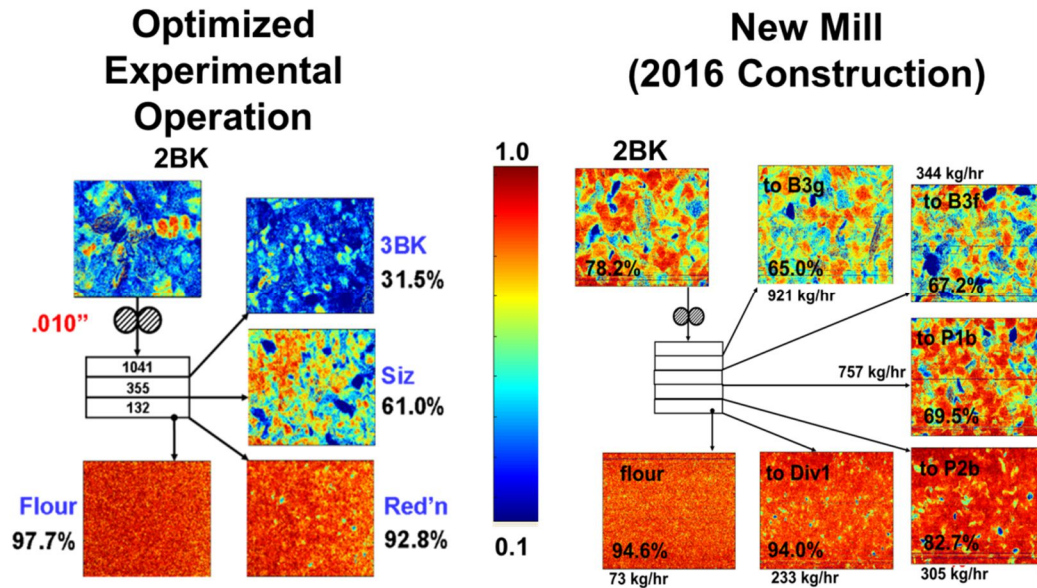


**Figure 4.11.** Purity comparisons of second break operations for a laboratory and commercial scale milling operations. Note that the experimental operation had an optimized first break and second break grinding with tempering of the wheat. The 2016 construction had limits for the incoming stock and grinding because of the lack of pretreatment and contracted engineer settings, respectively. Note the expanded color scale that indicates endosperm purity with warm false colors.

that the wheat kernel is 83% endosperm; this would suggest that there was a lot of endosperm still available for removal after the 1st break operation. This indicates a major deficiency or systematic limitation in the release of endosperm for the early steps of the milling process. There are six outgoing streams from the commercial second break operation. Note that the lower purity material is sent to the next break operation for additional particle size reduction. High purity break flour was produced under the current operation of B2, and other endosperm rich streams are sent to the Div 1 sifter and P2b purifier for further particle size classification.

The optimized experimental second break operation (with tempering) shown here for comparison corroborates the main deficiency with the current operation of the commercial mill (**Fig. 4.11**). The endosperm should be released at the early stages of the mill to maximize the material sent to the reduction stages. However, there is a reasonable distribution of purified

material being sent to additional particle based separation steps of importance (P1b, P2b, and Div 1).

One potential explanation for the discrepancies between duplicate milling processes is imbalance of flow. A slight difference in the angle of spouting could impact the amount or chemical makeup of material reaching the roll stand or sifter (6). Instantaneous surging of product particularly could cause this discontinuity in balance. This is contradictory to the desire to have a uniform product with respect to both particle size and endosperm purity.

#### **4.3.3 Reduction Operation**

The early stages of the reduction system (C2-C5) were studied after observation of the fluctuating amounts of flour production. A traditional flow typically features maximum flour production in the first reduction system that decreases for each subsequent process; however, the Jerusalem milling operation was deficient in that respect.

**Fig. 4.12** displays the distribution of endosperm after the C2 reduction operation. Note that the non-endosperm particles are fairly coarse. The purity of the incoming material was fairly high 85.2%, however, it is well below the intended ideal purity of flour. This operation featured more coarse than fine flour at a higher purity. The C4 fraction was almost negligible, but featured a relevant endosperm purity (84.5%), however, some of this material would have been better suited toward the C3 operation. The material sent to C3 had a significant flow rate. One of these streams had an endosperm purity reduction of 26%. The clear-cut, obvious way to optimize this operation would be to reconsider the destination of the output for the coarsest two sieves. The measured purity suggests sending it to C4. Also, the top sieves may need to be slightly fined downward to prevent excess non-endosperm material passing through.

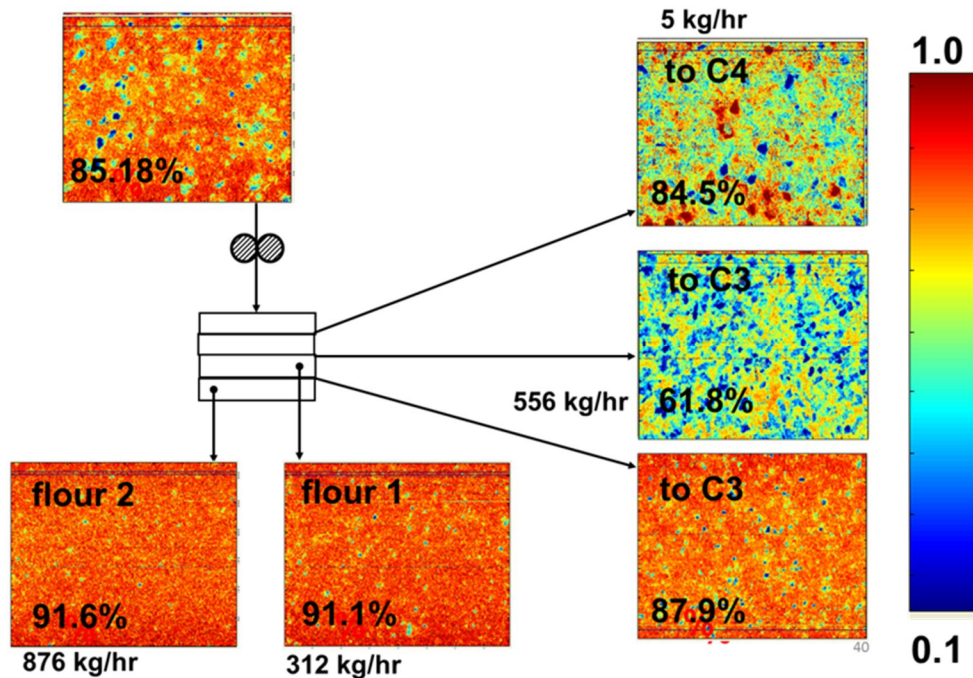


**Figure 4.12.** Chemical images indicating distribution of C2 stock into streams of varying purity. The destination operations included a coarse C4 stock, two C3 streams, a fine flour fraction, and a coarse flour fraction. Note the expanded color scale that indicates endosperm purity with warm false colors.

By the C4 operation, only 60% endosperm is present (**Fig. 4.13**). A single medium flour with an endosperm purity of 82.5% was produced. The material being sent to B4 had an appropriate purity with most of the endosperm having been removed. However, for the streams being sent to the C5 operation, the endosperm purity is higher than that of the incoming material. Optimization of the material entering this singular process is necessary to better reflect its function in the milling operation. One key place for improvement would be the optimization of the purifier settings, including selection of the sieves to be used. Ideally, the flour purity at this point of the reduction system should be much higher. If it was impossible to optimize the upstream process settings, the flour sieves chosen should definitely be changed and perhaps this operation could be divided into two destination streams. Another option was to decrease the gap

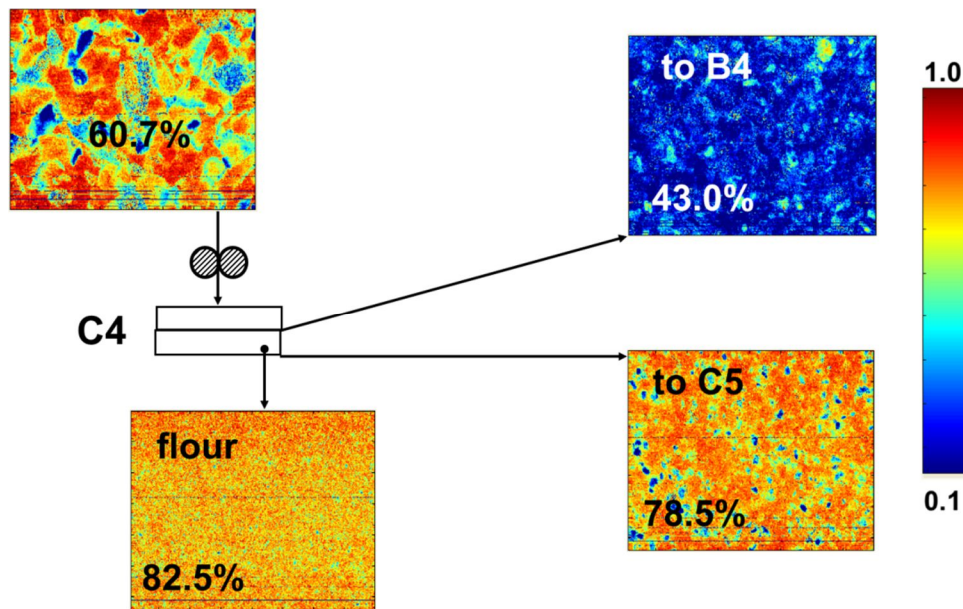


**Figure 4.13.** Chemical images indicating distribution of C4 stock into streams of varying purity. The destination operations included a coarse B4 stock, a C5 stream, and a single lower quality flour fraction. Note the expanded color scale that indicates endosperm purity with warm false colors.

setting of the C4 rolls to reduce the particle size and avoid having clean endosperm agglomerates being sent to the C5 operation.

The results of the commercial C2 reduction operation was compared to a laboratory sieving experiment (**Fig. 4.14**). The two reduction operations handle material of similar purity being ground. The main difference between these two operations is that the commercial mill delivers material to two reduction operations rather than to a reclamation step. The purity of one of the commercial mill C3 fractions was of inferior quality. Future operational changes could alter this distribution, but in the meantime, this material should be sent elsewhere in the reduction system.

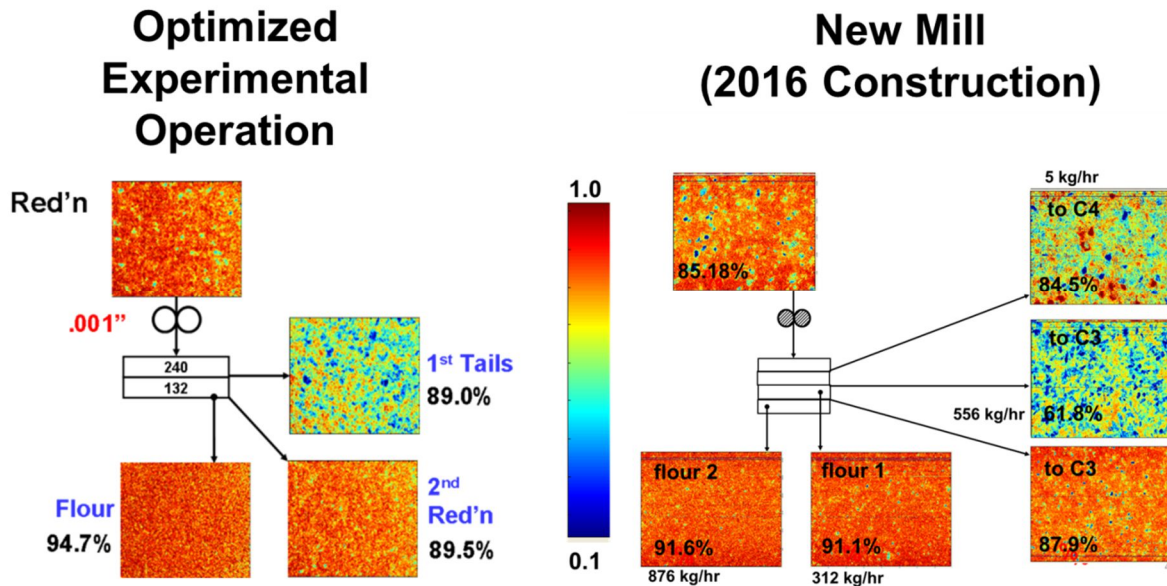


**Figure 4.14.** Purity comparisons of reduction operations for a laboratory and commercial scale mill flow. Note that the both operations feature relatively pure incoming stock and segregate it between a significant mass of product, the next reduction step, and some further processing step. The optimized experiment understandably had higher purity incoming stock and flour. Note the expanded color scale that indicates endosperm purity with warm false colors.

#### 4.4 Summary

Whereas the flour sieves are responsible for determining the final product, it is only logical significant optimization and analysis occurs at this level. However, previous methods of purity analysis for wheat milling have not enabled a sensitive and objective measurement. The technique of near infrared quantitative analysis provides these qualities (16, 17). Here we have shown near infrared quantitative numerical and imaging results that will enable optimization. Chemical images have revealed large particles of contamination that can be removed by alteration of the sifter aperture size. It also revealed small purity differences in between individual sieves, and identified the purity differences between the overs and thrus. As described previously (4), the presented endosperm values confirm the errors in the “purity” determination by ash. The near infrared chemical imaging technique as it stands would be very useful in

determining operational deficiencies for sifter set up in between weekly mill maintenance scheduled shutdowns of several hours.

Also, the optimization of each processing step is essential to redistribute material to different processing steps based upon particle size and the availability of endosperm (9). Near infrared quantitative chemical imaging enables the previously unavailable determination of endosperm concentration as a purity measurement. The objective, chemical structural technique produces high distinction between endosperm purity and particle size distribution within chemical images.

The current operation of the second break and early reduction system was highlighted and corrective action has been suggested for this particular milling operation based upon the results. Also, the mixed purity response of the primary reduction system was observed in chemical terms with false color imaging results. Optimization of the analytical technique and spectroscopic imaging software could eventually provide automation and direct results on the day of analysis for significant economic benefit.

#### **4.5 Abbreviations**

LCTF – Liquid Antimonide

SWIR – Short wavelength infrared

MCT – Mercury-cadmium-telluride

ENVI – Environment for visualizing images

PLS – Partial least squares

B – Break

P – Purifier

Br – Bran duster

D – Divisor

C – Reduction

#### 4.6 References

1. Posner, E.S.; Hibbs, A.N. (Eds.). (1997). *Wheat Flour Milling*. American Association of Cereal Chemists Inc: Minnesota.
2. Posner, E.S., personal communication, August 2017.
3. Gwartz, J.A. (2009) Product quality. *Milling Journal*. 3rd Quarter.
4. Wetzel, D.L. (2013). Positive assessment of mill stream endosperm purity using chemical imaging. *Cereal Foods World*. 58(3), 133-137.
5. Hosney, R.C. (Ed.). (1998). Structure of cereals. In: *Principles of Cereal Science and Technology*. American Association of Cereal Chemists Inc: Minnesota.
6. Seckinger, H.L., & Wolf, M.J. (1970). Electron microscopy of endosperm protein from hard and soft wheats. *Cereal Chem*. 47, 236-243.
7. Turnbull, K.M., & Rahman, S. (2002). Endosperm texture in wheat. *Journal of Cereal Science*. 36(3), 327-337.
8. Barron, C., Parker, M.L., Mills, E.N.C., Rouau, X., & Wilson, R.H. (2005). FTIR imaging of wheat endosperm cell walls in situ reveals compositional and architectural heterogeneity related to grain hardness. *Planta*. 220(5), 667-677.
9. Wheat Intake/Mill Performance/Quality Control. Module 11. (1989). In: *Workbook Series; The Incorporated National Association of British and Irish Millers Limited*. London, England.
10. Wetzel, D.L., Posner, E.S. & Dogan, H. (2010). Indium antimonide (InSb) focal plane array chemical imaging enables assessment of unit process efficiency for milling operation. *Appl. Spectrosc*. 64(12):1320-1324.
11. Lewis, E.N., Levin, I.W. & Treado, P.J. (1996). *U.S. Patent No. 5, 528, 368*.
12. Wingfield, J., & Ferrer, A. (1984). Multiple sieve sifter performance using various combinations of feed rates, circles and speeds. *Journal of Food Process Engineering*. 7(2), 91-110.
13. Official Publication of the Association of American Feed Control Officials. (1996). Association of American Feed Control Officials. Atlanta, GA.
14. King, R.W. (1989). Physiology of sprouting resistance. In: *Preharvest Field Sprouting in Cereals*. Derera, N.F. (Ed.). CRC Press: Boca Raton, Florida; pp. 2855.
15. Boatwright, M.D., Gwartz, J.A., Posner, E.S., & Wetzel, D.L. (2013). A quantitative near infrared imaging study of 1, 2, 3 break system endosperm yield from variation of 1BK/2BK roll gap combinations. *Int. Miller*. 3, 35.
16. Manley, M. (2014). Near-infrared spectroscopy and hyperspectral imaging: non-destructive analysis of biological materials. *Chemical Society Reviews*. 43(24), 8200-8214.
17. Lewis, E.N., Carroll, J.E., & Clark F. (2001). A Near-Infrared View of Pharmaceutical Formulation Analysis. *NIR News*. 12, 16-18.

## Chapter 5 - Summary and Future Direction

The novel aspect of the near infrared chemical imaging approach for wheat milling is that the enhanced sensitivity, compared to previous methods of analysis, enables optimization of the flour (product) sieves. Chemical imaging analysis of the material flowing over or passing through each individual flour (product) allows determination of an optimal sieve aperture size to achieve high purity and maximize the yield. Furthermore, this quantitative spectroscopic imaging method can be used for any intermediate stream or product streams of the wheat milling process. Additional opportunities for application of this analytical approach include the optimization of key unit processes at early stages in the processing flow, or customization of other coarse sieve openings to selectively separate the analyte from other material in the mixture.

Guidance with the near infrared spectroscopic quantitative determination of endosperm is a practical approach to increase mill production. Collection of samples is readily done while the mill is shut down for periodic routine maintenance. The optimization of the flour sieves has the potential to increase the yield by a minimum of 1% annually with the intent to extend the yield to 2-3%. Taking the worldwide wheat usage into consideration (approximately 730 million tons annually), the potential exists for a 1% increase of 7.3 million tons, or approximately \$2.2 billion annually. Even when considering a single average capacity flour mill (454 tons/24 hrs.); increasing the extraction rate by only 1% would produce an additional 1275 tons of flour. Thus, a 1% increase in extraction rate for the “average” mill would approximately produce an additional \$380,000 annually. Taking into account larger benefits, flour mills could potentially produce a > \$1,000,000 payoff.

Software and instrumental advances in the field of spectroscopy have picked up momentum in recent years. Computer scripts or “macros” can enable follow through of a

spectroscopic chemometrics procedure, and rapidly increase the throughput of the experimentation. In the field of instrumentation, the linear array is commercially available from multiple companies. Array instrumentation provides an enhanced output with data acquisition of thousands of pixels. An obvious target for instrumental development is the cost of the array detection. Previous experiments have determined that spectral libraries cannot provide enough data to cover the chemical differences within or between particles of the endosperm and non-endosperm standards without a large number of pixels. The imaging aspect is also important to reveal the varying chemical distribution and particle size statistics.

Near infrared spectroscopic imaging offers a chemical structural approach selective for the composite endosperm analyte. The technique looks at the purity in positive terms rather than the unfavorable material with an objective, binary approach of endosperm product vs. non-endosperm. These features are in contrast to the indirect methods used to determine impurity based upon inorganic residue (ash) or pigmentation (color). With the current instrumentation, chemical imaging can serve central laboratories for the milling industry, but there is also a future expectation to analyze samples at line within a timely manner for the purpose of making the necessary grinding and sieve configuration corrections. This would occur while the mill is shut down for scheduled maintenance. For these considerations, leasing of an expensive piece of diagnostic equipment is a realistic option for the reluctant miller.

## Appendix A - Copyright Permission for Chapter 2

**CEREAL FOODS  
WORLD®**

A PUBLICATION OF AACC INTERNATIONAL



October 24, 2017

Mark Boatwright  
141 Chalmers Hall  
Kansas State University  
Manhattan, KS 66506  
U.S.A.

Dear Mark,

This is to inform those who need to know that permission is hereby granted for use of all materials from the *Cereal Foods World* article referenced below in the dissertation authored by Mark D. Boatwright.

**Cereal Foods World Reference:**

Boatwright, M. D., Posner, E. S., Lopes, R., and Wetzel, D. L. Profiling endosperm purity of commercial mill streams preceded by debranning using quantitative chemical imaging. *Cereal Foods World* 60(5):211-216, 2015.

Sincerely,

Amy Hope  
Publisher  
*Cereal Foods World*

**AACC International**

3340 Pilot Knob Road, St. Paul, MN 55121, USA  
Telephone: +1.651.454.7250 • Facsimile: +1.651.454.0766 • E-Mail: [aacc@scisoc.org](mailto:aacc@scisoc.org)

## Appendix B - Reasoning for the term matza

12/7/2017

Mail - wetzellab@ksu.edu

Re: Matzo, Matzah, Matzos

Elieser Posner <elieser.posner@gmail.com>

Sun 11/12/2017 12:14 AM

To: Wetzellab <wetzellab@ksu.edu>;

Hi Mark

Based on different sources (matza, matzah, & matzos). The Hebrew name used in Israel is Matza which in my opinion you should use for the flour (matza flour & matza). Matzah and matzos are names used around the world where they are influenced by the accent of foreign languages.

Regards

Elie

On Sat, Nov 11, 2017 at 10:12 PM, Wetzellab <[wetzellab@ksu.edu](mailto:wetzellab@ksu.edu)> wrote:

Dear Dr. Posner:

What combination(s) of matzo, matzah, and matzos should I be using to describe the flour product of the mill and the bakery, respectively?

Thanks,

Mark

--

Dr. Elieser (Elie) Posner  
19 Hatichon St.  
P.O. Box 2189 Savyon, Israel 5653016  
Tel: ++972-3-534-2976  
Fax: ++972-3-535-3515